The role of protease-activated receptor-1 in pancreatic cancer progression

Tekin, C.

Publication date
2021
Document Version
Final published version

Citation for published version (APA):
Tekin, C. (2021). *The role of protease-activated receptor-1 in pancreatic cancer progression*. [Thesis, fully internal, Universiteit van Amsterdam].
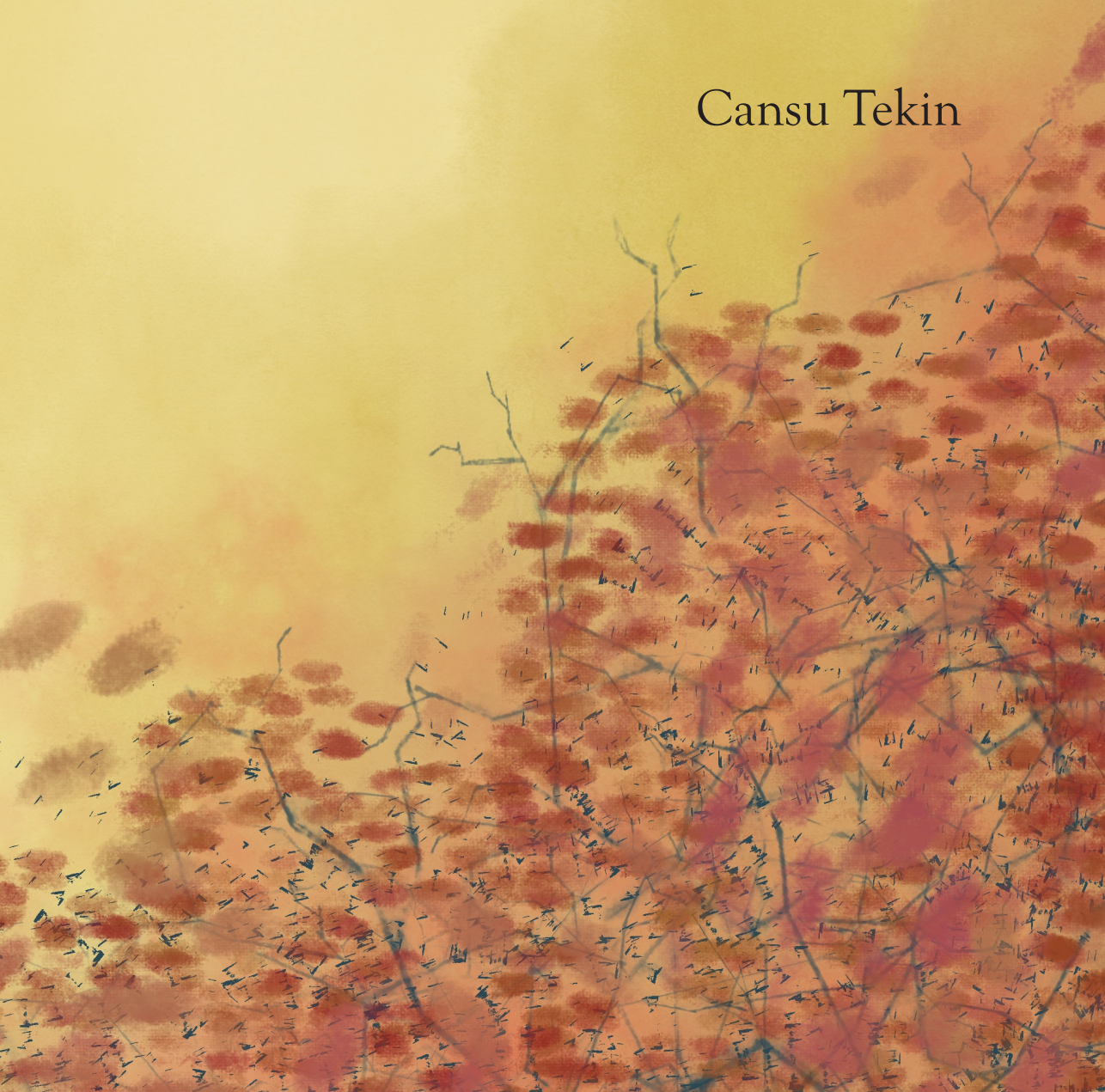
The Role of
Protease-activated Receptor-1 in
Pancreatic Cancer Progression

Cansu Tekin

The Role of Protease-activated Receptor-1 in Pancreatic Cancer Progression

Cansu Tekin

The Role of Protease-activated Receptor-1 in
Pancreatic Cancer Progression

ACADEMISCH PROEFSCHRIFT

ter verkrijging van de graad van doctor
aan de Universiteit van Amsterdam
op gezag van de Rector Magnificus
prof. dr. ir. K.I.J. Maex
ten overstaan van een door het College
voor Promoties ingestelde commissie,
in het openbaar te verdedigen
in de Agnietenkapel
op donderdag 7 oktober 2021, te 16.00 uur

door Cansu Tekin
geboren te Ankara

Promotiecommissie

Promotor:

    prof. dr. J.P. Medema   AMC-UvA

Co-promotores:

    dr. C.A. Spek   AMC-UvA

    dr. M.F. Bijlsma   AMC-UvA

Overige leden:

    prof. dr. H.W.M. van Laarhoven   AMC-UvA

    prof. dr. L. Vermeulen   AMC-UvA

    prof. dr. J.C.M. Meijers   AMC-UvA

    prof. dr. C.J.M. de Vries   AMC-UvA

    dr. A.F. de Vos   AMC-UvA

    prof. dr. H.H. Versteeg   Universiteit Leiden

Faculteit der Geneeskunde

Table of Contents

Chapter 1

Introduction and Outline

Pancreatic Ductal Adenocarcinoma epidemiology, and current therapeutic approaches

Pancreatic ductal adenocarcinoma (PDAC), a neoplasm of the ductal cells in the exocrine pancreas, is the most common type of pancreatic cancer, with 80-85% of diagnosed pancreatic neoplasms being PDAC [1,2]; hence the terms pancreatic cancer and PDAC are consequently used interchangeably. PDAC is a grim disease with a high mortality rate and, despite strenuous efforts to improve disease outcome, 5-year survival rates remain below 10% [3]. The high mortality rates are partly attributed to the fact that most patients are diagnosed at a late stage with advanced disease, and only around 20% of patients are eligible for surgical resection of the tumor [1,4]. The incidence rate for PDAC is increasing globally, and around 460.000 new cases are diagnosed every year [5]. Epidemiological predictions suggest that PDAC will surpass breast cancer and become the third leading cause of cancer-related death in the next decade [5].

Risk factors for PDAC include tobacco smoking, male gender, diabetes mellitus, high red or processed meat consumption, chronic pancreatitis [6], and alcohol abuse [7]. In addition, familial and inherited risk factors are identified in approximately 10% of PDAC patients, and these germline mutations include mutations in BRCA2, p16, ATM, STK11, PRSS1/PRSS2, SPINK1, PALB2 genes, and DNA mismatch repair genes [8].

Treatment of PDAC depends on its disease stage and comprises surgical resection, radiation therapy, chemotherapy, and palliative care. However, among all treatments, surgical resection is the only treatment with curative potential [9,10]. PDAC is divided into three stages as resectable/borderline resectable (10-20% of cases), locally advanced disease/non-resectable (~30% of cases), and metastatic disease (~60% of cases) [1,4,11]. Patients diagnosed with resectable/borderline resectable tumors may receive post-operative (adjuvant) chemotherapy, or alternatively preoperative (neoadjuvant) chemotherapy in combination with radiotherapy [12–14]. According to the PRODIGE-24 trial, patients with resectable/borderline resectable tumor who received 6 months of adjuvant (modified) fluorouracil plus leucovorin, oxaliplatin, and irinotecan (FOLFIRINOX) therapy had significantly increased disease-free survival (DFS) and around 20 months of increase in median overall survival (OS) when compared to gemcitabine mono-

therapy [13]. Importantly, however, treatment-associated toxicities are significant with FOLFIRINOX, and it is only recommended for patients with good performance status [4]. Based on these findings, for patients with good post-operation performance status, FOLFIRINOX became the recommended therapy. For resectable/borderline resectable patients with poor performance status or with contraindications, gemcitabine with or without capecitabine combination is still the treatment alternative [15].

Systemic chemotherapy is also a standard treatment for patients with locally advanced disease. Although a small portion of patients with a prominent response to chemotherapy might become eligible for surgery, the vast majority of patients with the locally advanced disease remain ineligible for surgery, and treatment only delays progression [15].

In the treatment of metastatic disease, chemotherapy is also the standard treatment, and until recently, gemcitabine monotherapy was used as first-line therapy [16]. Based on the ACCORD-11 phase III trial, which showed that standard-dose FOLFIRINOX yielded better treatment outcomes based on improved progression-free survival (PFS) and reduced OS when compared to gemcitabine monotherapy [17], gemcitabine has been replaced by FOLFIRINOX as first-line treatment modality [17]. Although the therapeutic benefits of FOLFIRINOX are superior, associated toxicities are also significant in this patient group, and, similar to resectable/borderline resectable patients, FOLFIRINOX is only recommended for those with good performance status [4]. Another phase III clinical trial (the MPACT trial [18]) demonstrated that nab-paclitaxel, in combination with gemcitabine, outperformed gemcitabine monotherapy in PFS and OS in patients with metastatic PDAC. Nab-paclitaxel / gemcitabine combination therapy was, however, slightly less effective than FOLFIRINOX. Of note, the reduced cytotoxicity of nab-paclitaxel with gemcitabine combination therapy allows it to be administered to older patients and those with lower performance status. Indeed, retrospective analyses suggest that younger and well-performing patients are likely to benefit from FOLFIRINOX with improved OS compared to patients with gemcitabine plus nab-paclitaxel [19,20]. Gemcitabine monotherapy is the only remaining option for patients whose performance status is not fit for FOLFIRINOX or nab-paclitaxel regiment [15].

Based on the above, it is evident that chemotherapy is the backbone of PDAC treatment, and a significant challenge in the management of PDAC progression is the development of chemoresistance. Prolonged exposure to chemotherapeutic reagents leads to increased therapy resistance, which limits therapeutic benefits [21]. Although resistance to other chemotherapeutics is also an increasing problem in the management of PDAC, interestingly, PDAC cells seem especially effective in developing resistance against gemcitabine [22]. It is enticing to speculate that overcoming resistance to gemcitabine could increase its broader therapeutic applicability. This is particularly important considering the substantial toxicity of FOLFIRINOX as compared to gemcitabine. Several mechanisms have been proposed that confer resistance to gemcitabine, including shifts in cell states and associated morphology.

Epithelial-to-mesenchymal transition in PDAC

Throughout embryonic development, cells can undergo transitions between epithelial and mesenchymal cell states. Epithelial cells shift towards the mesenchymal state through a process called epithelial-to-mesenchymal transition (EMT), which alters the cell membrane's adhesion molecules and presents with loss of cell polarity, enhancing the cells' migratory behavior. The reversal of EMT, called mesenchymal-to-epithelial transition (MET), results in the loss of migratory capacity and adaptation of cell polarity [23,24]. EMT is essential for normal embryonic development, but in cancer, EMT is often attributed to metastasis and chemotherapy resistance [24]. Tumor cells that gain mesenchymal traits through EMT can evade the primary tumor, intravasate into the bloodstream, and extravasate into distant tissues to initiate metastatic colonization [25]. Once extravasated, MET triggers the completion of migration and re-initiates proliferation, thereby promoting metastatic outgrowth (reviewed in reference [26]). Although it is thought that EMT is the primary driver of metastatic dissemination, it induces more changes than just invasiveness and motility. For instance, activation of EMT aids cells to evade cell death and confers resistance to senescence [25,27]. Altogether, activation of the EMT pathway results in therapy-resistant, invasive tumor cells with enhanced survival benefits.

The tumor microenvironment in PDAC

One of the most characteristic hallmarks of PDAC is a very desmoplastic tumor microenvironment (TME). Indeed, PDAC lesions can consist of 60-80% non-tumor cells, and only 20-40% is made up of tumor cells [28]. At the initial stage of tumor progression, tumor cells secrete cytokines and chemokines that attract immune cells to the TME. Recruitment of these immune cells can, in turn, create a niche environment that enhances tumor progression and induces an invasive phenotype [29–31]. For instance, recruited non-malignant cells such as myeloid cells and tissue-resident cells can gain tumor-promoting characteristics within the tumor microenvironment in response to tumor stimuli [32]. Apart from tumor cells and cells of the immune system, fibroblasts, extracellular matrix, lymphatic system, and vasculature, occasionally adipocytes and pericytes are parts of the TME. Intercellular communication within the tumor microenvironment ecosystem is done through an elaborate array of cytokines, chemokines, extracellular matrix remodeling enzymes, intercellular interactions, and inflammatory signals (reviewed in reference [33]).

One of the major players in the TME is the macrophage. Macrophages are specialized innate immune cells with phagocytic activities that play a critical role in host defense and tissue homeostasis and respond to intracellular cues, such as microbial products or cytokines, which result in macrophage polarization. Macrophages are ubiquitously present in all tissues, differentiated from peripheral-blood mononuclear cells [34]. In the past decade, macrophage phenotypes were categorized as either M1/Classically-activated or M2/Alternatively-activated macrophages [35,36]. In light of recent findings, macrophage polarization is now considered a spectrum of phenotypes, with considerable heterogeneity within tissues, and M1 and M2 phenotypes are considered the extremes of macrophage differentiation [37]. Upon entry into the tissue, monocytes/macrophages differentiate to sustain tissue homeostasis, and these differentiation patterns differ from inflammatory responses (M1 phenotype) to wound-healing responses (M2 phenotype) **(Fig.1)**. Th1 responses drive the M1 phenotype upon detection of pathogenic parasites or signals such as lipopolysaccharide (LPS). Due to their involvement in pathogen clearing and recruiting other lymphocytes, M1 macrophages are classified as pro-inflammatory [38]. In contrast to the M1 pheno-

type, M2 macrophages are driven by anti-inflammatory cytokines such as IL-4 and IL-13 [38]. However, as mentioned, macrophage plasticity goes beyond the dichotomous M1-M2 phenotypes and gains different characteristics in different tissue environments.
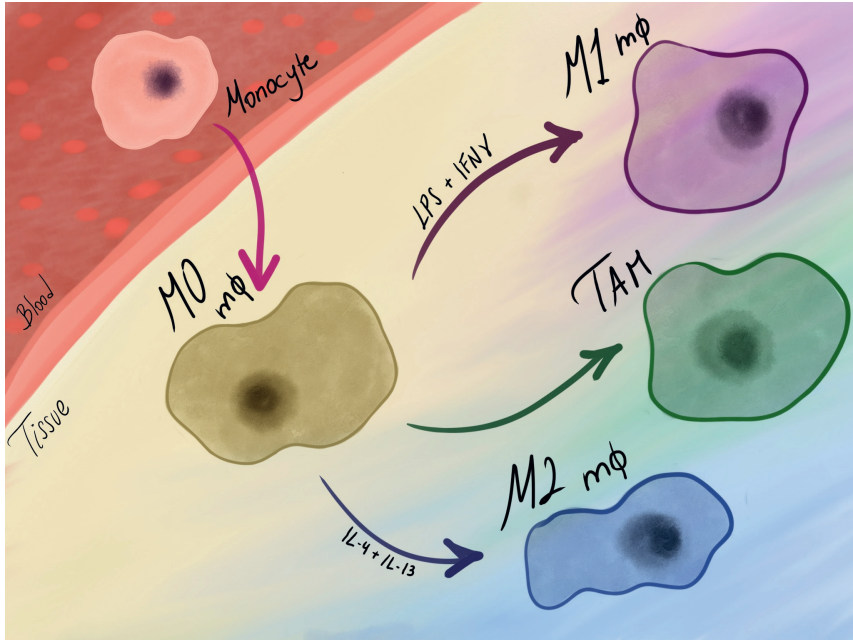
Figure 1

Schematic representation of macrophage differentiation. In response to inflammation or other types of tissue stress, monocytes are recruited from the blood stream into the tissue, where they are activated to become macrophages (Naïve, M0 macrophages (mΦ)). Depending on the environmental influence, i.e., dependence on the cytokines dominant in the tissue milieu, these M0 mΦ can further polarize into M1 (with LPS and IFN-γ stimulus) or M2 (with IL-4 and IL-13 stimulus) macrophages, or in the tumor microenvironment polarizes to become tumor associated macrophages (TAMs).

Macrophage infiltration in PDAC is a common phenomenon, and macrophage populations within the tumor often show high heterogeneity [39]. In cancer, macrophages have initially been considered to possess anti-tumorigenic capacities due to the secretion of cytotoxic molecules, such as; tumor necrosis factor-alpha (TNF-a), nitric oxide (NO), Interleukine-12 (IL-12), and reactive oxygen spe-

cies (ROS) [40,41]. However, despite their cytotoxic capacities, macrophages are now primarily considered to play a role in accelerated tumor progression [42]. Indeed, macrophages are omnipresent in/around tumors in many types of solid tumors, including PDAC, and typically high macrophage density is associated with poor prognosis and reduced OS [43–45]. Macrophages in tumors have distinct, albeit still heterogeneous phenotypes, broadly classified as tumor-associated macrophages (TAMs). TAMs are a diverse and heterogeneous macrophage population derived from either tissue-resident macrophages or monocytes [46]. TAMs exhibit high heterogeneity; for example, some subtypes are pro-angiogenic, some exhibit pro-tumorigenic activities and some subtypes secrete pro-inflammatory cytokines [47]. Although TAMs are considered an M2-like phenotype, the heterogeneous nature and secretion of anti-inflammatory and pro-inflammatory cytokines hint at their unique characteristics.

In addition to macrophages, cancer-associated fibroblasts (CAFs) are among the most substantial components of the TME. CAFs are the primary producers of fibrotic matrix components and other members of the extracellular matrix (ECM), such as hyaluronic acid (HA) and fibronectin, forming the desmoplastic stroma [48], which is a well-known hallmark of PDAC [49]. During early tumor progression, tumor-stroma crosstalk, oxidative stress, and pro-inflammatory cytokines drive the reprogramming of pancreatic stellate cells (PSCs) through which these quiescent cells activate and differentiate into CAFs [50,51]. Once differentiated, CAFs secrete numerous chemokines, cytokines, growth factors, the ECM components mentioned above, and metabolites that drive tumor cell growth and instruct other members of the TME [52–54].

The dense fibrotic deposition in the stroma has biomechanical consequences, such as increased tissue stiffness, hydrostatic pressure that hampers oxygenations and drug delivery and causes poor immune cell infiltration [55–57]. Consequently, it has been hypothesized that the stroma acts as a barrier for efficient delivery of chemotherapeutics, but clinical trials aimed to target stroma depletion did not improve outcome [58,59]. Of note, depletion of CAFs in genetically engineered mouse models of PDAC resulted in high-grade tumors with more aggressive growth and decreased survival, thereby questioning the stroma's tumor-promot-

ing role [60,61]. Reflecting these findings to the clinic also reveals that thera-peutic targeting of stroma in several trials with PDAC patients had no additive benefit; on the contrary, were reported to be more harmful than gemcitabine or FOLFIRINOX alone [62–64].

Acinar to Ductal Metaplasia in the Pancreas

In the human pancreas, two compartments can be defined. One of them is the endocrine pancreas, composed of islets, where alpha (glucagon production) and beta cells (insulin production) reside. The other part is the exocrine pancreas composed of acinar cells, which produces digestive enzymes, and ductal cells, which transport the digestive enzymes to the duodenum. Despite its nomencla-ture with emphasis on ductal characteristics (hence named ductal adenocarcino-ma), the origin of PDAC remains controversial. Nowadays, in light of accumu-lating evidence, acinar cells are considered more likely to be the cell-of-origin for PDAC [65–67].

The mechanism through which acinar cells give rise to PDAC relies on their ability to de-differentiate into duct-like cells under inflammatory stress and onco-genic hits [68]. This transdifferentiation process is called acinar-to-ductal meta-plasia (ADM) and is also a common, reversible phenomenon in the regeneration of the pancreas after (inflammatory) injury [68]. Prior studies have demonstrated that the premalignant lesions that harbor oncogenic mutations in genes such as proto-oncogene KRAS or tumor-suppressor TP53 can lead to the formation of PDAC [69]. Of note, such oncogenic mutations in acinar cells (particularly the activating KRAS mutation), aberrant growth factor signaling, and/or enhanced inflammatory states and tissue stress render ADM irreversible. This gives rise to pancreatic intraepithelial neoplasia (PanIN) [65]. Accumulation of additional on-cogenic mutations eventually leads to the progression of PanIN to PDAC **(Fig. 2)** [70]. More evidence is accumulating, showing that KRAS mutations are the main drivers of PanIN formation, further contributing to PDAC development [71–73]. In addition to its oncogenic effect, KRAS activation cooperates with the inflam-matory milieu, making cells more susceptible to malignant transformation [72].
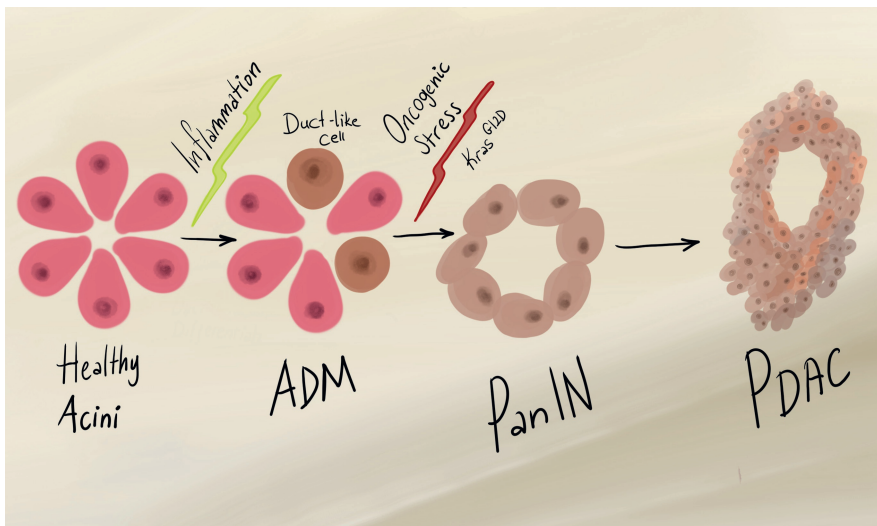
Figure 2

Schematic representation of ADM and progression towards PDAC. Severe stress conditions such as inflammation (pancreatitis) can initiate transdifferentiation of acinar cells into duct-like cells through a process called acinar-to-ductal metaplasia (ADM). This process is reversible and involved in tissue regeneration, where these cells proliferate to restore the injured tissue. However, the presence of oncogenic stress can render ADM irreversible, leading to the onset of low-grade neoplasia called pancreatic intraepithelial neoplasia (PanIN). PanIN lesions have cancerous potential and these lesions can progress into pancreatic ductal adenocarcinoma (PDAC).

Patients with chronic pancreatitis have a higher risk of developing PDAC, and increased macrophage infiltration in the pancreas is one of the hallmarks of acute and chronic pancreatitis. In the inflammatory stage, damaged acinar cells release digestive enzymes and pro-inflammatory cytokines that attract macrophages to the tissue. In this acute inflammatory milieu, acinar cells can undergo cell death or ADM [74]. Infiltrated immune cells such as macrophages clear damaged cells and cell debris but can also further stimulate an immune response by recruiting T-cells and neutrophils, which can ultimately exacerbate the inflammation[75,76]. A failure to overcome the inflammatory response prevents tissue renewal and leads to chronic pancreatitis [77]. Inflammatory macrophages drive ADM via the secretion of inflammatory cytokines such as IL-6, TNF, and CCL5(RANTES)

[78]. TNF and CCL5 secretion can also activate the NF-κB pathway in acinar cells, increasing extracellular matrix degradation and further accelerating inflammation and ADM [68,79].

Protease Activated Receptor-1 (PAR1)

Protease-activated receptors (PARs) are a family of G protein-coupled receptors (GPCRs) that mediate intracellular reactions to extracellular proteases. As the name suggests, PAR activation is dependent on proteolytic cleavage, whereas other GPCRs are dependent on ligand binding. The proteolytic cleavage of the N-terminal arm of PARs leads to a conformational change and releases the tethered ligand that interacts with the body of the receptor to initiate intracellular responses via G-proteins [80–82]. PAR1 is the quintessential member of the PAR family, which was initially reported to be activated by thrombin and PAR1 was initially named Thrombin (F2) Receptor [80]. Currently, various proteases are known to activate PAR1, such as activated protein C (APC), plasmin, coagulation factor Xa and VIIa, granzyme A and B, kallikrein 4, matrix metalloprotease (MMP)-1, -2, -9, and -13 (brief representation in **Figure 3** and in-depth review in reference [83]).
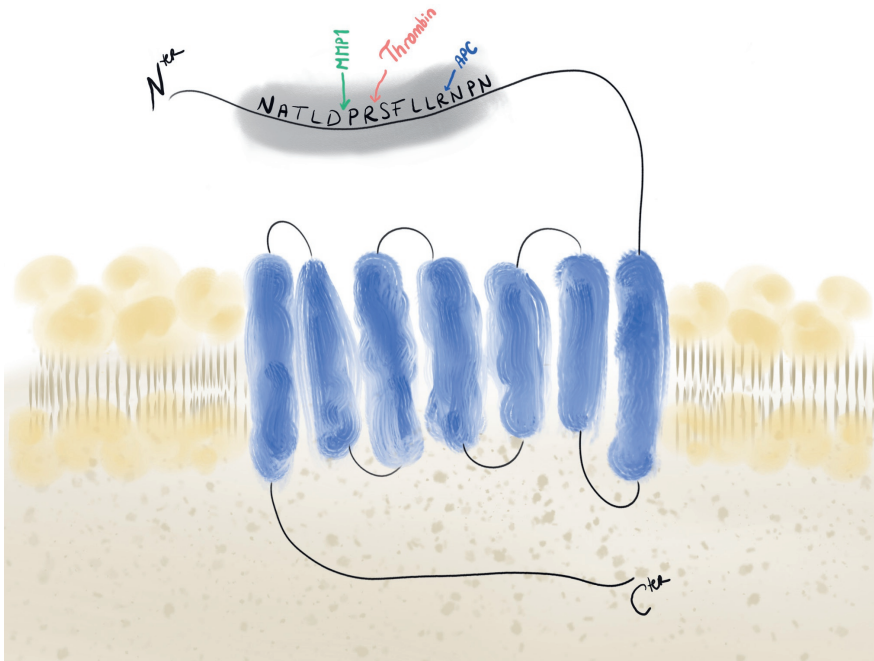
Figure 3

Schematic representation of PAR1 with the tethered ligand on the N-terminal arm and proteolytic cleavage sites. Cleavage of the N-terminal arm of PAR1 can be executed through different proteases, such as Thrombin, MMP1 and Activated Protein-C (APC). Different proteases have distinct cleavage sites on the N-terminal arm, each resulting in a different tethered ligand and a distinct cellular response.

Elevated levels of PAR1 are common in many solid tumor types, such as breast, lung, gallbladder, and prostate [84–87]. High PAR1 activity is associated with increased malignant progression and poor prognosis [84,88,89], cancer cell invasion, and metastasis [90,91]. In vivo studies have shown that PAR1 activity is tumor-promoting in lung cancer [85], and in a breast cancer model, PAR1 was shown to be indispensable for tumor growth [84]. Consistent with tumor-promoting activities of PAR1, pharmacological inhibition studies in preclinical setups have been promising. Indeed, PAR1 antagonist treatment significantly reduced tumor growth in breast, lung, and ovarian cancers [85,92,93]. In PDAC, high PAR1 expression is present in primary tumors and metastatic lesions; furthermore, PAR1 ablation in the host compartment limits tumor growth and re-establishes gemcitabine sensitivity in murine orthotopic tumor models [88].

Mechanistically, PAR1 activation is essential for the secretion of monocyte chemoattracting protein-1 (MCP-1, also known as CCL2), one of the critical cytokines that regulate monocyte/macrophage infiltration [94]. As mentioned above, increased macrophage influx in the tumor microenvironment is of the hallmarks of poor prognosis. In PDAC, it has been reported that PAR1 deficient mice had three-fold lower macrophage density in the tumor microenvironment and overall had decreased tumor size and improved response to gemcitabine therapy [88]. Interestingly, in the same study, it has been reported that PAR1 deficient mice had three-fold lower macrophage density in the tumor microenvironment and overall had decreased tumor size and improved response to gemcitabine therapy [88]. Altogether, these findings suggest that PAR1 acts as a gateway in the macrophage-tumor cell crosstalk in PDAC and is involved in PDAC progression. However, the exact mechanisms that govern these contributions remain to be fully elucidated.

Aim and Outline of this thesis

This thesis aims to elucidate the involvement of PAR1 in PDAC progression with particular emphasis on the tumor cell-PAR1-macrophage crosstalk. In Chapter 2 of this thesis, we explore the role of PAR1 in mesenchymal differentiation by using orthotopic tumor inoculation in parallel with shRNA-mediated PAR1 knockdown in human pancreatic cancer cell lines. Chapter 3 addresses the PAR1-macrophage-tumor cell crosstalk and its contributions to tumor progression. In this chapter, macrophage secreted proteases are assessed to identify a principal PAR1 activator. Also, in this chapter, the anti-tumorigenic properties of macrophages are investigated in the initial stages of tumorigenesis (i.e., the anti-tumor effects of naïve macrophages). In Chapter 4, the mechanisms that drive anti-tumorigenic activities of macrophages are explained in detail by using macrophage models based on peripheral blood-derived monocyte and monocyte cell cultures. Chapter 5 explains how acinar cells are transdifferentiated into ductal cells in a PAR1-dependent manner. We explore the mechanism ofPAR1 dependency on ductal cell fate and on the differentiation of acinar cells using cell lines, murine organoids, and ex vivo models. In Chapter 6, we discuss the involvement of PAR1 in various cancers and their effect on tumor growth. This commentary review provides a summary of PAR1 driven effects and observed discrepancies. Finally, in Chapter 7, we summarize and discuss all our data on PAR1 in early tumor formation, differentiation, and tumor growth.

REFERENCES

[1]   Ducreux M, Cuhna AS, Caramella C, Hollebecque A, Burtin P, Goéré D, et al. Cancer of the pancreas: ESMO Clinical Practice Guidelines for diagnosis, treatment and follow-up. Ann Oncol. 2015;26:v56–68.

[2]   Ryan DP, Hong TS, Bardeesy N. Pancreatic Adenocarcinoma. N Engl J Med. 2014;371:1039–49.

[3]   Siegel RL, Miller KD, Jemal A. Cancer statistics, 2020. CA Cancer J Clin. 2020;70:7–30.

[4]   Kamisawa T, Wood LD, Itoi T, Takaori K. Pancreatic cancer. Lancet. 2016;388:73–85.

[5]   Bray F, Ferlay J, Soerjomataram I, Siegel RL, Torre LA, Jemal A. Global cancer statistics 2018: GLOBOCAN estimates of incidence and mortality world-wide for 36 cancers in 185 countries. CA Cancer J Clin. 2018;68:394–424.

[6]   Raimondi S, Lowenfels AB, Morselli-Labate AM, Maisonneuve P, Pez-zilli R. Pancreatic cancer in chronic pancreatitis; Aetiology, incidence, and early detection. Best Pract Res Clin Gastroenterol. 2010;

[7]   Rawla P, Sunkara T, Gaduputi V. Epidemiology of Pancreatic Cancer: Global Trends, Etiology and Risk Factors. World J Oncol. 2019;10:10–27.

[8]   Yeo TP. Demographics, epidemiology, and inheritance of pancreatic duc-tal adenocarcinoma. Seminars in Oncology. 2015.

[9]   Okasha H, Elkholy S, El-Sayed R, Wifi M-N, El-Nady M, El-Nabawi W, et al. Real time endoscopic ultrasound elastography and strain ratio in the diag-nosis of solid pancreatic lesions. World J Gastroenterol. 2017;23:5962.

[10]   Millikan KW, Deziel DJ, Silverstein JC, Kanjo TM, Christein JD, Doo-las A, et al. Prognostic factors associated with resectable adenocarcinoma of the head of the pancreas. Am Surg. 1999;65:618–23; discussion 623-4.

[11]   Vincent A, Herman J, Schulick R, Hruban RH, Goggins M. Pancreatic cancer. Lancet. 2011;378:607–20.

[12]   Neoptolemos J, Dunn J, Stocken D, Almond J, Link K, Beger H, et al. Adjuvant chemoradiotherapy and chemotherapy in resectable pancreatic cancer: a randomised controlled trial. Lancet. 2001;358:1576–85.

[13]   Conroy T, Hammel P, Hebbar M, Ben Abdelghani M, Wei AC, Raoul J-L, et al. FOLFIRINOX or Gemcitabine as Adjuvant Therapy for Pancreatic Cancer. N Engl J Med. 2018;379:2395–406.

[14]   Versteijne E, Suker M, Groothuis K, Akkermans-Vogelaar JM, Besselink MG, Bonsing BA, et al. Preoperative Chemoradiotherapy Versus Immediate Sur-gery for Resectable and Borderline Resectable Pancreatic Cancer: Results of the Dutch Randomized Phase III PREOPANC Trial. J Clin Oncol. 2020;38:1763–73.

[15]   Mizrahi JD, Surana R, Valle JW, Shroff RT. Pancreatic cancer. Lancet. 2020;395:2008–20.

[16]   Burris HA, Moore MJ, Andersen J, Green MR, Rothenberg ML, Modia-

no MR, et al. Improvements in survival and clinical benefit with gemcitabine as first-line therapy for patients with advanced pancreas cancer: a randomized trial. J Clin Oncol. 1997;15:2403–13.

[17]   Conroy T, Desseigne F, Ychou M, Bouché O, Guimbaud R, Bécouarn Y, et al. FOLFIRINOX versus gemcitabine for metastatic pancreatic cancer. N Engl J Med. 2011;364:1817–25.

[18]   Von Hoff DD, Ervin T, Arena FP, Chiorean EG, Infante J, Moore M, et al. Increased Survival in Pancreatic Cancer with nab-Paclitaxel plus Gemcitabine. N Engl J Med. 2013;369:1691–703.

[19]   Chan KKW, Guo H, Cheng S, Beca JM, Redmond-Misner R, Isaranu-watchai W, et al. Real-world outcomes of FOLFIRINOX vs gemcitabine and nab-paclitaxel in advanced pancreatic cancer: A population-based propensity score-weighted analysis. Cancer Med. 2020;

[20]   Wang Y, Camateros P, Cheung WY. A Real-World Comparison of FOL-FIRINOX, Gemcitabine Plus nab-Paclitaxel, and Gemcitabine in Advanced Pancreatic Cancers. J Gastrointest Cancer. 2019;50:62–8.

[21]   Jia Y, Xie J. Promising molecular mechanisms responsible for gemcit-abine resistance in cancer. Genes Dis. 2015;2:299–306.

[22]   Zeng, Pöttler, Lan, Grützmann, Pilarsky, Yang, et al. Chemoresistance in Pancreatic Cancer. Int J Mol Sci. 2019;20:4504.

[23]   Kalluri R, Neilson EG. Epithelial-mesenchymal transition and its impli-cations for fibrosis. Vol. 112, Journal of Clinical Investigation. 2003. p. 1776–84.

[24]   Kalluri R, Weinberg RA. The basics of epithelial-mesenchymal transi-tion. J Clin Invest. 2009;119:1420–8.

[25]   Thiery JP, Acloque H, Huang RYJJ, Nieto MA. Epithelial-Mesenchymal Transitions in Development and Disease. Cell. 2009;139:871–90.

[26]   Nieto MA, Huang RYYJ, Jackson RAA, Thiery JPP. Emt: 2016. Cell. 2016;166:21–45.

[27]   Barrallo-Gimeno A, Nieto MA. The Snail genes as inducers of cell move-ment and survival: Implications in development and cancer. Development. 2005.

[28]   Dijk F, Veenstra VL, Soer EC, Dings MPG, Zhao L, Halfwerk JB, et al. Unsupervised class discovery in pancreatic ductal adenocarcinoma reveals cell-intrinsic mesenchymal features and high concordance between existing clas-sification systems. Sci Rep. 2020;10:1–12.

[29]   Brenot A, Knolhoff BL, DeNardo DG, Longmore GD. SNAIL1 action in tumor cells influences macrophage polarization and metastasis in breast cancer through altered GM-CSF secretion. Oncogenesis. 2018;7:32.

[30]   Cortés M, Sanchez-Moral L, de Barrios O, Fernández-Aceñero MJ, Martínez-Campanario M, Esteve-Codina A, et al. Tumor-associated macro-phages (TAMs) depend on ZEB1 for their cancer-promoting roles. EMBO J. 2017;36:3336–55.

[31]   Singh S, Chakrabarti R. Consequences of EMT-Driven Changes in the

Immune Microenvironment of Breast Cancer and Therapeutic Response of Cancer Cells. J Clin Med. 2019;8:642.

[32]   Hanahan D, Coussens LM. Accessories to the Crime: Functions of Cells Recruited to the Tumor Microenvironment. Cancer Cell. 2012;21:309–22.

[33]   Wörmann SM, Diakopoulos KN, Lesina M, Algül H. The immune network in pancreatic cancer development and progression. Oncogene. 2014;33:2956–67.

[34]   Gordon S, Taylor PR. Monocyte and macrophage heterogeneity. Vol. 5, Nature Reviews Immunology. 2005. p. 953–64.

[35]   Porta C, Riboldi E, Totaro MG, Strauss L, Sica A, Mantovani A. Macrophages in cancer and infectious diseases: the 'good' and the 'bad.' Immunotherapy. 2011;3:1185–202.

[36]   Mills CD, Kincaid K, Alt JM, Heilman MJ, Hill AM. M-1/M-2 Macrophages and the Th1/Th2 Paradigm. J Immunol. 2000;164:6166–73.

[37]   Mosser DM, Edwards JP. Exploring the full spectrum of macrophage activation. Nat Rev Immunol. 2008;8:958–69.

[38]   Sica A, Mantovani A. Macrophage plasticity and polarization: in vivo veritas. J Clin Invest. 2012;122:787–95.

[39]   Mantovani A, Sozzani S, Locati M, Allavena P, Sica A. Macrophage polarization: tumor-associated macrophages as a paradigm for polarized M2 mononuclear phagocytes. Trends Immunol. 2002;23:549–55.

[40]   Jadus MR, Irwin MRC, Horansky RD, Sekhon S, Pepper KA, Kohn DB, et al. Macrophages can recognize and kill tumor cells bearing the membrane isoform of macrophage colony-stimulating factor. Blood. 1996;87:5232–41.

[41]   Goswami KK, Ghosh T, Ghosh S, Sarkar M, Bose A, Baral R. Tumor promoting role of anti-tumor macrophages in tumor microenvironment. Cell Immunol. 2017;316:1–10.

[42]   Noy R, Pollard JW. Tumor-Associated Macrophages: From Mechanisms to Therapy. Immunity. 2014;41:49–61.

[43]   Jung KY, Cho SW, Kim YA, Kim D, Oh B-C, Park DJ, et al. Cancers with Higher Density of Tumor-Associated Macrophages Were Associated with Poor Survival Rates. J Pathol Transl Med. 2015;49:318–24.

[44]   Lindsten T, Hedbrant A, Ramberg A, Wijkander J, Solterbeck A, Eriksson M, et al. Effect of macrophages on breast cancer cell proliferation, and on expression of hormone receptors, uPAR and HER-2. Int J Oncol. 2017;51:104–14.

[45]   Zhang Q wen, Liu L, Gong C yang, Shi H shan, Zeng Y hui, Wang X ze, et al. Prognostic Significance of Tumor-Associated Macrophages in Solid Tumor: A Meta-Analysis of the Literature. Hoque MO, editor. PLoS One. 2012;7:e50946.

[46]   Lahmar Q, Keirsse J, Laoui D, Movahedi K, Van Overmeire E, Van Ginderachter JA. Tissue-resident versus monocyte-derived macrophages in the tumor microenvironment. Biochim Biophys Acta - Rev Cancer. 2016;1865:23–34.

[47]   Helm O, Held-Feindt J, Grage-Griebenow E, Reiling N, Ungefroren H, Vogel I, et al. Tumor-associated macrophages exhibit pro- and anti-inflammato-

ry properties by which they impact on pancreatic tumorigenesis. Int J Cancer. 2014;135:843–61.

[48]   Tian C, Clauser KR, Öhlund D, Rickelt S, Huang Y, Gupta M, et al. Proteomic analyses of ECM during pancreatic ductal adenocarcinoma progression reveal different contributions by tumor and stromal cells. Proc Natl Acad Sci. 2019;116:19609–18.

[49]   Mahadevan D, Von Hoff DD. Tumor-stroma interactions in pancreatic ductal adenocarcinoma. Mol Cancer Ther. 2007;6:1186–97.

[50]   Tape CJ, Ling S, Dimitriadi M, McMahon KM, Worboys JD, Leong HS, et al. Oncogenic KRAS Regulates Tumor Cell Signaling via Stromal Reciprocation. Cell. 2016;165:910–20.

[51]   Apte M, Pirola RC, Wilson JS. Pancreatic stellate cell. Curr Opin Gastroenterol. 2015;31:416–23.

[52]   Vennin C, Murphy KJ, Morton JP, Cox TR, Pajic M, Timpson P. Reshaping the Tumor Stroma for Treatment of Pancreatic Cancer. Gastroenterology. 2018;154:820–38.

[53]   Neesse A, Algül H, Tuveson DA, Gress TM. Stromal biology and therapy in pancreatic cancer: a changing paradigm. Gut. 2015;64:1476–84.

[54]   Pereira BA, Vennin C, Papanicolaou M, Chambers CR, Herrmann D, Morton JP, et al. CAF Subpopulations: A New Reservoir of Stromal Targets in Pancreatic Cancer. Trends in Cancer. 2019;5:724–41.

[55]   Olive KP, Jacobetz MA, Davidson CJ, Gopinathan A, McIntyre D, Honess D, et al. Inhibition of Hedgehog Signaling Enhances Delivery of Chemotherapy in a Mouse Model of Pancreatic Cancer. Science (80-). 2009;324:1457–61.

[56]   Provenzano PP, Cuevas C, Chang AE, Goel VK, Von Hoff DD, Hingorani SR. Enzymatic Targeting of the Stroma Ablates Physical Barriers to Treatment of Pancreatic Ductal Adenocarcinoma. Cancer Cell. 2012;

[57]   Jacobetz MA, Chan DS, Neesse A, Bapiro TE, Cook N, Frese KK, et al. Hyaluronan impairs vascular function and drug delivery in a mouse model of pancreatic cancer. Gut. 2013;62:112–20.

[58]   Gore J, Korc M. Pancreatic Cancer Stroma: Friend or Foe? Cancer Cell. 2014;25:711–2.

[59]   Van Mackelenbergh MG, Stroes CI, Spijker R, Van Eijck CHJ, Wilmink JW, Bijlsma MF, et al. Clinical trials targeting the stroma in pancreatic cancer: A systematic review and meta-analysis. Cancers (Basel). 2019;11:1–23.

[60]   Rhim AD, Oberstein PE, Thomas DH, Mirek ET, Palermo CF, Sastra SA, et al. Stromal elements act to restrain, rather than support, pancreatic ductal adenocarcinoma. Cancer Cell. 2014;25:735–47.

[61]   Özdemir BC, Pentcheva-Hoang T, Carstens JL, Zheng X, Wu CC, Simpson TR, et al. Depletion of carcinoma-associated fibroblasts and fibrosis induces immunosuppression and accelerates pancreas cancer with reduced survival. Cancer Cell. 2014;25:719–34.

[62]   Catenacci DVT, Junttila MR, Karrison T, Bahary N, Horiba MN, Nattam SR, et al. Randomized Phase Ib/II Study of Gemcitabine Plus Placebo or Vismodegib, a Hedgehog Pathway Inhibitor, in Patients With Metastatic Pancreatic Cancer. J Clin Oncol. 2015;33:4284–92.

[63]   Kim EJ, Sahai V, Abel E V., Griffith KA, Greenson JK, Takebe N, et al. Pilot Clinical Trial of Hedgehog Pathway Inhibitor GDC-0449 (Vismodegib) in Combination with Gemcitabine in Patients with Metastatic Pancreatic Adenocarcinoma. Clin Cancer Res. 2014;20:5937–45.

[64]   Ko AH, LoConte N, Tempero MA, Walker EJ, Kate Kelley R, Lewis S, et al. A Phase I Study of FOLFIRINOX Plus IPI-926, a Hedgehog Pathway Inhibitor, for Advanced Pancreatic Adenocarcinoma. Pancreas. 2016;45:370–5.

[65]   Kopp JL, von Figura G, Mayes E, Liu F-F, Dubois CL, Morris JP, et al. Identification of Sox9-Dependent Acinar-to-Ductal Reprogramming as the Principal Mechanism for Initiation of Pancreatic Ductal Adenocarcinoma. Cancer Cell. 2012;22:737–50.

[66]   Wei D, Wang L, Yan Y, Jia Z, Gagea M, Li Z, et al. KLF4 Is Essential for Induction of Cellular Identity Change and Acinar-to-Ductal Reprogramming during Early Pancreatic Carcinogenesis. Cancer Cell. 2016;29:324–38.

[67]   Wang L, Xie D, Wei D. Pancreatic Acinar-to-Ductal Metaplasia and Pancreatic Cancer. In: Methods in Molecular Biology. 2019. p. 299–308.

[68]   Storz P. Acinar cell plasticity and development of pancreatic ductal adenocarcinoma. Nat Rev Gastroenterol Hepatol. 2017;14:296–304.

[69]   Hezel AF. Genetics and biology of pancreatic ductal adenocarcinoma. Genes Dev. 2006;20:1218–49.

[70]   Feldmann G, Beaty R, Hruban RH, Maitra A. Molecular genetics of pancreatic intraepithelial neoplasia. J Hepatobiliary Pancreat Surg. 2007;14:224–32.

[71]   Morris JP, Wang SC, Hebrok M. KRAS, Hedgehog, Wnt and the twisted developmental biology of pancreatic ductal adenocarcinoma. Nat Rev Cancer. 2010;10:683–95.

[72]   Gruber R, Panayiotou R, Nye E, Spencer-Dene B, Stamp G, Behrens A. YAP1 and TAZ Control Pancreatic Cancer Initiation in Mice by Direct Up-regulation of JAK–STAT3 Signaling. Gastroenterology. 2016;151:526–39.

[73]   Collins MA, Brisset J-C, Zhang Y, Bednar F, Pierre J, Heist KA, et al. Metastatic Pancreatic Cancer Is Dependent on Oncogenic Kras in Mice. Algül H, editor. PLoS One. 2012;7:e49707.

[74]   Liou G-Y, Storz P. Inflammatory macrophages in pancreatic acinar cell metaplasia and initiation of pancreatic cancer. Oncoscience. 2015;2:247–51.

[75]   Mikami Y, Takeda K, Shibuya K, Qiu-Feng H, Egawa S, Sunamura M, et al. Peritoneal inflammatory cells in acute pancreatitis: Relationship of infiltration dynamics and cytokine production with severity of illness. Surgery. 2002;132:86–92.

[76]   Gea-Sorlí S. Role of macrophages in the progression of acute pancreati-

tis. World J Gastrointest Pharmacol Ther. 2010;1:107.

[77]   Greer JB, Whitcomb DC. Inflammation and pancreatic cancer: an evidence-based review. Curr Opin Pharmacol. 2009;9:411–8.

[78]   Liou GY, Döppler H, Necela B, Krishna M, Crawford HC, Raimondo M, et al. Macrophage-secreted cytokines drive pancreatic acinar-to-ductal metaplasia through NF-KB and MMPs. J Cell Biol. 2013;202:563–77.

[79]   Liou G-Y, Döppler H, Necela B, Edenfield B, Zhang L, Dawson DW, et al. Mutant KRAS–Induced Expression of ICAM-1 in Pancreatic Acinar Cells Causes Attraction of Macrophages to Expedite the Formation of Precancerous Lesions. Cancer Discov. 2015;5:52–63.

[80]   Vu TKH, Hung DT, Wheaton VI, Coughlin SR. Molecular cloning of a functional thrombin receptor reveals a novel proteolytic mechanism of receptor activation. Cell. 1991;64:1057–68.

[81]   Coughlin SR, Vu TK, Hung DT, Wheaton VI. Characterization of a functional thrombin receptor. Issues and opportunities. J Clin Invest. 1992;89:351–5.

[82]   Zhang C, Srinivasan Y, Arlow DH, Fung JJ, Palmer D, Zheng Y, et al. High-resolution crystal structure of human protease-activated receptor 1. Nature. 2012;492:387–92.

[83]   Flaumenhaft R, De Ceunynck K. Targeting PAR1: Now What? Trends Pharmacol Sci. 2017;38:701–16.

[84]   Boire A, Covic L, Agarwal A, Jacques S, Sherifi S, Kuliopulos A. PAR1 is a matrix metalloprotease-1 receptor that promotes invasion and tumorigenesis of breast cancer cells. Cell. 2005;120:303–13.

[85]   Cisowski J, O'Callaghan K, Kuliopulos A, Yang J, Nguyen N, Deng Q, et al. Targeting protease-activated receptor-1 with cell-penetrating pepducins in lung cancer. Am J Pathol. 2011;179:513–23.

[86]   Grisaru-Granovsky S, Salah Z, Maoz M, Pruss D, Beller U, Bar-Shavit R. Differential expression of protease activated receptor 1 (Par1) and pY397FAK in benign and malignant human ovarian tissue samples. Int J Cancer. 2005;113:372–8.

[87]   Zhu L, Wang X, Wu J, Mao D, Xu Z, He Z, et al. Cooperation of protease-activated receptor 1 and integrin alphanubeta5 in thrombin-mediated lung cancer cell invasion. Oncol Rep. 2012;28:553–60.

[88]   Queiroz KCS, Shi K, Duitman J, Aberson HL, Wilmink JW, Van Noesel CJM, et al. Protease-activated receptor-1 drives pancreatic cancer progression and chemoresistance. Int J Cancer. 2014;135:2294–304.

[89]   Even-Ram S, Uziely B, Cohen P, Grisaru-Granovsky S, Maoz M, Ginzburg Y, et al. Thrombin receptor overexpression in malignant and physiological invasion processes. Nat Med. 1998;4:909–14.

[90]   Yang E, Cisowski J, Nguyen N, O'Callaghan K, Xu J, Agarwal A, et al. Dysregulated protease activated receptor 1 (PAR1) promotes metastatic phenotype in breast cancer through HMGA2. Oncogene. 2016;35:1529–40.

[91]   Shi X, Gangadharan B, Brass LF, Ruf W, Mueller BM. Protease-activated receptors (PAR1 and PAR2) contribute to tumor cell motility and metastasis. Mol Cancer Res. 2004;2:395–402.

[92]   Yang E, Boire A, Agarwal A, Nguyen N, O'Callaghan K, Tu P, et al. Blockade of PAR1 Signaling with Cell-Penetrating Pepducins Inhibits Akt Survival Pathways in Breast Cancer Cells and Suppresses Tumor Survival and Metastasis. Cancer Res. 2009;69:6223–31.

[93]   Agarwal A, Covic L, Sevigny LM, Kaneider NC, Lazarides K, Azabdaftari G, et al. Targeting a metalloprotease-PAR1 signaling system with cell-penetrating pepducins inhibits angiogenesis, ascites, and progression of ovarian cancer. Mol Cancer Ther. 2008;7:2746–57.

[94]   Chen D, Carpenter A, Abrahams J, Chambers RC, Lechler RI, McVey JH, et al. Protease-activated receptor 1 activation is necessary for monocyte chemoattractant protein 1-dependent leukocyte recruitment in vivo. J Exp Med. 2008;205:1739–46.

1

Chapter 2

PAR1 signalling on tumor cells limits tumor growth by
maintaining a mesenchymal phenotype
in pancreatic cancer

Cansu Tekin, Kun Shi, Joost B. Daalhuisen, Marieke S. ten Brink,
Maarten F Bijlsma, C Arnold Spek

ABSTRACT

Protease activated receptor-1 (PAR1) expression is associated with disease progression and overall survival in a variety of cancers. However, the importance of tumor cell PAR1 in pancreatic ductal adenocarcinomas (PDAC) remains unexplored. Utilizing orthotopic models with wild type and PAR1-targeted PDAC cells, we show that tumor cell PAR1 negatively affects PDAC growth, yet promotes metastasis. Mechanistically, we show that tumor cell-specific PAR1 expression correlates with mesenchymal signatures in PDAC and that PAR1 is linked to the maintenance of a partial mesenchymal cell state. Indeed, loss of PAR1 expression results in well-differentiated pancreatic tumors in vivo, with enhanced epithelial characteristics both in vitro and in vivo. Taken together, we have identified a novel growth inhibitory role of PAR1 in PDAC, which is linked to the induction, and maintenance of a mesenchymal-like phenotype. The recognition that PAR1 actively limits pancreatic cancer cell growth suggest that the contributions of PAR1 to tumor growth differ between cancers of epithelial origin and that its targeting should be applied with care.

INTRODUCTION

Pancreatic ductal adenocarcinoma (PDAC) is a highly aggressive disease with an extremely low survival rate (5-year survival ~7.7%) [1,2]. This high mortality rate is largely due to late diagnosis with the vast majority of patients presenting with locally advanced or metastatic disease, and only around 20% of the patients are eligible for surgical resection. Progress in improving survival has been slow, and current treatment options are severely inadequate. The only noteworthy progress has been in lowering mortality rates for patients undergoing resections, and a small prolongation and improved quality of life in patients with unresectable disease by chemotherapeutic agents [3]. Novel combination therapies, like for instance FOLFIRINOX [4] or gemcitabine with Nab-paclitaxel [5], are superior over single-drug regimens but even in the specific group of patients eligible for treatment the survival benefit is limited.

A key factor responsible for the poor prognosis in PDAC is a high propensity for epithelial-to-mesenchymal transition (EMT) of pancreatic cancer cells [6]. EMT, a biological process where epithelial cells morphologically and phenotypically transition into mesenchymal cells [7], is associated with invasion and metastasis in various cancers [8–10]. Loss of epithelial characteristics, as revealed by a loss of E-cadherin expression in a Snail and/or zinc finger E-box-binding homeobox 1 (ZEB1) dependent manner [11,12], correlates with poor prognosis and poor therapeutic outcome [13,14]. Importantly, suppression of EMT enhances therapeutic efficacy and survival in a murine pancreatic cancer model [15].

Protease activated receptor 1 (PAR1), also known as the thrombin (F2) receptor, is a seven-transmembrane G-coupled receptor. As implied by its name, PAR1 is activated by proteolytic cleavage of a N-terminal extracellular region by proteases such as thrombin, activated protein C and matrix metalloproteases [16]. Interestingly, PAR1 expression is increased in breast, lung, ovarian, and prostate cancer [17–20] and PAR1 expression correlates with poor prognosis in breast [21] and lung cancer [22]. In line with these clinical data pointing to a tumor-promoting effect of PAR-1, experimental studies underscore the tumor-promoting actions of activated PAR1. For instance, PAR1 expression is shown to be required and sufficient for tumor growth in a breast carcinoma xenograft model

2

[17]. Moreover, pharmacological PAR1 inhibition inhibited lung tumor growth in nude mice [18]; PAR1 silencing decreased tumor growth and metastasis to the lung in a murine melanoma model [23]; and PAR1 inhibition in giant cell tumor of bone restrained tumor growth in vivo [24]. In the setting of pancreatic cancer, we recently showed that genetic ablation of PAR1 in the pancreatic stroma impeded tumor growth and metastasis [25] suggesting that PAR1 expression contributes to poor prognosis in pancreatic cancer.

In this manuscript, we addressed the hypothesis that PAR1 could be a prognostic marker for PDAC. However, we find that the survival of PDAC patients is not associated with PAR1 expression in bulk tumor tissue. We explain this by the observation that tumor cell-specific PAR1 expression is linked to the maintenance of a mesenchymal-like cell state. In an orthotopic pancreatic cancer model, the loss of tumor cell PAR1 induces well-differentiated tumors with increased epithelial characteristics, and enhanced tumor growth. We thus conclude that tumor cell PAR1 actively limits the growth of PDAC likely by playing a role in the induction and maintenance of a partial mesenchymal phenotype in PDAC.

MATERIALS AND METHODS

Animals
C57BL/6 mice (Charles River Laboratories) were housed at the animal facility of the Academic Medical Center of Amsterdam. All mice had access to food and water ad libitum. Institutional Animal Care and Use Committee of Academic Medical Center approved all animal experiments according to protocol number DIX102373 and DIX107AA.

Orthotopic pancreatic cancer model
Cultures of Panc02 (kindly provided by Dr. Schmitz, Universitatsklinikum Bonn, Bonn, Germany) and KP cells (derived from pancreatic adenocarcinomas from p48-CRE/LSL-KRAS/P53flox/flox KPC mice, kindly provided by Dr. DeNardo, Washington University Medical School, St. Louis, MO) were trypsinized at 80% confluency, pelleted, washed twice in phosphate buffered saline (PBS) and re-suspended in 0.9% sterile saline (Sigma, St Louis, MO). During tumor inoculation mice were given with Tamgesic (0.05mg/kg) and anaesthetized with isoflurane (2% in CO2). Tumor cells ($4x10^5$ cells per animal) were injected directly into the tail of the pancreas of 8- to 10-week-old mice essentially described as before [25]. Mice were evaluated for changes in body weight and signs of discomfort or morbidity, and they were euthanized 4 weeks after tumor cell injection. Whole pancreata were removed and weighed, followed by fixation in 4% formalin and embedding in paraffin for further analysis.

Cell culturing
Murine KP and Panc02 cells and human PANC-1, Capan-2, and MIA PaCa-2 cells (ATCC, Manassas, VA) were cultured in high glucose (4.5g/mL) DMEM, 10% fetal bovine serum (FBS), L-glutamine (2mM), penicillin (100 units/mL), and streptomycin (500 μg/mL) (Lonza, Basel, Switzerland) according to routine cell culture procedures. Cells were incubated in 5% CO2 incubators at 37oC. Human cell lines were authenticated by STR profiling (Promega PowerPlex) and tested for mycoplasma by PCR monthly.

Lentiviral silencing of PAR1

PAR-1 knock down cells were established as described before [25]. Briefly, PAR-1 (clone TRCN0000026806 for murine cells and clone TRCN0000003690 for human cells) and control (clone SHC004) shRNA in the pLKO.1-puro backbone were purchased from the MISSION shRNA library (Sigma-Aldrich, St. Louis, MO). Lentivirus was produced by transfecting HEK293T cells with 3rd generation transfer and packaging plasmids pVSV, pMDL, and pRES using Lipofectamine 2000 (ThermoFisher Scientific, Waltham, MA). 48 and 72 hours after transfection, supernatant was harvested and 0.45 μm filtered (Millipore, Billerica, MA, USA). 75% confluent PANC-1, MIA PaCa-2 and Capan-2 cells were transduced with 20 μl lentivirus and incubated for 24h. Transduced cells were selected with 2 μg/ml puromycin (Sigma, St.Louis, MO) for 72h.

PAR1 overexpression

PANC-1 cells were transfected using Lipofectamine 2000 according routine procedures (ThermoFisher Scientific, Waltham, MA) with pcDNA3.1(+) plasmid containing PAR1-P2A-eGFP (Genscript, Piscataway, NJ) and pcDNA3.1(+) coding for eGFP as control (Addgene, Cambridge, MA). 48 hours after transfection, GFP-positive and GFP-negative single cells were sorted using a Sony Cell Sorter SH800S (Sony Biotechnology, San Jose, CA). Cells were sorted directly into RNA lysis buffer of the RNeasy Mini Isolation Kit (Qiagen, Hilden, Germany) after which RNA was isolated following manufacturer's instructions.

Flow Cytometry

Cells were harvested with 5 mM EDTA and washed with FACS buffer (1% FBS/PBS). Cells were stained either with PAR1 (ATAP-2: sc-13503, Santa Cruz Biotechnology, Dallas, TX) or E-cadherin (24E10; Cell Signaling Technology, Danvers, MA) as primary antibodies and anti-mouse APC (550826; BD, Franklin Lakes, NJ) and anti-rabbit Alexa 488 (A-11008; Invitrogen, Carlsbad, CA) secondary antibodies with 1:400 dilution for each antibody. For PAR1 inhibition on PANC-1, MIA PaCa-2 and Capan-2 wildtype cells, 250 nM Vorapaxar (SCH530348, Adooq Biosciences, Irvine, CA) was added and cells were analyzed 48 hours later. In all assays, samples were prepared following the manufacturer's instructions, and analyzed on FACS Canto II (BD, Franklin Lakes, NJ). Data were analyzed using FLOWJO v10 (FlowJo LLC, Ashland, OR). Cells

were gates initially based on FCS and SSC for the main cell population and later FCS-H vs FCS-W for single cells. APC or FITC positive populations were gated on single cell population based on antibody control samples.

Quantitative Real-Time PCR

Total RNA was isolated with TriReagent (Sigma, St. Louis, MO) and chloroform separation with repeated ethanol washes. cDNA was synthesized from DNase treated total RNA by using M-MLV-RT enzyme (Promega, Leiden, Netherlands) with random hexamers (Qiagen, Hilden, Germany). Real-time quantitative RT-PCR was performed with Sensifast SYBR No-Rox Kit (Bioline, London, UK) on a lightcycler LC 480 II (Roche, Basel, Switzerland). Relative expression of genes was calculated using the comparative threshold cycle (dCt method) and were normalized for expression of reference gene TBP. Primer sequences of the analyzed genes are;

hTBP (fw 5'- ATCCCAAGCGGTTTGCTGC-3';
rv 5'-ACTGTTCTTCACTCTTGGCTC-3'),
hF2R(PAR1) (fw 5'-GCAGGCCAGAATCAAAAGCAACAAATGC-3';
rv 5'-TCCTCATCCTCCCAAAATGGTTCA-3'),
hCDH1 (fw 5'-TGGAGGAATTCTTGCTTTGC-3';
rv 5'-CGCTCTCCTCCGAAGAAAC-3'),
 hZEB1 (fw 5'-GCACAAGAAGAGCCACAAGTA-3';
rv 5'-GCAAGACAAGTTCAAGGGTTC-3'),
hVIM1 (fw 5'- AGTCCACTGAGTACCGGAGAC-3';
rv 5'- CATTTCACGCATCTGGCGTTC-3').

Western Blot

PANC-1 cells were seeded in 6-well plates in DMEM supplemented with 10% FCS. After 48 hours, cells were lysed in RIPA buffer and Western blots were performed as described before [49]. In brief, protein samples were boiled in Lae-mmli buffer with 3% beta-mercaptoethanol for 10 minutes at 95°C, separated by 10% SDS-PAGE and transferred to a PVDF membrane (Millipore, Billerica, MA). Membranes were blocked for 1 hour in 4% milk in TBS-T and incubated overnight with antibodies against a-tubulin (1:1000, Santa Cruz, CA) or E-cad-herin (1:1000, 24E10; Cell Signaling Technology, Danvers, MA) at 4°C. All sec-ondary antibodies were horseradish peroxidase (HRP)-conjugated from Dako

Cytomation (Glostrup, Denmark) and diluted according to the manufacturer's instructions. Blots were imaged using Lumilight Plus ECL substrate from Roche (Almere, The Netherlands) on a LAS 4000 imager from Fuji (FujiFilm, Tokyo, Japan).

Kaplan-Meier Survival Analysis
The following datasets were used: The Cancer Genome Atlas (TCGA)-PDAC [50], GSE17891 [51], GSE62452 [52], GSE15471 [53], GSE21501 [54]. Kaplan-Meier survival analysis was based on median PAR1 (F2R) expression. Kaplan-meier analysis and gene expression data were collected and processed for use in the AMC in-house R2: Genomics Analysis and Visualization Platform (http://r2.amc.nl). For visualization of gene expression, data were plotted in GraphPad Prism 7.0 (GraphPad Software Inc, La Jolla, CA, USA).

Gene Set Enrichment Analysis
Datasets used were the tumor expression datasets GSE28735 [55], GSE16515 [56], The Cancer Genome Atlas (TCGA)-PDAC [50], GSE62452 [52], GSE21501 [54], micro dissected tissue expression data: E-MEXP-1121 [57] and cell line expression data: GSE36133 [58]. GSEA software (Broad Institute, Cambridge, MA, USA) was downloaded from the Broad Institute website (http://www.broad.mit.edu/gsea/) and signature sets for cancer mesenchymal transition [59], and hallmark epithelial to mesenchymal transition (Broad Institute) were downloaded from the Molecular Signature Database (MSigDB). Expression datasets were compiled with annotated gene names (.gct), samples were segmented for median PAR1/F2R expression (i.e. high and low) as phenotype label files (.cls), and signature sets were assembled (.gmx). One thousand permutations were run on the phenotype. Datasets were not collapsed to gene symbols (collapse to gene symbols=false) in the GSEA software.

Immunohistochemistry
Histological examination was performed essentially as described before [25]. Briefly, the excised tumor was fixed in formalin, embedded in paraffin and 4-µm-thick slides were subsequently deparaffinized, rehydrated and washed in deionized water. Slides were stained with hematoxylin and eosin (H&E) according to routine procedures. For immunohistochemistry, endogenous peroxidase activity

was quenched with 0.3% hydrogen peroxide for 15 min at room temperature, with antigen retrieval for 10 min at 100°C in 10mM sodium citrate buffer, pH 7.4. Slides were blocked for 10 min with 5% normal goat serum. Primary antibodies against, Anti-alpha smooth muscle Actin antibody (ab5694; Abcam, Cambridge, UK), E-cadherin (24E10; Cell Signaling Technology, Danvers, MA), or Ki67 (1:500, clone Sp6; Neomarkers, Fremont, CA), were added for overnight incubation at 4°C. Slides were subsequently incubated with appropriate HRP-conjugated secondary antibodies and DAB staining was used to visualize peroxidase activity. Slides were photographed with a microscope equipped with a digital camera (Leica CTR500, Leica Microsystems, Wetzlar, Germany). The number of Ki67 positive cells were counted in five different fields at 20X magnification, counting was performed with ImageJ and the expressed count per image.

Immunofluorescence

Cells grown on coverslips were fixed with 4% formaldehyde. F-actin was stained with (1:1000) Acti-stain 535 (rhodamine) Phalloidin (Tebu Bio, Heerhugowaard, Netherlands), (1:400) ZEB1 antibody (HPA027524, Atlas Antibodies, Sigma, St. Louis, MO), (1:400) E-cadherin antibody (24E10; Cell Signaling Technology, Danvers, MA), (1:1000) DAPI (ThermoFisher Scientific, Waltham, MA), 1:400 secondary antibody Alexa488 conjugated anti-rabbit IgG (ThermoFisher Scientific, Waltham, MA). All reagents/antibodies were dissolved in 1% bovine serum albumin (Sigma, St. Louis, MO) in PBS with 0.1% Triton X-100 (Sigma, St. Louis, MO) in PBS. Images were acquired on a Leica SP-8 Confocal Microscope (Leica, Wetzlar, Germany) at 63X magnification. LUT values of channels were improved for better visualization in LAS AF software (Leica, Wetzlar, Germany).

Calcium-flux assay

Calcium signaling responses were analyzed using the Fluo-4 Direct™ Calcium Assay Kit (Invitrogen, Carlsbad, CA) as described before [27]. Cells were challenged with thrombin (1 U/ml) or PBS. Ca2+ flux was monitored for the indicated time points on a Bio-Tek HT Multi-Detection Microplate Reader (Winooski, United States).

MTT cell proliferation assay

Cells at 70% confluency in 96-well plates were serum starved overnight after

which cell viability was determined using a 3-(4,5-dimethylthiazol- 2-yl)-2,5-di-phenyltetrazolium (MTT) assay at 0, 24, 48 and 72 hours according to routine procedures. Measurements were performed on a Synergy HT Biotek Microplate Reader (Biotek Instrumens, Winooski, VT) at 560nm. Fold changes were calculated based on optical density at t=0.

Wound-scratch assay

Cells were seeded onto six-well plates and maintained in 10% FCS/DMEM until confluence. Next, cells were serum staved overnight and a scratch was created in the center (on the vertical axis) with a p200 pipette tip. Cells were incubated up to 72h with serum-free DMEM with 25 µM PAR1 agonist peptide TFLLR-NH2 (GL Biochem, Shanghai, China) or solvent control (PBS) as mock. Scratched area were scanned every 24 hours at 4X magnification with EVOS® FL Cell Imaging System. Wound area analysis was performed at fixed locations (400x400) along the scratch area at each time point. Wound area at t=0 is taken as 100% and the changes in wound area at each time point was calculated based on the difference from the area at t=0. Three independent replicates were included for each measurement (n=3).

Statistical Analysis

Data were presented as Mean ± SEM. Statistical analysis was performed with built-in analysis tool of GraphPad PRISM 7.0. For further details see figure legends.

RESULTS

Bulk tumor PAR1 expression does not associate with prognosis in PDAC

Previous work on PAR1 has demonstrated a role for PAR1 in tumor progression in different tumor types leading to poor prognosis in patients with high PAR1 expression levels [17,21,22,25,26]. Therefore, we hypothesized that PAR1 expression also holds prognostic value in PDAC. To assess this hypothesis, Kaplan-Meier survival analysis was performed on four PDAC gene expression sets dichotomized by median PAR1 expression. Surprisingly, PAR1 expression did not associate with overall survival in any of the expression sets **(Supp. Fig. 1A-D)**. However, given that PAR1 expression in these sets is the cumulative expression obtained from tumor cells, stromal content, and possibly adjacent non-tumor tissue, we reasoned that further analyses should address if PAR1 signaling in tumor and stromal compartments contribute differently to tumor growth.

PAR1 regulates tumor cell differentiation and proliferation

Previously, we showed that PAR1 expression in PDAC stroma drives tumor progression [25] and the lack of association between PAR1 and overall survival in PDAC patients lead us to reason that tumor cell-specific PAR1 might counteract the tumorigenic stromal PAR1 activity and reduces the detrimental effect on overall survival. To assess the effect of PAR1 expression on tumor cells and the suspected counterbalancing activity, cells derived from p48-CRE/LSL-KRAS/P53flox/flox mice (named KP hereafter) and Panc02 murine pancreatic cancer cells were transduced with short hairpin RNA against PAR1 (shPAR1) or with control short hairpin RNA (shCtrl). PAR1 knockdown was confirmed by measuring PAR1-dependent calcium fluxes as described before [27] **(Supp. Fig.2A and B)**. Importantly, PAR1 knockdown did not affect in vitro proliferation of both cell lines **(Supp. Fig.3A and B)**. After subsequent orthotopic engraftment to wildtype C57Bl/6 animals, shPAR1 knockdown cells formed significantly bigger tumors as compared to vector control cells **(Figure 1A and B)**. Subsequent stainings for the proliferation marker Ki67 showed a higher density of Ki67 positive cells in shPAR1 tumors than in shCtrl tumors **(Figure 1C)**. Histopathological examination of KP pancreatic cancer sections showed abundant ductal structures throughout the tumor in the shPAR1 group, whereas poorly differentiated tumors

2

lacking apparent ductal structures were observed in the control group **(Figure 1D)**. We next analyzed alpha smooth muscle actin (a-SMA); a marker for activated stromal fibroblasts, but did not find any difference in expression of this marker between shPAR1 and shCtrl tumors **(Figure 1E)**, indicating that PAR1 knockdown on tumor cells does not effect stromal recruitment and activation. In contrast, expression and membrane localization of the epithelial marker E-cadherin was markedly increased in shPAR1 tumors as compared to shCtrl tumors **(Figure 1E)**. Furthermore, in the shPAR1 KP engrafted animals significantly less macro-metastasis were found compared to shCtrl animals **(Figure 1F)**, mainly to the spleen. Overall, these data thus suggest that tumor cell PAR1 contributes to enhanced mesenchymal features.

KP		shCtrl	shPAR1
Spleen Metastasis		5/7	1/8
Liver Metastasis		1/7	1/8
Kidney Metastasis		0/7	1/8
Total Metastasis Count		5/7	3/8
No metastasis		2/7	5/8
Metastasis (%)		71.43	37.5
Chi square p-value			0.021

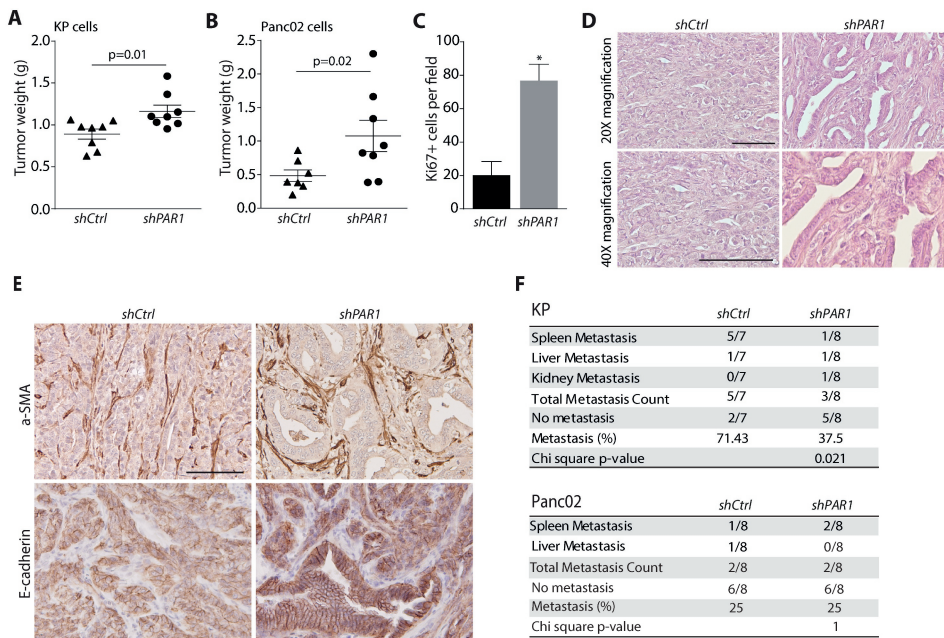| Panc02		shCtrl	shPAR1
Spleen Metastasis		1/8	2/8
Liver Metastasis		1/8	0/8
Total Metastasis Count		2/8	2/8
No metastasis		6/8	6/8
Metastasis (%)		25	25
Chi square p-value			1

Figure 1

PAR1 negatively regulates tumor differentiation and growth. Orthotopic inoculation of (A) shCtrl (n=8) and shPAR1 (n=8) KP cells and (B) shCtrl (n=7) and shPAR1 (n=8) Panc02 cells. Symbols show individual samples. Error bars show mean ± SEM: Mann-Whitney test (two-tailed). (C) For the KP model, Ki67+ counts per field (at 200X magnification) for shCtrl (n=5) and shPAR1 (n=5) tumors, error bars show mean ± SEM. Mann-Whitney (two-tailed), ****<0.0001. (D) KP shCtrl (left) and shPAR1 (right) tumor staining with hematoxylin and eosin at 200X (upper panels) and 400X (lower panels) magnification. (E) KP shCtrl (left) and shPAR1 (right) tumor immunohistochemistry with a-SMA (upper panels) and E-cadherin (lower panels) staining. Scale bar is 200µm. (F) Macro-metastasis scores of the KP and Panc02 models, for shCtrl and shPAR1 animals. Group differences were tested with chi-square distribution tests (for KP group p=0.021, for Panc02 group p=1).

PAR1 associates with tumor cell-intrinsic mesenchymal programs

To elucidate the mechanism through which PAR1 impacts on tumor cell differentiation, we performed gene set enrichment analysis (GSEA) [28] for mesenchymal cell state, and differentiation-related genes on PDAC gene expression sets. The analyses shows that high PAR1 expression was associated with a mesenchymal cancer signature, as well as with a hallmark epithelial-to-mesenchymal transition signature in all expression sets analyzed, including a micro-dissected tumor cell set. This suggests that tumor cell PAR1 expression is linked to a mesenchymal cell state in PDAC **(Figure 2A and B)**. To further confirm that PAR1 activity on tumor cells is associated with a mesenchymal phenotype and with decreased epithelial characteristics, we correlated PAR1 expression with different epithelial and mesenchymal markers in a large panel of PDAC cell lines available in the GSE36133 and GSE57083 datasets. As mesenchymal markers, Zinc Finger E-Box Binding Homeobox 1 (ZEB1) and Vimentin (VIM) were used and E-cadherin (CDH1), cytokeratin 19 (KRT19), CD24, and Epithelial cell adhesion molecule (EPCAM) were used as epithelial markers. PAR1/F2R followed similar expression patterns with ZEB1 and VIM, whereas PAR1 expression was inversely correlated with the epithelial markers (especially prominent for CDH1, KRT19 and EPCAM, see **Figure 2C**). Furthermore, quantitative correlation analysis confirmed the strong positive association of F2R with ZEB1 **(Figure 2D)** and VIM **(Figure 2E)** and showed a negative correlation between F2R and CDH1 **(Figure 2F)**.
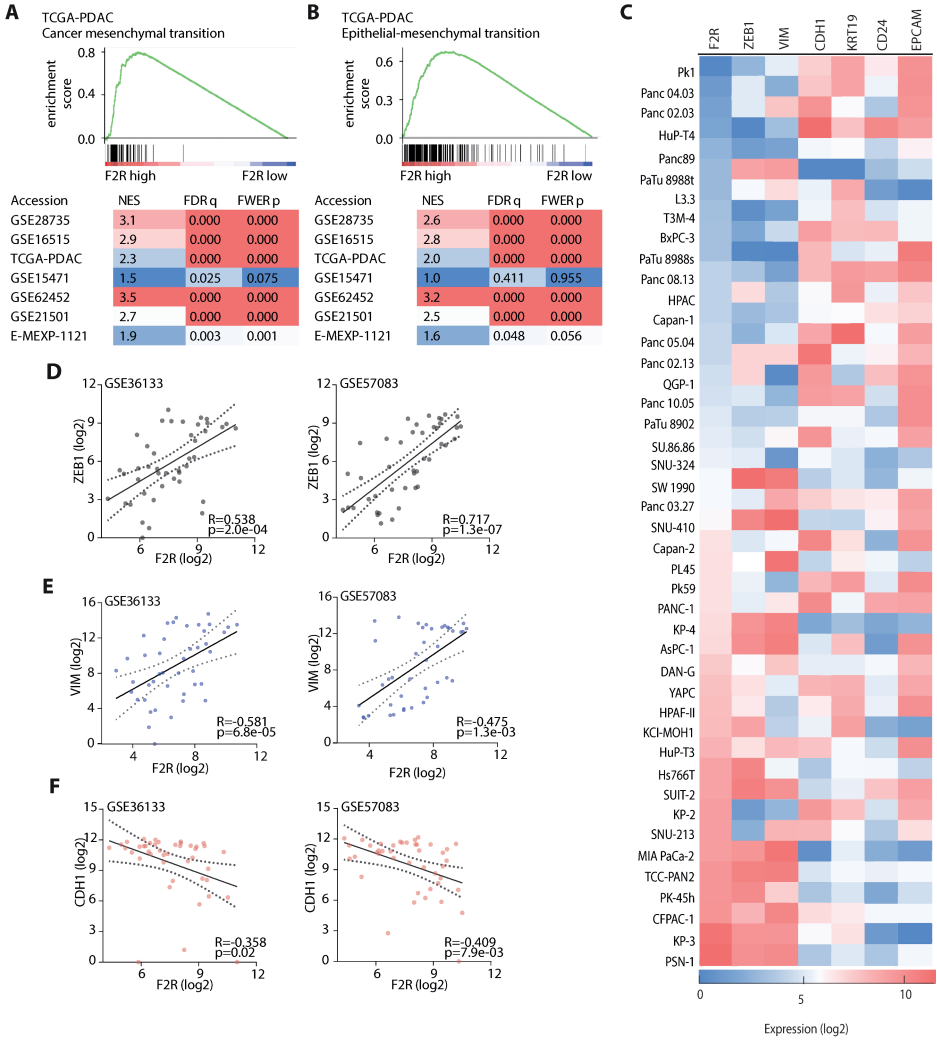
A TCGA-PDAC
Cancer mesenchymal transition

Accession	NES	FDR q	FWER p
GSE28735	3.1	0.000	0.000
GSE16515	2.9	0.000	0.000
TCGA-PDAC	2.3	0.000	0.000
GSE15471	1.5	0.025	0.075
GSE62452	3.5	0.000	0.000
GSE21501	2.7	0.000	0.000
E-MEXP-1121	1.9	0.003	0.001

B TCGA-PDAC
Epithelial-mesenchymal transition

Accession	NES	FDR q	FWER p
GSE28735	2.6	0.000	0.000
GSE16515	2.8	0.000	0.000
TCGA-PDAC	2.0	0.000	0.000
GSE15471	1.0	0.411	0.955
GSE62452	3.2	0.000	0.000
GSE21501	2.5	0.000	0.000
E-MEXP-1121	1.6	0.048	0.056

D GSE36133 / GSE57083

R=0.538 p=2.0e-04
R=0.717 p=1.3e-07

E GSE36133 / GSE57083

R=-0.581 p=6.8e-05
R=-0.475 p=1.3e-03

F GSE36133 / GSE57083

R=-0.358 p=0.02
R=-0.409 p=7.9e-03

C

Expression (log2)

Figure 2

PAR1 expression correlates with EMT signatures. (A-B) Gene Set Enrichment Analysis (GSEA) results of different PDAC gene expression sets with the EMT signature set (A) [35] and the EMT hallmark gene set (B) (Broad Institute). Enrichment plots are shown for both signature sets in the TCGA-PDAC expression dataset. Normalized Enrichment Score (NES), False Discover Rate (FDR) q-value and Family-Wise Error Rate (FWER) p-value are shown for each tested gene expression set. (C) Gene expression heat map of pancreatic cancer cell line expression from GSE36133 and GSE57083 for F2R (PAR1), ZEB1, VIM, CDH1, KRT19, CD24 and EPCAM. Color coding of the heatmap is by log2 transformed gene expression. (D-F) Correlation of PAR1 expression in PDAC cell lines with ZEB1, Vim and CDH1 in the GSE36133 and GSE57083 datasets. Dots show expression levels for individual cell lines. 95% confidence interval and linear regression line are shown; p value is corrected for multiple testing (FDR correction).

For conclusive evaluation of the in silico analysis, we next assessed PAR1 expression in pancreatic cancer cells isolated from tumors with different differentiation status [29] by flow cytometry and qPCR. These data confirmed that PAR1 levels were high in poorly differentiated MIA PaCa-2 cells; intermediate in moderately differentiated PANC-1 cells and relatively low in well-differentiated Capan-2 cells **(Figure 3A)**. Subsequently, we performed qPCR-based transcript analysis for ZEB1 and CDH1 expression and, in line with the in silico data, ZEB1 expression patterns mirrored that of PAR1; high in MIA PaCa-2 cells and low in Capan-2 cells, whereas E-cadherin (CDH1) expression patterns were opposite to that of PAR1 **(Figure 3B)**. To functionally ascertain that PAR1 activity is linked to ZEB1 upregulation and E-cadherin downregulation, we generated PAR1 shRNA knockdown MIA PaCa-2, PANC-1 and Capan-2 cell lines **(Figure 3C, D)**. In agreement with the results above, PAR1 knockdown resulted in a significant increase in CDH1 expression **(Figure 3E)** in all of the shPAR1cell lines compared to their controls. ZEB1 expression was decreased in PANC-1 and MIA PaCa-2 shPAR1 cell lines compared to control cell lines and remained invariably low in the Capan-2 cell line **(Figure 3F)**. Expression levels of the mesenchymal marker VIM were significantly decreased in PANC-1 shRNA cells but remained unchanged in high Vimentin expressing MIA PaCa-2 or low expressing Capan-2 cells **(Figure 3G)**.

To confirm the expression data on the protein level, we analyzed E-cadherin levels on PANC-1 shCtrl and shPAR1 cells with flow cytometry, western blot, and immunofluorescence. We opted for PANC-1 cells in these experiments as they express intermediate levels of PAR1, E-cadherin and ZEB1 allowing efficient visualization of PAR1 knockdown, without confounding high endogenous ZEB1 or low/undetectably E-cadherin expression. Consistent with aforementioned results, all assays showed that PANC-1 shPAR1 cells had a markedly enhanced E-cadherin expression **(Figure 3H and Supp. Fig. 4A)**. Increased E-cadherin expression was accompanied by decreased ZEB1 nuclear localization **(Supp. Fig. 4A)**. Increased E-cadherin expression upon PAR1 knockdown in these cell lines led us question whether we can achieve the same affect with PAR1 inhibition. To test this, we treated PANC-1, MIA PaCa2 and Capan-2 cells with the PAR1 inhibitor Vorapaxar and determined E-cadherin surface expression by flow cytometry. In all cell lines analyzed, treatment with Vorapaxar increased E-cadherin expression **(Supp. Fig. 4B)**.

Finally, we generated PAR1 overexpressing (PAR1-OE) PANC-1 cells to assess whether E-cadherin expression could be reduced. To this end, PANC-1 cells were transfected with PAR1-GFP or control-GFP plasmids after which cells were sorted based on GFP positivity **(Supp. Fig. 5A, B)**. As expected, E-cadherin expression was nearly absent in GFP-positive PAR1-OE cells but not in GFP-positive control vector transfected cells, or in cells from the GFP-negative gates **(Fig. 3I)**. Taken together, we conclude that PAR1 levels are associated with a mesenchymal cell state and that loss of PAR1 enhances epithelial characteristics of pancreatic cancer cells, whereas gain of PAR1 diminishes such epithelial characteristics.
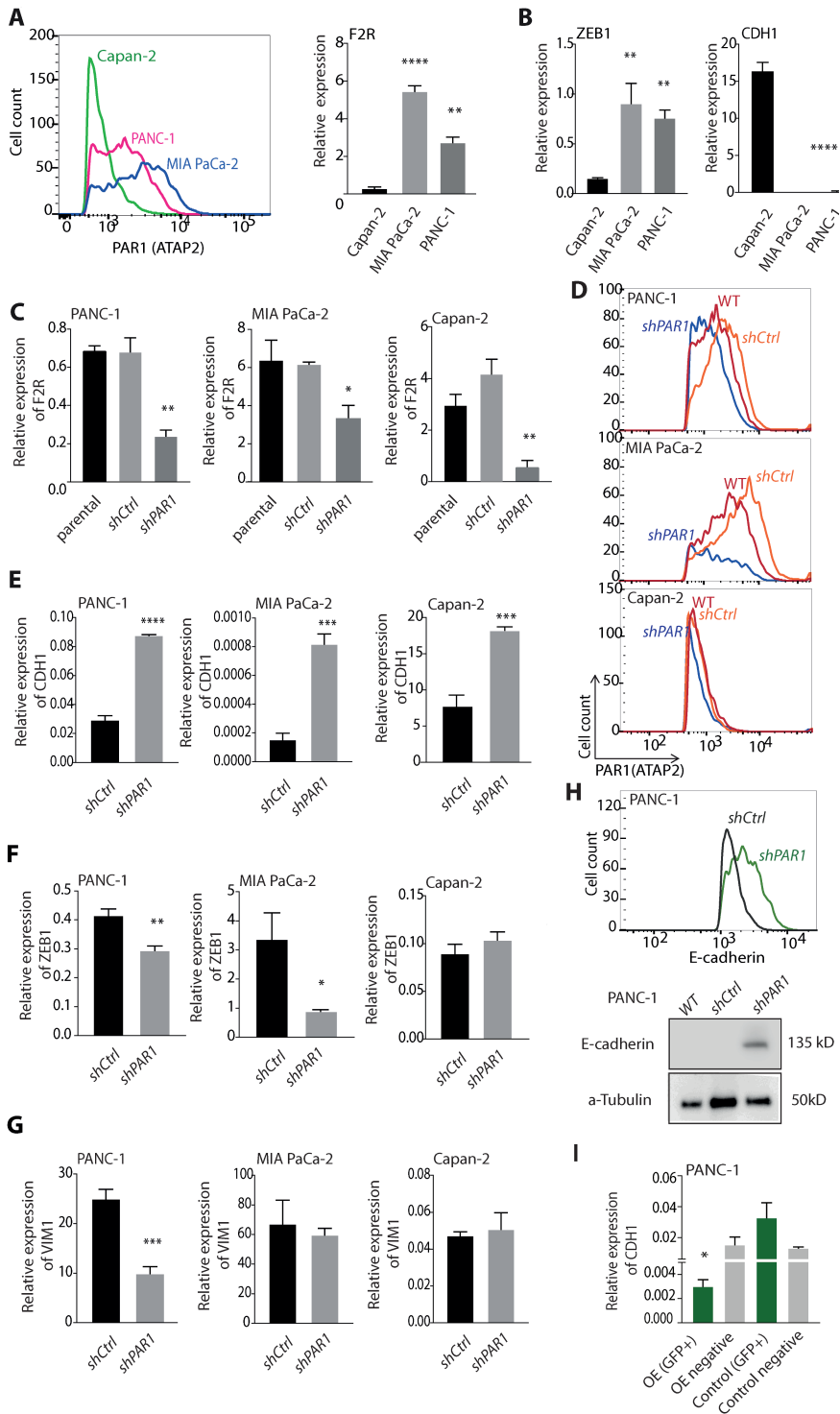
Figure 3

Short hairpin RNA mediated PAR1 knockdown induces E-cadherin and reduces ZEB-1 expression. (A) PAR1 expression on MIA PaCa-2, PANC-1 and Capan-2 cell lines by flow cytometry and qPCR analysis. Flow cytometry histograms show cell counts versus PAR1 (ATAP-2)/APC intensity of the cell lines. Error bars in the qPCR graph show mean ± SEM: one-way ANOVA, ****<0.0001 (B) Relative mRNA expression levels for CDH1 and ZEB1 in three pancreatic cell lines (Capan-2, PANC-1, MIA PaCa-2). Symbols show triplicates. Error bars show mean ± SEM: one-way ANOVA, ****<0.0001. (C) Relative PAR1 expression of shPAR1 and shCtrl transduced MIA PaCa-2, PANC-1 and Capan-2 cell lines in comparison to non-transduced (parent) cells. (D) Flow cytometry histogram showing the cell count versus PAR1 (ATAP-2)/APC intensity of wildtype (WT), shCtrl and shPAR1 cell lines. Initial gating was based on FCS and SSC for the main cell population and later FCS-H vs FCS-W for single cells. APC (PAR1) positive populations were gated on single cell population based on secondary antibody control. (E-G) Relative expression of CDH1 (E), ZEB1 (F), and VIM1 (G) in MIA PaCa-2, PANC-1 and Capan-2 shCtrl and PANC-1 shPAR1 cells. Symbols show quadruplicates. Error bars show mean ± SEM: Student's t-test, ****<0.0001. (H) Upper panel; flow cytometry histogram showing cell counts versus E-cadherin/Alexa 488 intensity of PANC-1 shCtrl (dark gray) and PANC-1 shPAR1 (green) cells. FITC (Alexa 488/E-cadherin) positive populations were gated on single cell population based on secondary antibody control. Lower panel; Western blot analysis for E-cadherin in PANC-1 wildtype, shCtrl and shPAR1 cells. a-Tubulin was used as loading control. (I) Relative E-cadherin mRNA expression levels in PANC-1 PAR1 OE (GFP+), OE negative (GFP negative) with Control (GFP+) and Control negative (GFP negative) cells. Symbols show quadruplicates. Error bars show mean ± SEM: one-way ANOVA, ****<0.0001.

PAR1 signaling drives tumor cell migration

One of the functional outcomes of the transition to a more mesenchymal state is an enhanced migratory behavior and previously ZEB1 was reported to induce tumor cell invasion and enhanced metastatic potential [7,30],. The abovementioned ZEB1 downregulation following PAR1 knockdown (shPAR1) in PANC-1 cells thus raises the question whether this affects the migratory capacities of the cells. To test this, we performed scratch/wound-healing assays with PANC-1 shCtrl and shPAR1 cells in the absence or presence of PAR1 agonist peptide TFLLR-NH2 (PAR1-AP) **(Figure 4A and B)**. After 72 hours, PANC-1 shCtrl cells stimulated with PAR1-AP had higher migration rates than mock controls **(Figure 4C)**, whereas mock or PAR1-AP treated PANC-1 shPAR1 cells had lower migration

rates than shCtrl cells in all cases **(Figure 4D)**. These findings show that activation of PAR1 induces the migration of PANC-1 cells. Although not as strong as agonist peptide induced shCtrl cells, mock treated shCtrl cells also present higher migration rates than shPAR1 cells both with or without PAR1-AP stimulation, meaning that endogenous PAR1 activity already operates the migratory activity of pancreatic cancer cells. Overall, our findings suggest that PAR1 activity on tumor cells promotes migration and exhibits enhanced metastatic potential.
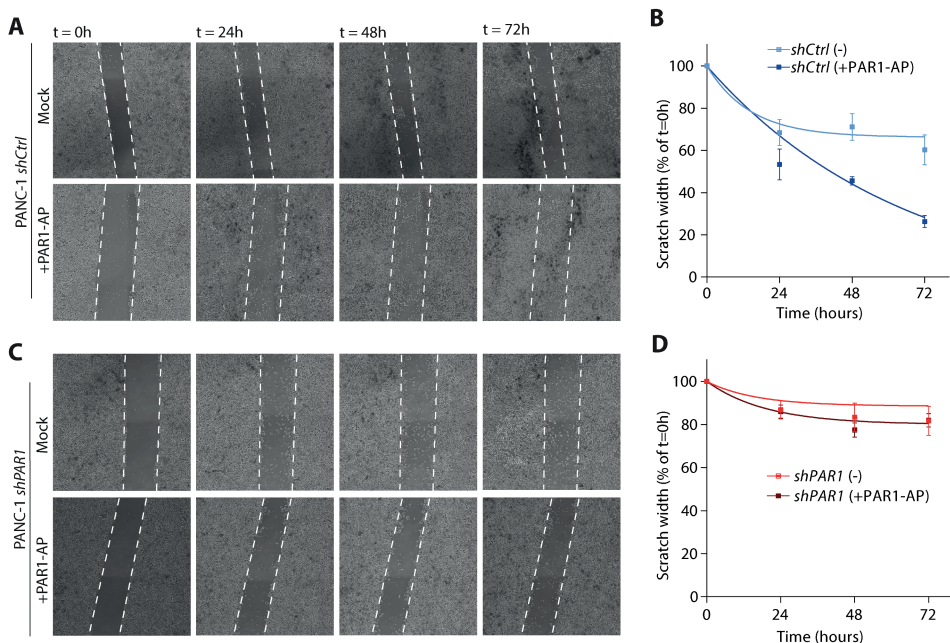
Figure 4

PAR-1 signaling contributes to tumor cell migration. Scratch-healing assays were performed on PANC-1 shCtrl (A) and PANC-1 shPAR1 (C) with mock or 25µM TFLLR-NH2 (PAR1 agonist peptide). At 80% confluency, cells were scratched on the vertical axis of the well with a sterile p200 tip. Images were taken at along the scratch every 24 hours up until 72 hours at 4X magnification on an EVOS FL Cell Imaging System. Scratch size was measured with ImageJ and calculated based on scratch size at t=0 as 100% (n=3). Scratch size over time for PANC-1 shCtrl (B) and PANC-1 shPAR1 (D) with or without the agonist peptide was calculated and put on non-linear one-phase decay curve in Graph-Pad Prism 7.0.

DISCUSSION

PAR1 is generally accepted to promote tumor progression [17,25,31], cancer cell invasion and metastasis [32,33]. This notion is based on the fact that PAR1 expression is increased in various cancers types [17–20] and that PAR1 expression correlates with poor prognosis in breast [21] and lung cancer [22]. Experimental animal studies also support the notion of PAR1 as a potential tumor-promoting factor in lung cancer [18]. Correspondingly, PAR1 is shown to be indispensible and sufficient to promote tumor growth in a breast cancer model [17]. In the current manuscript, we however show that PAR1 expression levels are not associated with the overall survival of PDAC patients and that PAR1 silencing in pancreatic cancer cells potentiates tumor growth. The observed increase in tumor growth of orthotopically implanted PAR1 knockdown cells is particularly interesting since we previously described that PAR1 depletion in the stroma in fact limits tumor growth [25]. These findings suggest that PAR1 has an opposing activity in the stroma and tumor cells, and that PAR1 activity in the stroma appears to promote tumor growth. The opposite role of PAR1 in tumor cells compared to stromal cells likely explains the lack of association between bulk tumor PAR1 levels and overall survival in PDAC patients. In addition, it further highlights the complexity of pancreatic cancer and strengthens the notion that specific compartments need to be targeted in PDAC for efficient tumor control.

Our investigation of PAR1 expression in PDAC bulk tumors and in micro-dissected tumor cells together with PDAC cell line gene expression datasets shows that PAR1 expression correlates with EMT related genes. Moreover, downregulation of PAR1 in the tumor compartment results in enhanced epithelial characteristics and lower tumor grade. Although the exact molecular mechanism between PAR1 activation and ZEB1 expression are not yet discovered, the increase in E-cadherin expression in all shPAR1 knockdown cell lines with a simultaneous decrease in ZEB1 and the decreased Vimentin expression in PANC-1 shPAR1 cells indicates that PAR1 plays a role in the initiation and maintenance of mesenchymal differentiation. In addition to its role in maintaining mesenchymal characteristics in tumor cells, PAR1 activation induces migration in PANC-1 shCtrl cells, indicating a further shift into a mesenchymal phenotype. Moreover, we observed dif-

ferences in macro-metastases scores in the KP model between shPAR1 and shCtrl tumors. Altogether, these findings strongly suggest that PAR1 activation on tumor cells initiates mesenchymal differentiation and increases the metastatic potential. Recent studies have shown that suppression and reversion of EMT stimulates proliferation and that growth at the metastatic site is dependent on mesenchymal to epithelial reversion [15,34]. Furthermore, it has recently been reported that the epithelial status and E-cadherin expression levels mediate cell proliferation in vitro and promotes xenograft growth in vivo [35,36]. The mechanistic link between PAR1 and E-cadherin has been demonstrated in a follow up study where doxycycline was proposed as a novel PAR1 inhibitor and doxycycline treated cells exhibited increased E-cadherin expression and a significantly decreased metastatic potential [37,38]. Considering these findings we might bring an additional explanation for the increased proliferation in shPAR1 tumors in vivo. Decreasing PAR1 activity on tumor cell increases E-cadherin expression, thereby diminishing further differentiation and increasing the proliferative capacity. Furthermore, our observations are in line with work of Krebs et al. [39], who show less metastasis and more differentiated tumors in ZEB1 conditional knockdown KPC animals as compared to ZEB1 expressing KPC animals. Despite the notion to consider these changes as bona fide EMT, we do not observe full conversion of cells into a mesenchymal phenotype. Recent discussions on EMT also report intermediate phenotypes in different cell types and refer to them as "metastable", implying that these changes can be pushed further or conversely – reversed [40]. Moreover, several intriguing studies indeed show that stable intermediate cell fates with hybrid epithelial and mesenchymal features exist and play a key role in metastasis [41,42]. Therefore, we conclude that PAR1-induced changes result in a hybrid epithelial/mesenchymal state.

PAR1 silencing in both Panc02 and KP cells results in increased tumor growth in vivo, however metastasis is only significantly reduced by PAR1 silencing in the KP model. This could be explained by the fact that the metastatic potential of grafted wildtype Panc02 cells is low, not allowing a further decrease to become evident. Indeed, Panc02 cells have been suggested to have a limited metastatic phenotype [43]. Finally, the different genetic background of the used tumor cell lines may contribute. KP cells are both Kras and Tp53 mutant whereas Panc02

2

cells are Kras wildtype [43,44]. Considering the importance of Kras in human pancreatic cancer [45] we focused on the KP model for detailed experimental characterization of PAR1 mediated cell state transitions.

As opposed to the growth inhibitory effect of PAR-1 in vivo, PAR-1 deficiency does not seem to affect proliferation in vitro. Obviously, 2-D cultures do not accurately mimic the complex nature of stroma-rich pancreatic tumors and indeed stromal components play crucial roles in cancer cell proliferation. In addition, the in vitro experiments are performed in growth factor-rich fully oxygenated conditions that may obscure the effect of PAR1 on proliferation under growth factor and/or oxygen depleted circumstances that exist in vivo. Finally, the growth advantage of PAR1 deficient cells in vivo is observed after 4 weeks and it may well be that small differences in growth rate are not observed on a short time scale in vitro. Overall, this underscores that conclusions based on in vitro proliferation experiments may not accurately reflect in vivo results and should be interpreted with care.

Several clinical studies have evaluated the potential clinical efficacy of anticoagulants in pancreatic cancer patients. Indeed, in a retrospective analysis of patients who received chemotherapy for advanced pancreatic adenocarcinoma the addition of low molecular weight heparin (LMWH) to standard chemotherapy significantly improved survival in patients with locally advanced or metastatic pancreatic carcinoma [46]. Opposed to these studies suggesting anticoagulants may increase overall survival of pancreatic cancer patients, a large randomized-placebo controlled trial did not show any benefit of LMWH in pancreatic cancer patients [47]. Our data showing that tumor cell PAR1 limits pancreatic cancer progression may provide an explanation for the disappointing efficacy of anticoagulants in PDAC. Indeed, thrombin is the prototypical PAR1 agonist and thrombin inhibition will thus inhibit PAR1 signaling on tumor cells, suppress mesenchymal transition, and enhance tumor cell proliferation. In line with this notion, we previously showed that thrombin inhibition is less effective in the setting of pancreatic cancer as compared to stromal PAR-1 depletion and we hypothesized this may be due to the counteracting effect of thrombin-PAR1 signaling on tumor cells [48].

Overall, we show that, against its anticipated oncogenic role, tumor cell PAR1

limits PDAC progression by enhancing a mesenchymal phenotype of pancreatic cancer cells. This implies that PAR1 plays a dual role in pancreatic cancer progression and that any therapeutic strategy focusing on PAR1 should be on the stromal compartment. Such compartmentalized PAR1 targeting might be challenging although PAR1-dependent biased signaling, in which different agonists induce different functional responses, may provide an opportunity. Indeed, identifying and targeting PAR1 agonists that drive tumor progression in the tumor compartment, without affecting tumor inhibitory PAR1 signaling on tumor cells, would be a promising strategy to pursue.

DECLARATIONS

REFERENCES

[1]   Ghaneh P, Costello E, Neoptolemos JP. Biology and management of pancreatic cancer. Gut. 2008;84:478–97.

[2]   Miller KD, Siegel RL, Lin CC, Mariotto AB, Kramer JL, Rowland JH, et al. Cancer treatment and survivorship statistics, 2016. CA Cancer J Clin. 2016;66:271–89.

[3]   Adamska A, Domenichini A, Falasca M. Pancreatic Ductal Adenocarcinoma: Current and Evolving Therapies. Int J Mol Sci. 2017;18:1338.

[4]   Conroy T, Desseigne F, Ychou M, Bouché O, Guimbaud R, Bécouarn Y, et al. FOLFIRINOX versus gemcitabine for metastatic pancreatic cancer. N Engl J Med. 2011;364:1817–25.

[5]   Von Hoff DD, Ervin T, Arena FP, Chiorean EG, Infante J, Moore M, et al. Increased Survival in Pancreatic Cancer with nab-Paclitaxel plus Gemcitabine. N Engl J Med. 2013;369:1691–703.

[6]   Khalafalla FG, Khan MW. Inflammation and Epithelial-Mesenchymal Transition in Pancreatic Ductal Adenocarcinoma: Fighting Against Multiple Opponents. Cancer Growth Metastasis. 2017;10:117906441770928.

[7]   Kalluri R, Weinberg RA. The basics of epithelial-mesenchymal transition. J Clin Invest. 2009;119:1420–8.

[8]   Murai T, Yamada S, Fuchs BC, Fujii T, Nakayama G, Sugimoto H, et al. Epithelial-to-mesenchymal transition predicts prognosis in clinical gastric cancer. J Surg Oncol. 2014;109:684–9.

[9]   Zhang W, Wu Y, Yan Q, Ma F, Shi X, Zhao Y, et al. Deferoxamine enhances cell migration and invasion through promotion of HIF-1α expression and epithelial-mesenchymal transition in colorectal cancer. Oncol Rep. 2014;31:111–6.

[10]   Leibovich-Rivkin T, Liubomirski Y, Bernstein B, Meshel T, Ben-Baruch A. Inflammatory factors of the tumor microenvironment induce plasticity in nontransformed breast epithelial cells: EMT, invasion, and collapse of normally organized breast textures. Neoplasia. 2013;15:1330–46.

[11]   Bolos V, Peinado H, Perez-Moreno MA, Fraga MF, Esteller M, Cano A. The transcription factor Slug represses E-cadherin expression and induces epithelial to mesenchymal transitions: a comparison with Snail and E47 repressors. J Cell Sci. 2016;129:1283–1283.

[12]   Aigner K, Descovich L, Mikula M, Sultan A, Dampier B, Bonné S, et al. The transcription factor ZEB1 (deltaEF1) represses Plakophilin 3 during human cancer progression. FEBS Lett. 2007;581:1617–24.

[13]   Zhang GJ, Zhou T, Tian HP, Liu ZL, Xia S Sen. High expression of ZEB1 correlates with liver metastasis and poor prognosis in colorectal cancer. Oncol Lett. 2013;5:564–8.

[14]   Bronsert P, Kohler I, Timme S, Kiefer S, Werner M, Schilling O, et al.

Prognostic significance of Zinc finger E-box binding homeobox 1 (ZEB1) expression in cancer cells and cancer-associated fibroblasts in pancreatic head cancer. Surg (United States). 2014;156:97–108.

[15]   Zheng X, Carstens JL, Kim J, Scheible M, Kaye J, Sugimoto H, et al. Epithelial-to-mesenchymal transition is dispensable for metastasis but induces chemoresistance in pancreatic cancer. Nature. 2015;527:525–30.

[16]   Macfarlane SR, Seatter MJ, Kanke T, Hunter GD, Plevin R. Proteinase-Activated Receptors. Pharmacol Rev. 2001;53:245 LP – 282.

[17]   Boire A, Covic L, Agarwal A, Jacques S, Sherifi S, Kuliopulos A. PAR1 is a matrix metalloprotease-1 receptor that promotes invasion and tumorigenesis of breast cancer cells. Cell. 2005;120:303–13.

[18]   Cisowski J, O'Callaghan K, Kuliopulos A, Yang J, Nguyen N, Deng Q, et al. Targeting protease-activated receptor-1 with cell-penetrating pepducins in lung cancer. Am J Pathol. 2011;179:513–23.

[19]   Ghio P, Cappia S, Selvaggi G, Novello S, Lausi P, Zecchina G, et al. Prognostic role of protease-activated receptors 1 and 4 in resected stage IB non-small-cell lung cancer. Clin Lung Cancer. 2006;7:395–400.

[20]   Grisaru-Granovsky S, Salah Z, Maoz M, Pruss D, Beller U, Bar-Shavit R. Differential expression of protease activated receptor 1 (Par1) and pY397FAK in benign and malignant human ovarian tissue samples. Int J Cancer. 2005;113:372–8.

[21]   Diaz J, Aranda E, Henriquez S, Quezada M, Espinoza E, Bravo ML, et al. Progesterone promotes focal adhesion formation and migration in breast cancer cells through induction of protease-activated receptor-1. J Endocrinol. 2012;214:165–75.

[22]   Zhu L, Wang X, Wu J, Mao D, Xu Z, He Z, et al. Cooperation of protease-activated receptor 1 and integrin alphanubeta5 in thrombin-mediated lung cancer cell invasion. Oncol Rep. 2012;28:553–60.

[23]   Villares GJ, Zigler M, Wang H, Melnikova VO, Wu H, Friedman R, et al. Targeting melanoma growth and metastasis with systemic delivery of liposome-incorporated protease-activated receptor-1 small interfering RNA. Cancer Res. 2008;68:9078–86.

[24]   Wang T, Jiao J, Zhang H, Zhou W, Li Z, Han S, et al. TGF-β induced PAR-1 expression promotes tumor progression and osteoclast differentiation in giant cell tumor of bone. Int J Cancer. 2017;141:1630–42.

[25]   Queiroz KCS, Shi K, Duitman J, Aberson HL, Wilmink JW, Van Noesel CJM, et al. Protease-activated receptor-1 drives pancreatic cancer progression and chemoresistance. Int J Cancer. 2014;135:2294–304.

[26]   Han N, Jin K, He K, Cao J, Teng L. Protease-activated receptors in cancer: A systematic review. Oncol Lett. 2011;2:599–608.

[27]   Lin C, Rezaee F, Waasdorp M, Shi K, van der Poll T, Borensztajn K, et al. Protease activated receptor-1 regulates macrophage-mediated cellular senes-

cence: a risk for idiopathic pulmonary fibrosis. Oncotarget. 2015;6:35304–14.

[28]   Subramanian A, Tamayo P, Mootha VK, Mukherjee S, Ebert BL, Gillette MA, et al. Gene set enrichment analysis: a knowledge-based approach for interpreting genome-wide expression profiles. Proc Natl Acad Sci U S A. 2005;102:15545–50.

[29]   Deer EL, Gonzalez-Hernandez J, Coursen JD, Shea JE, Ngatia J, Scaife CL, et al. Phenotype and Genotype of Pancreatic Cancer Cell Lines. Pancreas. 2010;39:425–35.

[30]   Brabletz T. To differentiate or not-routes towards metastasis. Nat Rev Cancer. 2012;12:425–36.

[31]   Even-Ram S, Uziely B, Cohen P, Grisaru-Granovsky S, Maoz M, Ginzburg Y, et al. Thrombin receptor overexpression in malignant and physiological invasion processes. Nat Med. 1998;4:909–14.

[32]   Yang E, Cisowski J, Nguyen N, O'Callaghan K, Xu J, Agarwal A, et al. Dysregulated protease activated receptor 1 (PAR1) promotes metastatic phenotype in breast cancer through HMGA2. Oncogene. 2016;35:1529–40.

[33]   Shi X, Gangadharan B, Brass LF, Ruf W, Mueller BM. Protease-activated receptors (PAR1 and PAR2) contribute to tumor cell motility and metastasis. Mol Cancer Res. 2004;2:395–402.

[34]   Tsai JH, Donaher JL, Murphy DA, Chau S, Yang J. Spatiotemporal Regulation of Epithelial-Mesenchymal Transition Is Essential for Squamous Cell Carcinoma Metastasis. Cancer Cell. 2012;22:725–36.

[35]   Hugo HJ, Gunasinghe NPAD, Hollier BG, Tanaka T, Blick T, Toh A, et al. Epithelial requirement for in vitro proliferation and xenograft growth and metastasis of MDA-MB-468 human breast cancer cells: oncogenic rather than tumor-suppressive role of E-cadherin. Breast Cancer Res. 2017;19:86.

[36]   Park SY, Shin JH, Kee SH. E-cadherin expression increases cell proliferation by regulating energy metabolism through nuclear factor-κB in AGS cells. Cancer Sci. 2017;108:1769–77.

[37]   Zhong W, Chen S, Zhang Q, Xiao T, Qin Y, Gu J, et al. Doxycycline directly targets PAR1 to suppress tumor progression. Oncotarget. 2017;8:16829–42.

[38]   Zhong W, Chen S, Qin Y, Zhang H, Wang H, Meng J, et al. Doxycycline inhibits breast cancer EMT and metastasis through PAR-1/NF-κB/miR-17/E-cadherin pathway. Oncotarget. 2017;8:104855–66.

[39]   Krebs AM, Mitschke J, Losada ML, Schmalhofer O, Boerries M, Busch H, et al. The EMT-activator Zeb1 is a key factor for cell plasticity and promotes metastasis in pancreatic cancer. Nat Cell Biol. 2017;19:518–29.

[40]   Nieto MA, Huang RYYJ, Jackson RAA, Thiery JPP. Emt: 2016. Cell. 2016;166:21–45.

[41]   Jolly MK. Implications of the Hybrid Epithelial/Mesenchymal Phenotype in Metastasis. Front Oncol. 2015;5:1–19.

[42]   Jolly MK, Tripathi SC, Jia D, Mooney SM, Celiktas M, Hanash SM, et al. Stability of the hybrid epithelial/mesenchymal phenotype. Oncotarget. 2016;7:27067–84.

[43]   Wang Y, Zhang Y, Yang J, Ni X, Liu S, Li Z, et al. Genomic sequencing of key genes in mouse pancreatic cancer cells. Curr Mol Med. 2012;12:331–41.

[44]   Jiang H, Hegde S, Knolhoff BL, Zhu Y, Herndon JM, Meyer MA, et al. Targeting focal adhesion kinase renders pancreatic cancers responsive to checkpoint immunotherapy. Nat Med. 2016;22:851–60.

[45]   Hingorani SR, Petricoin EF, Maitra A, Rajapakse V, King C, Jacobetz MA, et al. Preinvasive and invasive ductal pancreatic cancer and its early detection in the mouse. Cancer Cell. 2004;5:103.

[46]   von Delius S, Ayvaz M, Wagenpfeil S, Eckel F, Schmid RM, Lersch C. Effect of low-molecular-weight heparin on survival in patients with advanced pancreatic adenocarcinoma. Thromb Haemost. 2007;98:434–9.

[47]   Van Doormaal FF, Di Nisio M, Otten HM, Richel DJ, Prins M, Buller HR. Randomized trial of the effect of the low molecular weight heparin nadroparin on survival in patients with cancer. J Clin Oncol. 2011;29:2071–6.

[48]   Shi K, Damhofer H, Daalhuisen J, ten Brink M, Richel DJ, Spek CA. Dabigatran Potentiates Gemcitabine-Induced Growth Inhibition of Pancreatic Cancer in Mice. Mol Med. 2017;23:13–23.

[49]   Lin C, Duitman JW, Daalhuisen J, Ten Brink M, Von Der Thüsen J, Van Der Poll T, et al. Targeting protease activated receptor-1 with P1pal-12 limits bleomycin-induced pulmonary fibrosis. Thorax. 2014;69:152–60.

[50]   Raphael BJ, Hruban RH, Aguirre AJ, Moffitt RA, Yeh JJ, Stewart C, et al. Integrated Genomic Characterization of Pancreatic Ductal Adenocarcinoma. Cancer Cell. 2017;32:185-203.e13.

[51]   Collisson EA, Sadanandam A, Olson P, Gibb WJ, Truitt M, Gu S, et al. Subtypes of pancreatic ductal adenocarcinoma and their differing responses to therapy. Nat Med. 2011;17:500–3.

[52]   Wang J, Yang S, He P, Schetter AJ, Gaedcke J, Ghadimi BM, et al. Endothelial nitric oxide synthase traffic inducer (NOSTRIN) is a negative regulator of disease aggressiveness in pancreatic cancer. Clin Cancer Res. 2016;22:5992–6001.

[53]   Badea L, Herlea V, Dima SO, Dumitrascu T, Popescu I. Combined gene expression analysis of whole-tissue and microdissected pancreatic ductal adenocarcinoma identifies genes specifically overexpressed in tumor epithelia. Hepato-gastroenterology. 2008;55:2016–27.

[54]   Stratford JK, Bentrem DJ, Anderson JM, Fan C, Volmar KA, Marron JS, et al. A Six-Gene Signature Predicts Survival of Patients with Localized Pancreatic Ductal Adenocarcinoma. Hanash SM, editor. PLoS Med. 2010;7:e1000307.

[55]   Zhang G, Schetter A, He P, Funamizu N, Gaedcke J, Ghadimi BM, et al. DPEP1 Inhibits Tumor Cell Invasiveness, Enhances Chemosensitivity and Pre-

2

dicts Clinical Outcome in Pancreatic Ductal Adenocarcinoma. El-Rifai W, editor. PLoS One. 2012;7:e31507.
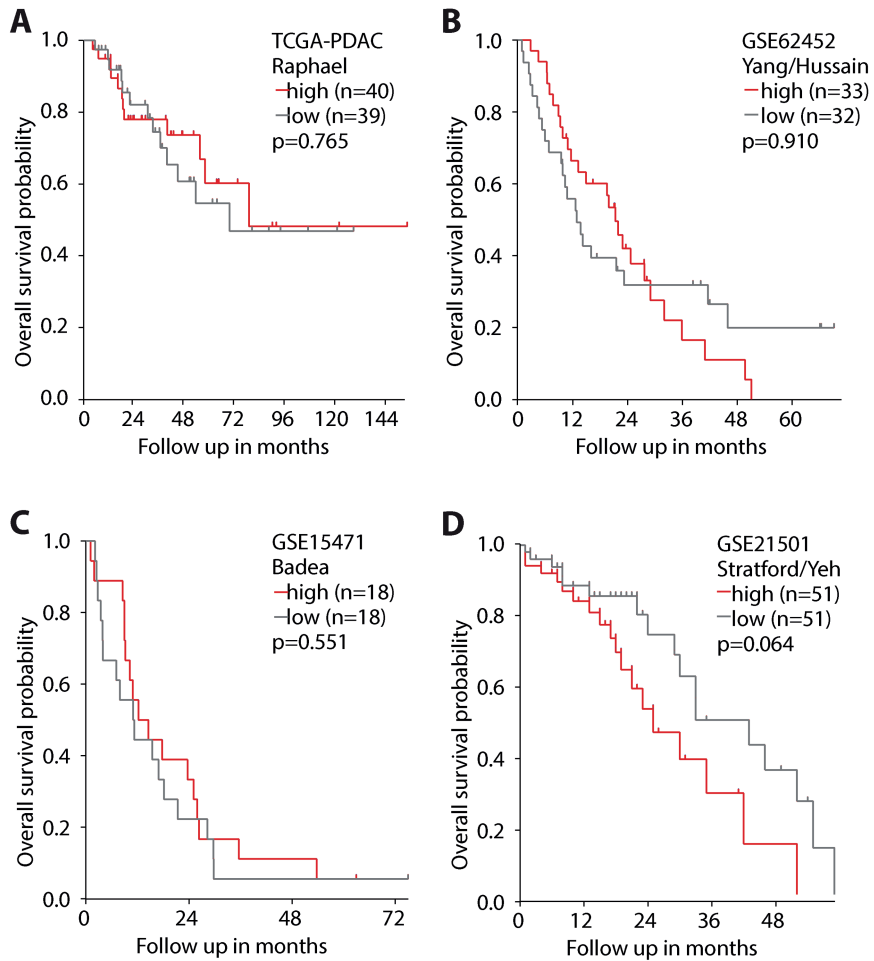
[56]   Pei H, Li L, Fridley BL, Jenkins GD, Kalari KR, Lingle W, et al. FKBP51 Affects Cancer Cell Response to Chemotherapy by Negatively Regulating Akt. Cancer Cell. 2009;16:259–66.

[57]   Rückert F, Hennig M, Petraki CD, Wehrum D, Distler M, Denz a, et al. Co-expression of KLK6 and KLK10 as prognostic factors for survival in pancreatic ductal adenocarcinoma. Br J Cancer. 2008;99:1484–92.

[58]   Barretina J, Caponigro G, Stransky N, Venkatesan K, Margolin AA, Kim S, et al. The Cancer Cell Line Encyclopedia enables predictive modelling of anticancer drug sensitivity. Nature. 2012;483:603–7.

[59]   Anastassiou D, Rumjantseva V, Cheng W, Huang J, Canoll PD, Yamashiro DJ, et al. Human cancer cells express Slug-based epithelial-mesenchymal transition gene expression signature obtained in vivo. BMC Cancer. 2011;11:529.

SUPPLEMENTARY INFORMATION

A TCGA-PDAC Raphael — high (n=40), low (n=39), p=0.765
B GSE62452 Yang/Hussain — high (n=33), low (n=32), p=0.910
C GSE15471 Badea — high (n=18), low (n=18), p=0.551
D GSE21501 Stratford/Yeh — high (n=51), low (n=51), p=0.064
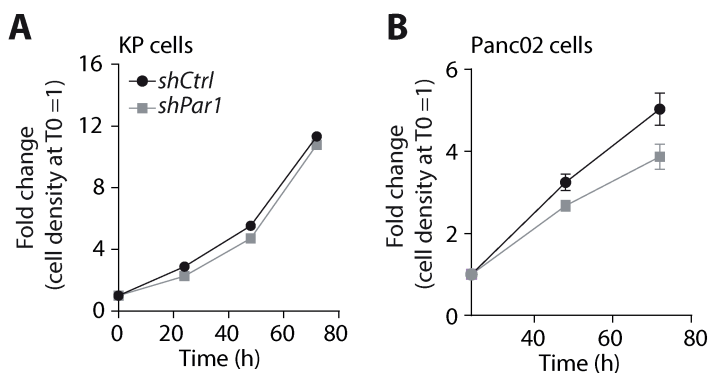
Supplementary Figure 1

Bulk tumor PAR1 expression does not associate with survival in PDAC. PAR1 high (red) vs. PAR1 low (gray) Kaplan-Meier overall survival analysis of pancreatic ductal adenocarcinoma expression sets: (A) TCGA-PDAC; (B) GSE62452; (C) GSE15471; and (D) GSE21501. Dichotomization for analysis was by median expression of PAR1 and performed in R2: Genomics Analysis and Visualization platform (http://r2.amc.nl).
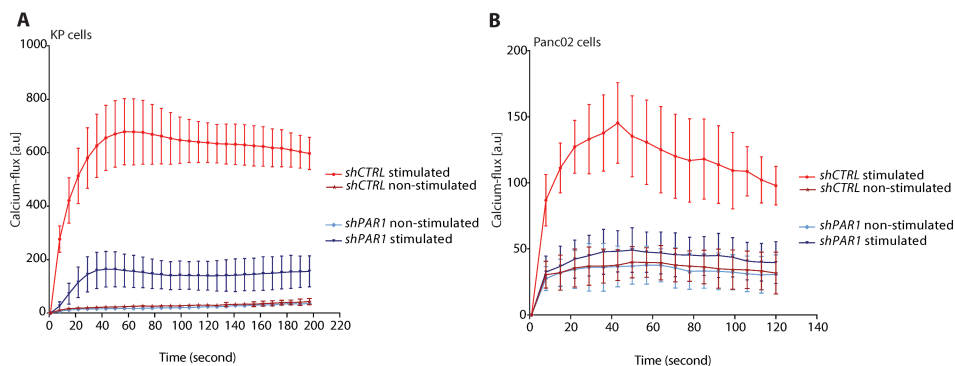
Supplementary Figure 2

Short hairpin RNA knockdown confirmation of KP and Panc02 cells via calcium-flux assay. Calcium-flux response curves of KP (A) and Panc02 (B) shCtrl and shPAR1 cells. Cells were induced with 1 U/ml thrombin or PBS. Calcium flux was monitored at indicated time points and measured kinetically on a plate reader.
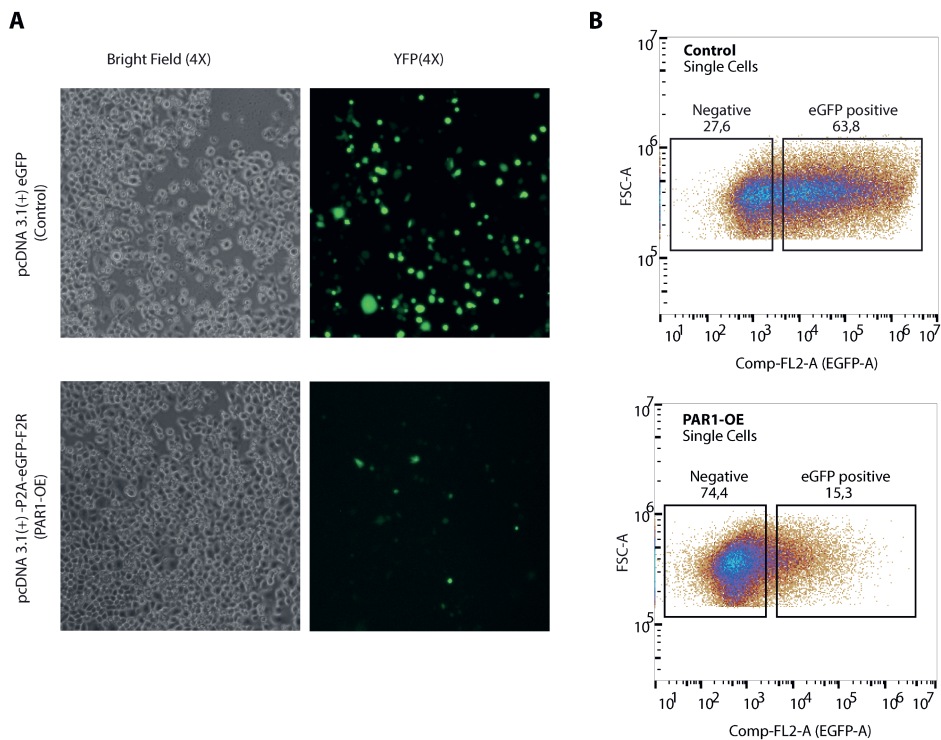

Supplementary Figure 3

Short hairpin RNA mediated PAR1 knockdown in KP (A) and Panc02 (B) murine pancreatic cancer cell lines does not affect their proliferation rate. Both KP and Panc02 (shCtrl/shPAR1) cell line proliferation was tested with MTT assays at different time points 0, 24, 48 and 72h. Measurements were performed at 560nm. Fold changes were calculated based on optical density at t=0.
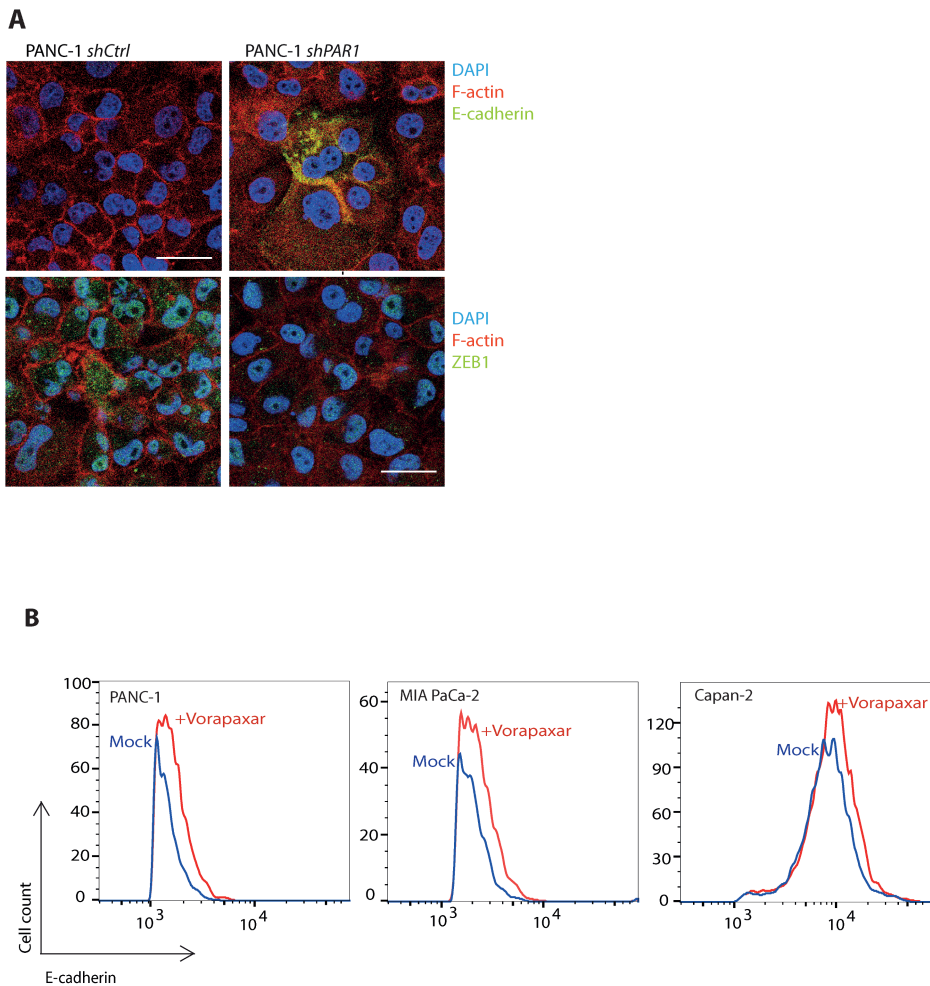
Supplementary Figure 4

Suppressing PAR1 decreases ZEB1 nuclear co-localization and increases E-cadherin expression. (A) Immunofluorescence for E-cadherin (upper panels) and ZEB1 (lower panels) on PANC-1 shCtrl and PANC-1 shPAR1 cells. Filamentous (F-) actin was stained with rhodamine phalloidin, nuclei were stained with DAPI. Detection was done using an Alexa488 conjugated secondary antibody. Scale bar is 20 μm. Images were acquired with a Leica SP-8 Confocal Microscope at 63X magnification. (B) Flow cytometry histogram shows the cell count versus E-cadherin/Alexa 488 intensity of Mock (blue) and 250 nM Vorapaxar treated (red) PANC-1, MIA PaCa-2 and Capan-2 cells (Left to right, respectively).

Supplementary Figure 5

Sorting PAR1-GFP (PAR1-OE) or control-GFP (Control) transfected PANC-1 cells based on GFP positivity. (A) Bright field and YFP fluorescence images at 4X magnification of transfected PANC-1 cells. (B) Sorted populations. Initial gates are based on live population and further gate was set on single cells. GFP positivity was gated on single cell population. In both sets, GFP positive and negative populations were sorted.

Chapter 3

Macrophage-secreted MMP9 induces mesenchymal transition in pancreatic cancer cells via PAR1 activation

Cansu Tekin, Hella L Aberson, Cynthia Waasdorp, Gerrit K J Hooijer, Onno J de Boer, Frederike Dijk, Maarten F Bijlsma, C Arnold Spek

ABSTRACT

Purpose: Targeting tumor-infiltrating macrophages limits progression and improves chemotherapeutic responses in pancreatic ductal adenocarcinoma (PDAC). Protease-activated receptor (PAR)1 drives monocyte/macrophage recruitment, and stromal ablation of PAR1 limits cancer growth and enhances gemcitabine sensitivity in experimental PDAC. However, the functional interplay between PAR1, macrophages, and tumor cells remains unexplored. Here we address the PAR1-macrophage-tumor cell crosstalk and assess its contributions to tumor progression.

Methods: PAR1 expression and macrophage infiltration were correlated in PDAC biopsies using gene expression datasets and tissue microarrays. Medium transfer experiments were used to evaluate the functional consequences of macrophage-tumor cell crosstalk and to assess the contributions of PAR1 to the observed responses. PAR1 cleavage assays were used to identify the macrophage-secreted PAR1 agonist, and the effects of candidate proteases were assessed in medium transfer experiments with specific inhibitors and/or recombinant agonist.

Results: PAR1 expression correlates with macrophage infiltration in PDAC, and macrophages induce mesenchymal transition of PDAC cells through PAR1 activation. Protease profiling identified macrophage-secreted matrix metalloprotease 9 (MMP9) as the relevant PAR1 agonist in PDAC. PAR1 and/or MMP9 inhibition limited macrophage-driven mesenchymal transition. Likewise, preventing mesenchymal transition by silencing ZEB1 or by pharmacological inhibition of the MMP9/PAR1 axis significantly reduced the ability of tumor cells to survive the anti-tumor activities of macrophages.

Conclusion: Macrophages secrete MMP9, which acts upon PDAC cells PAR1 to induce mesenchymal transition. This macrophage-induced mesenchymal transition supports the tumor-promoting role of macrophage influx, explaining the dichotomous contributions of these immune cells to tumor growth.

INTRODUCTION

Pancreatic ductal adenocarcinoma (PDAC) is one of the most lethal cancers with reported 5-year survival rates of less than 8% [1, 2]. The high mortality rate of PDAC is mostly due to late diagnosis with the vast majority of patients presenting with locally advanced or metastatic disease, and only around 20% of the patients are eligible for surgical resection of the tumor. Despite intense research efforts to improve and develop therapies, progress in therapeutic outcome has been slow, and current treatment options are still inadequate [2]. In the recent past, gemcitabine was used as first-line therapy, but survival benefits were limited [3]. Novel combination therapies like, for instance, FOLFIRINOX [4] or gemcitabine with Nab-paclitaxel [5], are superior over single-drug gemcitabine regimens, but even these intense combination treatments have limited efficacy. To increase PDAC survival rates, a better understanding of the mechanisms that contribute to the poor prognosis is urgently needed.

Macrophages are specialized mononuclear phagocytic immune cells critically involved in host defense and tissue homeostasis [6]. In cancer, macrophages have traditionally been considered to harbor cytotoxic activity, and numerous studies indeed show that macrophages may kill tumor cells by secreting cytotoxic molecules, such as TNF-α, IL-12, nitric oxide (NO), and reactive oxygen species (ROS) [7, 8]. Despite their cytotoxic capacity, however, macrophages are now increasingly believed to be pro-tumorigenic and to potentiate tumor growth [9–11]. High densities of macrophages are commonly seen in many different cancer types, including PDAC, and they are typically associated with poor prognosis [9]. Indeed, tumor-associated macrophages have been reported to induce epithelial-to-mesenchymal transition (EMT) [12–14], and blocking macrophage infiltration to decrease the number of metastatic lesions [15]. Furthermore, macrophage numbers have been reported to be associated with therapy resistance in pancreatic cancer [16, 17].

Protease-activated receptor (PAR)1, a seven-transmembrane G protein-coupled receptor (GPCR), is expressed in many tumor types, and its expression is associated with tumor progression and poor prognosis [18–21]. In contrast to most GPCRs, PAR1 activation requires proteolytic cleavage rather than classical ligand

binding. PAR1 was initially identified as the thrombin receptor (F2R), but recently other agonists, such as activated protein C, matrix metalloproteases (MMPs), and kallikreins, have been described [22]. Agonist-dependent proteolytic removal of the N-terminal extracellular region of PAR1 releases a tethered ligand that interacts with the body of the receptor to activate signaling pathways that affect numerous pathophysiological responses. In PDAC, PAR1 is abundantly expressed in both primary tumors as well as in metastases, and genetic ablation of PAR1 from the tumor microenvironment limits cancer growth and enhances gemcitabine sensitivity in experimental animals [23]. Of note, stromal PAR1 deficiency is accompanied by a reduced macrophage infiltration into the tumor microenvironment, which is a direct effect of PAR1-dependent chemokine production [23]. In the current study, we explore the functional interplay between PAR1, macrophages, and tumor cells. In doing so, we uncovered a mechanism through which macrophage-induced mesenchymal transition allows tumor cells to escape macrophage-dependent cell death.

MATERIALS AND METHODS

Patients

A tissue microarray was prepared from tumor specimens of pancreatic cancer patients obtained during surgery according to the guidelines of the Medical Ethical Committee of the Amsterdam University Medical Centers (Amsterdam UMC). We used anonymized formalin-fixed paraffin-embedded (FFPE) human tissue samples that were obtained during standard diagnostic procedures, and which were later made available for scientific research (so-called 'further use' of human tissue). According to the Code of Conduct for dealing responsibly with human tissue in the context of health research, these biological materials are as such not subject to any requirement for ethical review or consent from patients [24]. From selected FFPE blocks with primary PDAC (n = 30), one core of tumor with a diameter of 1 mm was collected using a TMA instrument (Beecher Instruments, Silver Springs MD, USA) and inserted in a recipient block. Each recipient block was sectioned at 4 µm, and dried overnight at 37ºC.

Immunohistochemistry

PDAC FFPE tissue sections were stained for PAR1 (ATAP-2: sc-13503, Santa Cruz Biotechnology, Dallas, TX, USA), CD68 (PG-M1, Dako Omnis, Agilent, Santa Clara, CA) and CD163 (10D6, Thermo Fischer Scientific, Waltham, MA). Slides were deparaffinized and rehydrated, after which endogenous peroxidase activity was quenched in 0.5% hydrogen peroxide-methanol solution. Antigen retrieval was performed for 20 minutes in Tris/EDTA pH 9.0 buffer in a pressure cooker. Primary antibodies directed against CD163 and CD68 were applied for 60 minutes at room temperature, whereas an anti-PAR1 antibody was applied overnight at 4oC. Slides were subsequently incubated with the appropriate HRP-conjugated secondary antibodies. To obtain triple staining of single slides, the same slide was sequentially stained. Following each staining, the sections were digitized (scanned) using a Philips IntelliSite UFS (Philips Digital Pathology Solutions, Best, the Netherlands) followed by a stripping step in which the colors and bound complexes were eluted from the sections, as described before [25]. De-stained sections were examined prior to the subsequent immunostaining to ensure that the previous staining was no longer present. From the acquired digital images, areas of interest were selected and aligned by non-linear registration

of the separate images. After creating image stacks and color deconvolution for NovaRed, false-color images were created for each staining and re-stacked using Fiji/Image J analysis software (NIH, Bethesda, MD, USA).

Reagents

The following reagents were used: GM6001 (ChemCruz, Dallas, TX, USA), Vorapaxar (250 nM, Adooq Bioscience, Irvine, CA, USA), L-glutamine (Lonza, Basel, Switzerland), Penicillin and Streptomycin (Lonza, Basel, Switzerland), Trypsin-EDTA (Gibco, Thermo Fischer Scientific, Waltham, MA, USA), Puromycin (Sigma, St. Louis, MO, USA), phorbol 12-myristate 13-acetate (PMA; Merck-Millipore, Burlington, MA, USA), 3-(4,5-dimethylthiazol- 2-yl)-2,5-diphenyltetrazolium (MTT), pre-activated recombinant MMP9 and Crystal Violet (both from Sigma, St. Louis, MO, USA).

Cell culture

Human PANC-1, MIA PaCa-2 and Capan-2 pancreatic cancer cells (ATCC, Manassas, VA, USA) were cultured in high glucose (4.5g/ml) DMEM (Gibco, Thermo Fischer Scientific, Waltham, MA, USA) and human THP-1 (ATCC, Manassas, VA, USA) cells were cultured in RPMI-1640 (Gibco, Thermo Fischer Scientific, Waltham, MA, USA). All media were supplemented with 10% fetal bovine serum (FBS, #F7524, Sigma, St. Louis, MO, USA), L-glutamine (2 mM), except RPMI-1640 for conditioned media experiments, which was supplemented with 1X GlutaMAX (Gibco, Thermo Fischer Scientific, Waltham, MA, USA), penicillin (100 units/ml), and streptomycin (500 µg/ml) (Lonza, Basel, Switzerland) according to routine cell culture procedures. Cells were incubated in 5% CO_2 incubators at 37oC. All PDAC cell lines were authenticated by STR profiling (Promega PowerPlex, Leiden, Netherlands), and tested for mycoplasma by PCR monthly.

Generation of macrophages and conditioned media

THP-1 cells seeded at 106 in a T75 culture flask (Greiner Bio-One, Kremsmünster, Austria) were treated with 150 nM phorbol 12-myristate 13-acetate (PMA) for 24 hours in RPMI-1640 (Gibco, Thermo Fischer Scientific, Waltham, MA, USA) medium. Next, adherent activated THP-1 cells were washed with fresh medium to remove PMA, and cells were cultured in fresh medium for another 24

hours, after which the medium was refreshed once more. Conditioned medium from these M0 macrophages (M0-CM), which express CD68 and CD163 but not CD206 (Sup. Fig. 2A), was collected 48 hours later. After collection, M0-CM was centrifuged at 1200 RPM for 4 minutes to remove cell debris, filtered using 0.2 µm syringe filters (Corning, New York, NY, USA), and stored at 4oC. For experimental procedures, the M0-CM medium was diluted 1:1 with fresh media to refresh the nutrients and serum content of the medium. M2 macrophages for phenotype testing (Sup. Fig. 2A), were generated from THP-1 cells, as described previously [26].

MMP9 cleavage prediction of PAR1
The FASTA sequence of human PAR1 (F2R), Uniprot ID: P25116, was loaded into the CleavePredict MMP substrate cleavage prediction tool for MMPs (http://cleavpredict.sanfordburnham.org [27]). After analysis, position weight matrices (PWM) representative of prediction scores for PAR1 cleavage were exported. In this analysis, higher PWM scores indicate a more substantial likelihood of cleavage at a specific site. A model representing the PAR1 N-terminal arm between amino acids 33 and 44, as shown in Figure 4, was generated in SWISS-MODEL (https://swissmodel.expasy.org/) and agonist-specific cleavage sites were colored using PyMol (https://pymol.org).

MMP9 ELISA
MMP9 concentrations in M0-CM were determined using a commercially available MMP9 ELISA kit (DY911-05, R&D Systems, Minneapolis, MN, USA) according to the manufacturer's instructions.

Quantitative Real-Time PCR
Total RNA was isolated using a NucleoSpin RNA miniprep kit (Macherey Nagel, Düren, Germany). cDNA was synthesized from DNase-treated total RNA using M-MLV-RT (Promega, Leiden, Netherlands) and random hexamers (Qiagen, Hilden, Germany). Real-time quantitative RT-PCR was performed using a Sensifast SYBR No-Rox Kit (Bioline, London, UK) on a LightCycler 480 II (Roche, Basel, Switzerland). Relative expression levels were calculated using the comparative threshold cycle (dCt method) and normalized for expression of

the reference gene TBP. Primer sequences of the analyzed genes are shown in Supplementary Table 1.

PDAC expression datasets

Gene expression datasets were derived from the Gene Expression Omnibus (http://www.ncbi.nlm.nih.gov/gds) using the R2 microarray analysis and visualization platform (http://r2.amc.nl). Pancreatic tumor expression sets (GSE62452 [28], GSE28735 [29], GSE15471 [30], TCGA-PDAC [31], E-MTAB-6830 [32], GSE93326 [33] and GSE49149 [34]) were used for expression analysis of PAR1 (F2R), CD68 and CD163. Datasets were dichotomized for F2R, CD68, or CD163 based on the median expression and further analyzed on the same platform.

Secreted alkaline phosphatase (SEAP) assay to detect PAR1 cleavage

HEK 293 cells stably expressing PAR1-SEAP (kindly provided by Dr. Mosnier, The Scripps Research Institute, La Jolla, CA, USA) were used for reporter assays as described previously [35]. PAR1-SEAP cells were incubated with 100 nM recombinant MMP9 (pre-activated, Sigma, St. Louis, MO, USA), 0.1 U/ml thrombin, or solvent control for 30 minutes in serum-free Opti-MEM (Gibco, Thermo Fischer Scientific, Waltham, MA, USA). Next, the supernatant was removed, and alkaline phosphatase activity was measured according to the manufacturer's instructions on a Synergy HT Biotek Microplate Reader (Biotek Instruments, Winooski, VT, USA).

Phase contrast microscopy and fluorescence microscopy

M0-CM-induced cellular changes were visualized at 20x magnification with phase-contrast on a Zeiss AxioVert microscope. Tracking cell behavior in time was performed with the scanning function on the EVOS® FL Cell Imaging System (Thermo Fischer Scientific, Waltham, MA, USA) at 10x magnification. Unlabelled Capan-2 cells were visualized with the phase contrast channel on the EVOS system. Scanned images were analyzed using ImageJ for area measurement (Capan-2).

MTT cell proliferation and Crystal Violet cell viability assays

Cells at 70% confluence in 96-well plates were serum-starved overnight after which cell proliferation/viability was determined using 3-(4,5-dimethylthiazol-

2-yl)-2,5-diphenyltetrazolium (MTT; 5 mg/ml) or Crystal Violet (0.5% Crystal Violet in 6% Glutaraldehyde in PBS) at 72 hours according to routine procedures. Cells were incubated with MTT reagent for 3 hours or with Crystal Violet for 30 minutes. Measurements were performed on a Synergy HT Biotek Microplate Reader (Biotek Instruments, Winooski, VT, USA) at 560 nm for MTT and 600 nm for Crystal Violet. The decrease in proliferation/viability was calculated based on optical density at t = 0 as 0%.

Flow cytometric detection of Annexin-V for apoptosis

After overnight serum starvation, cells were treated with M0-CM or control media for 48 hours after which free-floating and attached cells were collected, re-suspended in Annexin-V binding buffer (BD, Franklin Lakes, NJ, USA) and transferred to 96-well plates for staining. To each well containing 100 µl cell suspension, 1 µl anti-Annexin-V FITC antibody (BD, Franklin Lakes, NJ) was added. After incubation in the dark for 1 hour, cells were washed twice with Annexin-V binding buffer and re-suspended in 200 µl fresh buffer. Annexin-V positivity was next analyzed on a FACS Canto II (BD, Franklin Lakes, NJ, USA). The gating strategy for FITC positivity was set on the single-cell population (see Fig. 5C). The AnnexinV+ population was determined using antibody control samples (isotype control) applied to all conditions. For analysis, Geometric Mean Fluorescent Intensity (gMFI) on the FITC channel was used. Gating and data analysis were performed using FLOWJO v10 (FlowJo LLC, Ashland, OR, USA).

Lentiviral gene silencing

PAR1 silenced PANC-1, MIA PaCa-2, and Capan-2 cells were established with knockdown efficiencies of around 70% for PANC-1 and Capan-2 and around 50% for MIA PaCa-2 cells [36]. For lentiviral silencing of ZEB1, shRNA clones TRCN0000017565 and TRCN0000017567 were used. Clone shc004 was used as control. Lentivirus was produced by transfecting HEK293T cells with 3rd generation transfer and packaging plasmids pVSV, pMDL, and pRES using Lipofectamine 2000 (Thermo Fisher Scientific, Waltham, MA, USA). 48 and 72 hours after transfection, the supernatant was harvested and 0.45 µm filtered (Millipore, Billerica, MA, USA). PANC-1 cells were transduced with 40 µl lentivirus and incubated for 48 hours. Transduced cells were selected with 2 µg/ml puromycin

(Sigma, St. Louis, MO, USA) for 72 hours, after which the transduction efficiency was analyzed by qRT-PCR for the target gene.

Statistical analysis

Data are presented as mean ± SEM. Statistical analysis was performed using GraphPad PRISM 8.0 (Graphpad Software Inc., La Jolla, CA, USA). Statistically significant differences were considered with a p-value < 0.05. For further details of the statistical analyses, see figure legends. P-values are indicated by asterisks with * $p < 0.05$, ** $p < 0.01$, *** $p < 0.001$, and **** $p < 0.0001$.

RESULTS

PAR1 expression correlates with macrophage markers in human pancreatic tumors

To explore the functional interplay between PAR1, macrophages, and tumor cells, we first determined the correlation between PAR1/F2R and macrophages in both tumor and control pancreatic tissues. To this end, four different PDAC gene expression sets were dichotomized for tissue status (i.e., tumor or non-tumor), after which the expression of the macrophage marker CD68 and F2R(PAR1) was assessed. Both these markers were predominantly high in pancreatic tumor tissue **(Fig. 1A)**. Next, we plotted the expression of the general macrophage marker CD68 and the tumor-associated macrophage marker CD163 versus F2R in tumor-only datasets **(Fig. 1B)**. In these sets, CD68 and CD163 expression significantly correlated **(Sup. Fig 1)**, and both markers correlated with PAR1/F2R expression **(Fig. 1B)**. Subsequent immunohistochemical analysis of our in-house PDAC-TMA showed abundant PAR1, CD68, and CD163 expression, but no co-expression of PAR1 on either CD68- or CD163-positive cells **(Fig. 1C)**. Overall, these data confirm that PAR1 is overexpressed in pancreatic tumor tissues and that PAR1 expression correlates with macrophage numbers in the tumor microenvironment, but that macrophages themselves are PAR1-negative.
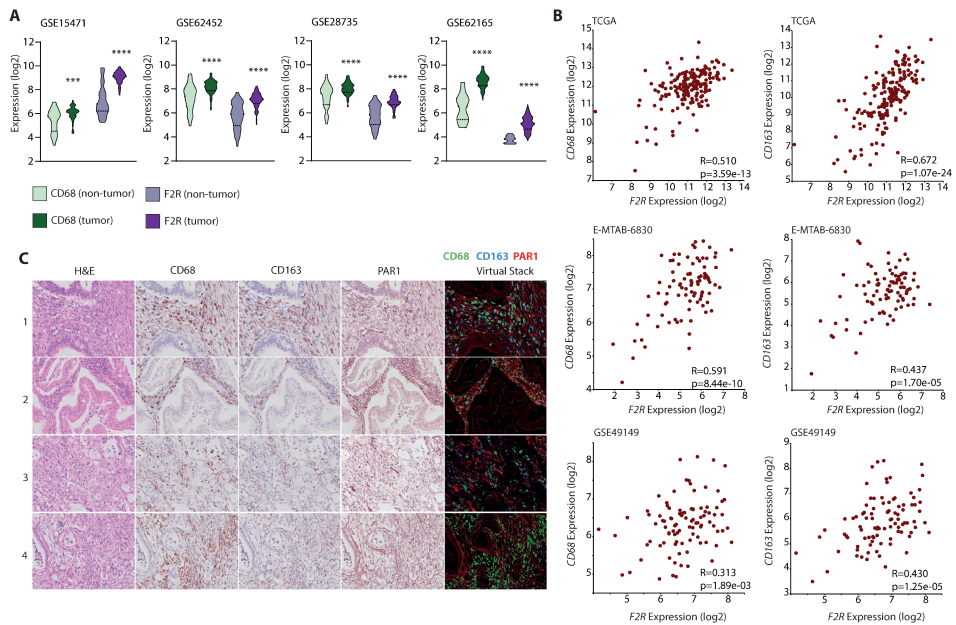
Figure 1

PAR1 is predominantly expressed in tumor tissue and correlates with macrophage markers. (A) Density plots for expression of CD68 (green) and PAR1(F2R) (purple) in the GSE15471, GSE62452, GSE28735 and GSE62165 datasets. For each set, expression in pancreatic cancer patients (dark) and non-tumor controls (light) is indicated. Student's t-tests were used to determine the significance of the differences in expression between the tumor and non-tumor control groups. (B) Correlations between F2R and CD68 or CD163 expression (log2 scale) in the TCGA-PDAC, E-MTAB-6830, and GSE49149 datasets. On the lower right corner of each graph, p-values and Pearson correlation coefficients (R) are shown. (C) Pancreatic tumor micro-array staining for CD68, CD163, PAR1, and H&E. Each layer was scanned separately and generated as virtual stacks in ImageJ. The virtual image stack on the right represents CD68 (green), CD163 (blue), and PAR1 (red) staining.

Macrophages induce EMT in a PAR1-dependent manner

To assess whether the observed correlation between PAR1 expression and macrophage infiltration has any functional consequence, we next focused on the role of PAR1 in the macrophage-tumor cell crosstalk. Conditioned medium (CM) from PMA-induced THP-1 monocytes (characterization shown in **Sup. Fig 2A**), hereafter called M0 macrophages, was applied to PANC-1 pancreatic cancer cells in the absence or presence of the PAR1 inhibitor Vorapaxar **(Fig. 2A)**. We found that M0-CM induced fibroblast-like morphological changes in PANC-1 cells, which was reduced by Vorapaxar-dependent PAR1 inhibition **(Fig. 2A)**. Importantly, the control conditioned medium (PANC-1-CM) did not induce any morphological changes **(Sup. Fig. 2B)**, excluding nutrient depletion to cause the effects of M0-CM. To confirm the specificity of the Vorapaxar results and to show that PAR1 acts on tumor cells, we next incubated PAR1-silenced PANC-1 cells (shPAR1) (as generated previously [36]) and their controls (shCtrl) with M0-CM. Control cells showed similar morphological changes as non-transduced PANC-1 cells, whereas these changes were less apparent in shPAR1 cells **(Fig. 2B)**.

To molecularly characterize the macrophage-induced morphological changes, we measured the expression of cell state markers E-cadherin (CDH1), Zinc finger E-box binding homeobox 1 (ZEB1), and Vimentin (VIM). M0-CM treatment of PANC-1 and MIA PaCa-2 cells resulted in decreased CDH1 expression and increased ZEB1 and VIM expression **(Fig. 2C-D)**. In line with the reduction in morphological changes observed by microscopy **(Fig. 2A and 2B)**, PAR1 inhibition diminished M0-CM-induced changes of cell state markers. PAR1 silenced PANC-1, and MIA PaCa-2 cells showed similar changes as Vorapaxar treated control PAR1 expressing cells **(Fig. 2E-F)**; M0-CM treatment decreased CDH1 and increased ZEB1 and VIM expression in shCtrl cells, but not in shPAR1 cells (that already show enhanced epithelial characteristics as described previously [36]). Of note, and in line with our previous study on the contributions of PAR1 signaling to tumor cell state [36], we found that also in the absence of M0-CM inhibition of PAR1 (using Vorapaxar) resulted in an epithelial phenotype shift in cancer cells.
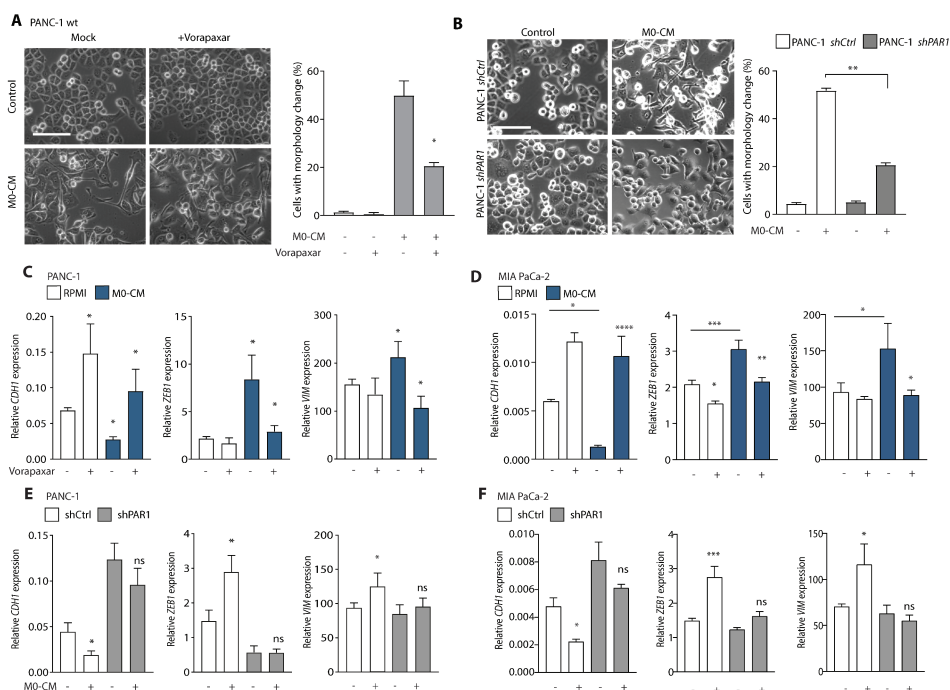
Figure 2

Macrophages induce EMT of pancreatic cancer cells in a PAR1-dependent manner. (A) Phase-contrast microscope images of PANC-1 wildtype cells treated with control or M0-CM medium. PAR1 was inhibited by Vorapaxar (500 nM) using DMSO as a mock control. Spindle-shaped cells were quantified using the cell counter tool of Image J, after which the percentage per field was calculated according to the total number of cells. Shown is the mean ± SEM (n = 3); Student′s t-test. (B) Morphology assessment of shCtrl and shPAR1 PANC-1 cells treated with M0-CM. Spindle-shaped cells were quantified using the cell counter tool of Image J, after which the percentage per field was calculated according to the total number of cells. Shown is the mean ± SEM (n = 3); Student′s t-test. In panels A and B, magnification is 20x, and the scale bar indicates 50 μm. (C-D) Relative mRNA expression of CDH1, ZEB1, and VIM in RPMI-1640 (white) or M0-CM (blue) treated PANC-1 (C) and MIA PaCa-2 (D) cells. PAR1 was inhibited by Vorapaxar (500 nM) using DMSO as a mock control. Shown is the mean ± SEM (n = 4); Student′s t-test. (E-F) Relative mRNA expression of CDH1, ZEB1 and VIM in RPMI-1640 (-) or M0-CM (+) treated PANC-1 (E) or MIA PaCa-2 (F) shCtrl (white) and shPAR1 (gray) cells. Shown is the mean ± SEM (n = 4); Student′s t-test. Relative expression levels, as depicted in panels C-F, were calculated using the comparative threshold cycle (dCt method) and normalized to the expression of the reference gene TBP.

To substantiate our findings that loss of PAR1 seems to block a macrophage-mediated mesenchymal cell state transition, we correlated stromal macrophage content with tumor cell phenotype in PDAC. To avoid confounding by stromal cells expressing mesenchymal markers, we performed these analyses using a laser capture micro-dissected gene expression set (GSE93326) containing paired stromal and tumor epithelium samples. We used the median expression of CD68 and CD163 from the stromal samples to dichotomize the matched tumor samples. Next, we generated differential gene expression plots between CD68 **(Fig. 3A)** or CD163 **(Fig. 3B)** high and low tumor samples. The association with EMT was highlighted using the Hallmark_EMT gene set (derived from MSigDB). Interestingly, most EMT related genes were increased in the CD68 or CD163 high groups. In line with these findings, gene set enrichment analysis (GSEA) showed that both CD68 and CD163 expression positively correlated with epithelial signatures **(Fig. 3C and D)**. Overall, these data suggest that macrophage influx correlates with a mesenchymal tumor state.
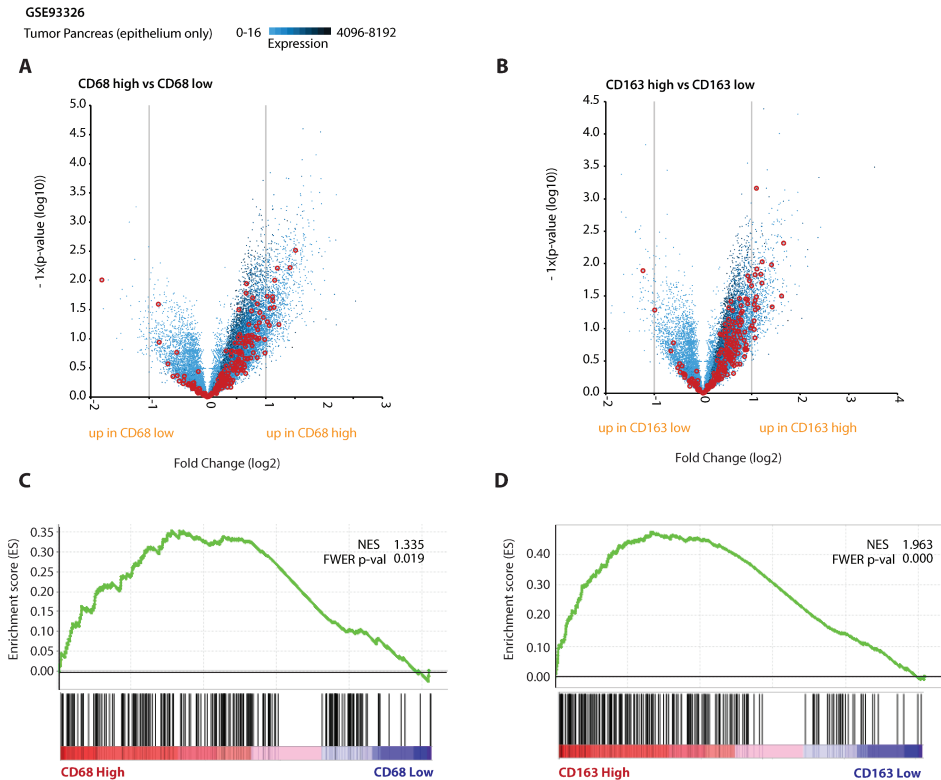
3

Figure 3

Macrophage influx correlates with EMT of cancer cells. High CD68 and CD163 macrophage marker expression in stroma indicate enhanced EMT in epithelial cells. (A-B) Differential expression analysis of tumor cells dichotomized on the stromal expression of CD68 (A) or CD163 (B) with genes from the Hallmark_EMT signature highlighted in red. (C-D) Gene Set Enrichment Analysis (GSEA) results for human PDAC cells from the GSE93326 expression set (dichotomized for median CD68 (C) or CD163 (D)) with the Hallmark_EMT signature. Normalized Enhancement Score (NES) and Family-Wise Error Rate (FWER) p-values are shown on the enrichment plots.

Macrophage-secreted MMP9 activates PAR1 and drives EMT

In order to identify the PAR1 agonist that mediates cancer cell differentiation, we next analyzed expression levels of all confirmed or suggested PAR1-cleaving proteases in M0 macrophages. Although several proteases were found to be expressed by M0 macrophages, MMP9 was most abundantly expressed with levels approximately 1000-fold higher than those of granzyme B, proteinase 3, and kallikrein 4 **(Fig. 4A)**. Although MMP9 has been suggested to act as a PAR1 cleaving protease [37, 38], detailed experimental proof for its activity on PAR1 has so far not been provided. Therefore, we next assessed whether the N-terminal tethered ligand of PAR1 contains a putative MMP9 cleavage site using the CleavPredict algorithm [27]. As shown in **Figure 4B**, this in silico analysis identified three potential MMP9 cleavage sites in the N-terminal part of PAR1 with the most robust proteolytic cleavage for the P1 position at Serine 42. Interestingly, this predicted MMP9 cleavage site lies directly adjacent to the thrombin cleavage site and is similar to the proposed MMP13 cleavage site [39]. To demonstrate that MMP9 may cleave PAR1, SEAP-PAR1 reporter cells [35] were incubated with recombinant MMP9, thrombin (positive control), or PBS (negative control). Both recombinant MMP9 and thrombin efficiently induced the proteolytic release of SEAP indicative of PAR1 cleavage **(Fig. 4C)**. To confirm that macrophage-secreted MMP9 is indeed responsible for the observed macrophage-dependent mesenchymal transition of PANC-1 and MIA PaCa-2 cells, we next determined MMP9 levels in M0-CM and found that the medium indeed contains high MMP9 levels **(Fig. 4D)**. Finally, we assessed whether MMP9 inhibition could block the M0-CM-induced mesenchymal transition. As shown in **Figure 4E and 4F**, the effects of MMP9 inhibition with GM6001 indeed mim-

ic that of Vorapaxar and significantly limited the M0-CM-induced decrease in CDH1 and increases in ZEB1 and VIM expression. As for Figure 2 and our previous work [36], inhibition of MMP9 in the absence of any macrophage-derived cues conferred an increased epithelial phenotype in MIA PaCa-2 cells **(Fig. 4F)**.

To confirm the role of the MMP9-PAR1 axis in mesenchymal transition and to assess the general applicability of our findings, we next used Capan-2 cells that are particularly epithelial and could, therefore, be expected to be more resilient to fully transition into a mesenchymal state [40]. Capan-2 cells were incubated in M0-CM or control medium. M0-CM indeed induced morphological changes (Fig. 4G, white arrows), and these changes were accompanied by decreased CDH1 and increased ZEB1 and Vimentin expression **(Fig. 4H)**. Vorapaxar and GM6001 treatment significantly decreased the M0-CM-induced morphological changes **(Sup. Fig. 3A)**. Similar to PANC-1 and MIA PaCa-2 cells, direct PAR1 inhibition by Vorapaxar or indirect inhibition by GM6001 prevented M0-CM-induced mesenchymal transition of Capan-2 cells as evident from reduced morphological changes as well as reduced expression of the cell state markers CDH1, ZEB1 and VIM. Considering these results, a picture emerges that macrophage-secreted MMP9 activates PAR1, which further orchestrates mesenchymal differentiation.

PAR1 signaling limits macrophage-induced cytotoxicity
Mesenchymal transition is known to cause drug resistance [41], and we aimed to assess whether macrophage-MMP9-PAR1 driven EMT also impacts resistance. Contrary to our expectations, however, we found that M0-CM already caused a substantial decrease in cell viability by itself **(Fig. 5A and Sup. Fig. 3B-C)**. The M0-CM induced cytotoxicity was dependent on the MMP9-PAR1 signaling axis as both Vorapaxar and GM6001 significantly potentiated macrophage-induced cytotoxicity in PANC-1, MIA PaCa-2 and Capan-2 cells **(Fig. 5A-B, and Sup. Fig.3B-C)**. To exclude that the decreased viability after M0-CM medium transfer may be due to nutrient depletion, we compared time-matched medium form PANC-1 cells (PANC-1-CM) with M0-CM and found that the decrease in viability was specific to M0-CM **(Sup. Fig. 4)**. To formally discriminate between cytotoxicity or decreased proliferation after M0-CM treatment, we analyzed Annexin-V positivity in control, and M0-CM-treated PANC-1 and MIA PaCa-2
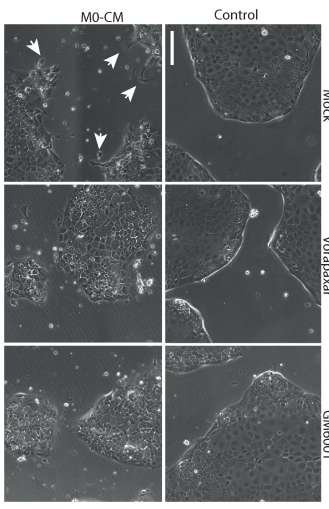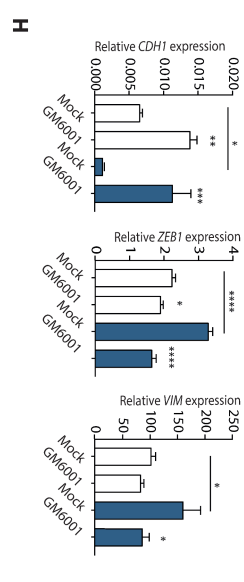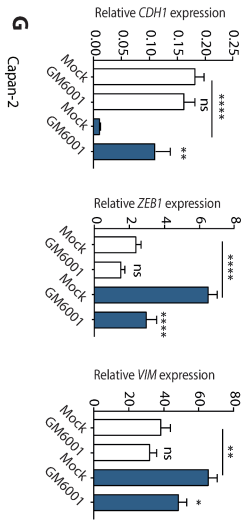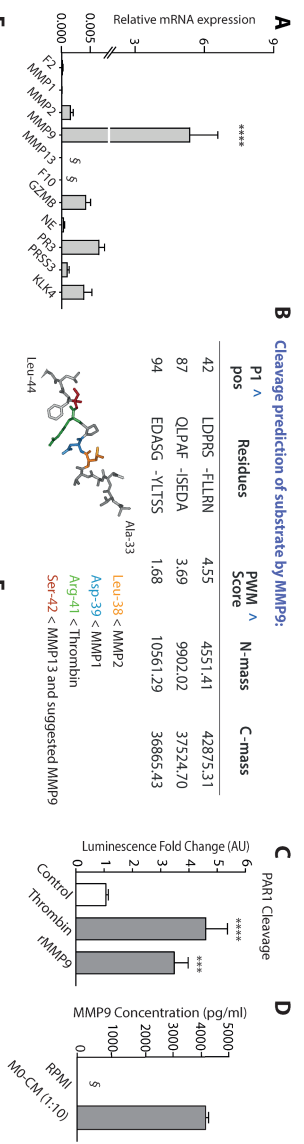
Figure 4

Macrophage-secreted MMP9 activates PAR1. (A) Relative mRNA expression levels of PAR1-cleaving proteases in M0 macrophages. The expression levels of F2 (Thrombin), MMP1, MMP2, MMP9, MMP13, F10 (FX), GZMB, NE, PR3, PRSS3, and KLK4 are shown as mean ± SEM (n = 4); Student´s t-test. § indicates signals below the detection limit. (B) MMP9 cleavage prediction of the PAR1 N-terminal amino acid sequence, derived from the FASTA sequence of Uniprot ID: P25116. P1 position, sequence, and PWM (position weight matrices) are shown together with the mass of the N- and C-terminal sequences after cleavage. Below the table, a stick representation for the PAR1 N-terminal amino acid sequence, where protease cleavage sites are concentrated, is shown. In this representation, locations for MMP2 (yellow), MMP1 (blue), Thrombin (Green) and MMP13, together with MMP9 (red) are indicated. (C) Quantification of PAR1 cleavage with 100 nM recombinant MMP9 (rMMP9) and 0.1 U/ml Thrombin in PAR1-SEAP assays. N = 4. Error bars show mean ± SEM. One-way ANOVA. (D) MMP9 levels in M0-CM and RPMI-1640 media. Shown is the mean ± SEM (n = 4); Student´s t-test. § indicates signals below the detection limit. (E-F) Relative mRNA expression of CDH1, ZEB1, and VIM in RPMI-1640 (white) or M0-CM (blue) treated PANC-1 (E) and MIA PaCa-2 (F) cells. MMP9 was inhibited by GM6001 (5 µM) using DMSO as a mock control. Shown is the mean ± SEM (n = 4); Student´s t-test. (G) Phase-contrast microscope image of Capan-2 cells after control (1:1 DMEM+RPMI-1640) and M0-CM treatment. PAR1 was inhibited by Vorapaxar (500 nM), MMP9 was inhibited by GM6001 (5 µM), and DMSO served as a mock control. Shown are images at t = 72 hours after the addition of M0-CM. Magnification is 10x, and scale bars indicate 100 µm. (H) Relative mRNA expression of CDH1, ZEB1, and VIM in RPMI-1640 (white) or M0-CM (blue) treated Capan-2 cells. PAR1 was inhibited by Vorapaxar (500 nM), MMP9 was inhibited by GM6001 (5 µM), and DMSO served as a mock control. Shown is the mean ± SEM (n = 4); Student´s t-test. Relative expression levels, as depicted in panels E, F, and H, were calculated using the comparative threshold cycle (dCt method) and normalized to the expression of the reference gene TBP.
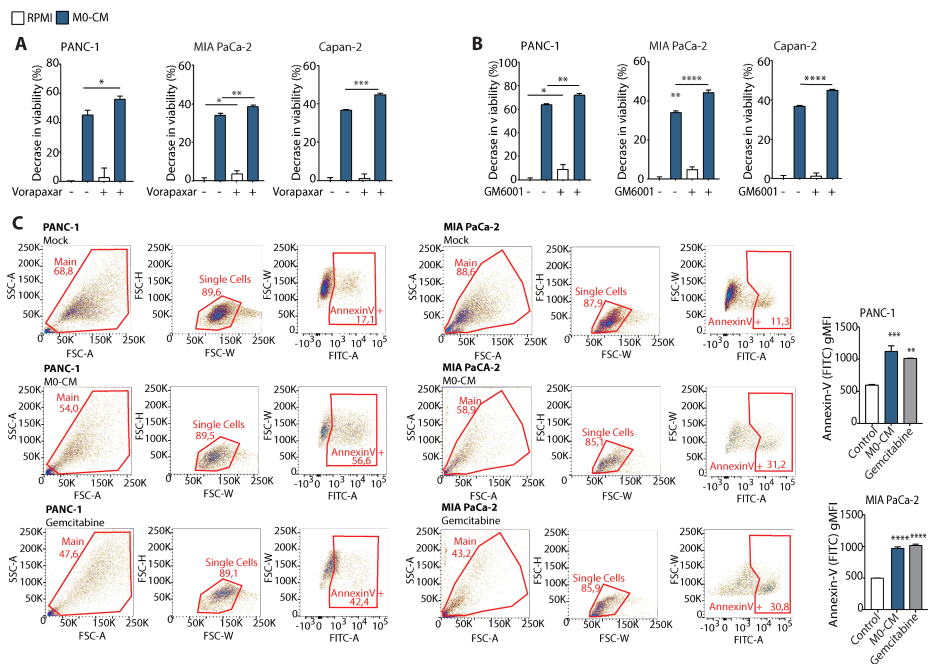
Figure 5

The PAR1-MMP9 axis reduces macrophage induced cytotoxicity. (A-B) MTT viability assay of PANC-1, MIA PaCa-2, and Capan-2 cells in RPMI-1640 (white) or M0-CM (blue) medium. Shown in the effect of PAR1 inhibition with 500 nM Vorapaxar (A) or MMP9 inhibition with 5 μM GM6001 (B). Decreased viability is calculated relative to the viability of control-treated cells. Shown is the mean ± SEM (n = 6); One-way ANOVA. (C) Annexin V-FITC+ cells in mock (RPMI-1640), M0-CM, or positive-control (Gemcitabine) treated PANC-1 and MIA PaCa-2 cells at t = 48 h. Left panel: gating strategy for the Annexin V+ population. The FITC gate was set on antibody controls. Right panel: geometric Mean Fluorescent Intensity (gMFI) on the FITC channel (Annexin V density) for Mock, M0-CM, and positive-control treated cells from the previous panel is given. Shown is the mean ± SEM (n = 3); One-way ANOVA.

cells. M0-CM treatment indeed induced Annexin-V positivity in both cell lines, showing that M0-CM drives PDAC cells into apoptosis **(Fig. 5C)**. To substantiate these findings, we next analyzed the effect of PAR1 silencing on M0-CM-induced cytotoxicity. Under M0-CM treatment, the addition of GM6001 only increased cytotoxicity in shCtrl cells but did not change the response in shPAR1 PANC-1, MIA PaCa-2, and Capan-2 cells **(Sup. Fig. 5A-B)**. Overall, these data suggest that the MMP9-PAR1 axis allows tumor cells to escape macrophage-dependent cell death.

Mesenchymal transition is a prerequisite for tumor cells to survive macrophage-induced cytotoxicity

Activation of PAR1 by macrophage-secreted MMP9 results in increased mesenchymal transition and reduced cell death of PDAC cells. To functionally ascertain that the mesenchymal transition is causal in the escape of PDAC cells from macrophage-dependent cell death, we generated ZEB1-silenced PANC-1 cells to block their capacity to undergo EMT and, subsequently, exposed these cells to M0-CM. ZEB1-silenced cells (knockdown efficiency depicted in **Sup. Fig. 6**) indeed showed largely diminished cell viability in response to M0-CM compared to control silenced cells that are capable of mesenchymal transition **(Fig. 6A)**. Moreover, targeting the MMP9-PAR1 axis in ZEB1-silenced cells did not further affect cell viability, confirming that MMP9-PAR1-dependent mesenchymal transition is the mechanism by which tumor cells escape macrophage-dependent cytotoxicity **(Fig. 6A)**. Overall, these data thus show that mesenchymal transition protects tumor cells from macrophage-induced cytotoxicity **(Fig. 6B)**.
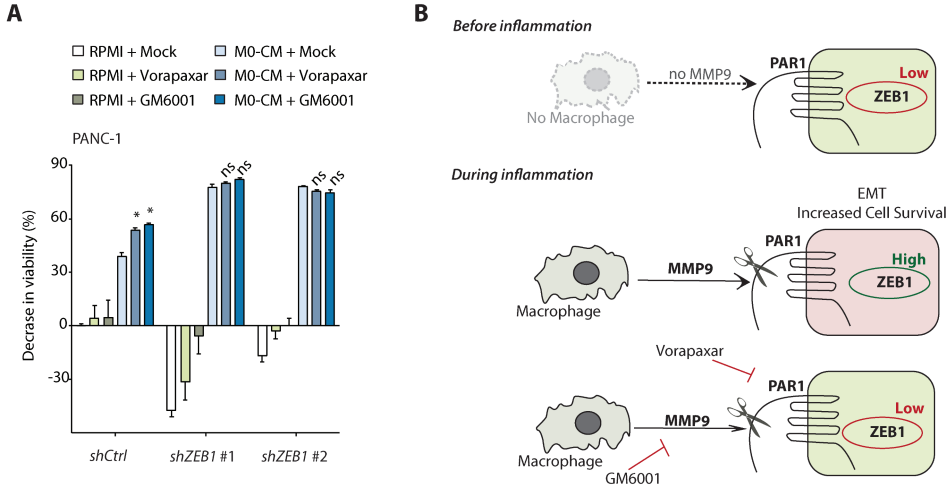
Figure 6

Mesenchymal transition protects tumor cells from macrophage induced cytotoxicity. (A) MTT viability assays of PANC-1 shCtrl, shZEB1 #1, and shZEB1 #2 cells treated with RPMI-1640 (green bars) or M0-CM (blue bars). PAR1 was inhibited by Vorapaxar (500 nM), MMP9 was inhibited by GM6001 (5 µM), and DMSO served as a mock control. Decreased viability was calculated relative to the viability of control-treated cells. Shown is the mean ± SEM (n = 6); One-way ANOVA. (B) Schematic representation showing that macrophages secrete MMP9 that activates PAR1 on pancreatic cancer cells, thereby inducing mesenchymal transition and subsequent resistance to macrophage-induced cytotoxicity.

DISCUSSION

Previous work has shown that stromal PAR1 ablation limits pancreatic cancer progression and potentiates gemcitabine efficacy [23]. In these experiments, diminished tumor growth was accompanied by reduced macrophage infiltration into the tumor [23], and macrophages were found to play a key role in PDAC development and progression [42]. Consequently, we hypothesized that PAR1-dependent macrophage-tumor cell crosstalk may contribute to the poor prognosis of PDAC. Using patient tumor biopsies, we confirmed that PAR1 is overexpressed in pancreatic tumor tissues and that its expression correlates with macrophage infiltration into the tumor microenvironment. Of note, we found that macrophage-derived signals act on PAR1 to mediate tumor-promoting effects. This is of particular interest in light of the dichotomous contributions of macrophages to cancer.

Early during tumor development, bone marrow-derived monocytes are recruited into the tumor microenvironment as an anti-tumor immune response. These cells then differentiate into naive (M0) macrophages, and depending on specific signals from the tumor microenvironment, they subsequently polarize into M2 or tumor-associated macrophages (TAMs), which have been described to induce EMT in cancer cells and drive metastasis and drug resistance [15–17]. Here, we assessed the functional interplay between M0 macrophages, PAR1 and tumor cells and found that M0 macrophages induce distinct morphological changes in PDAC cells reminiscent of EMT. This effect was dependent on an MMP9-PAR1 signaling axis, and subsequent experiments with ZEB1-silenced PDAC cells further underscored the contributions of mesenchymal transition programs to the escape of tumor cells from macrophage-induced cytotoxicity. This suggests that early in the sequence of macrophage recruitment to the tumor microenvironment, M0 macrophage differentiation results in MMP9-PAR1-EMT dependent crosstalk that facilitates tumor progression.

We found that M0 macrophages secrete a PAR1 agonist leading to PAR1-dependent mesenchymal transition of pancreatic cancer cells. Although thrombin is the first described and best-known PAR-1 agonist, more recently, other agonists like matrix metalloproteases (MMPs) and kallikreins have been described [22].

Of these potential PAR1 agonists, we here identified MMP9 as the most likely endogenous agonist secreted by M0 macrophages. Based on MMP9-dependent PAR1 internalization, it has previously been hypothesized that MMP9 may activate PAR1 [38], but functional evidence was not provided. Here, we substantiate these findings by showing that MMP9 indeed cleaves PAR1. Our in silico analysis identified Ser-42 of PAR1 as the most likely MMP9 cleavage site, which is particularly interesting as Ser-42 was previously identified as an MMP13 cleavage site leading to pathological activation of Gαq- and ErbB receptor-dependent pathways in the heart [39], suggesting that MMP9-dependent cleavage indeed activates PAR1. In line with this notion, we found that MMP9 inhibition mimics PAR1 inhibition. Indeed, GM6001 and Vorapaxar both block M0-CM-induced mesenchymal transition and prevent macrophage-induced cytotoxicity. It should be noted that the genetic silencing of PAR1 by shRNA transduction and pharmacological inhibition of PAR1 (Vorapaxar) or MMP9 (GM6001) did not completely reverse M0-CM-induced EMT. Most likely, this may be due to residual PAR1 expression/signaling, although it cannot be ruled out that macrophages secrete alternative mediators that induce morphological changes independent of PAR1.

In the current study, we revealed a tumor-promoting effect of the MMP9/PAR1 axis, suggesting that targeting this axis may have clinical benefit. Although PAR1 is generally considered to promote cancer progression [43], PAR1 may, however, not be the most attractive target to pursue in a cancer setting due to recent observations showing that genetic elimination of PAR1, in fact, aggravates tumor development [36, 44]. The context-dependent role of PAR1 in tumor biology is not fully understood, but it is well conceivable that the outcome of PAR1 activation depends on the activating agonist. Indeed, PAR1 is well known to exert biased agonism, a process in which different agonists activate multiple signaling pathways that have distinct or even opposite effects on cell function [35]. Instead of PAR1, it may thus be better to target MMP9. Interestingly, MMP9 levels have already been shown to correlate with lymph node involvement and the occurrence of distant metastases in pancreatic cancer patients [45]. Moreover, tumor cell MMP9 levels [46], as well as preoperative serum MMP9 concentrations [47], have been found to significantly correlate with the survival of pancreatic cancer patients, identifying MMP9 as a prognostic marker for PDAC survival. Although the clinical efficacy of MMP9 inhibition in PDAC remains to be established,

recent observations that selective MMP9 inhibition in combination with mFOLF-OX6 showed encouraging clinical activity without additional toxicity in patients with HER2-negative gastric and gastric/gastroesophageal junction adenocarcinomas [48], which suggests that MMP9 inhibition may be promising for enhancing combined therapeutic benefits.

CONCLUSION

In the early stages of tumor progression, macrophages exert anti-tumor effects. Here we show that in response to macrophage-secreted MMP9, tumor cells undergo mesenchymal transition in a PAR1-dependent manner. This adds to our understanding of the pro-tumor contributions of macrophages and may explain the contradictory contributions of macrophages to pancreatic as well as other cancers.

DECLARATIONS

Ethics approval and consent to participate
This research project used human tissues that were removed from patients during the course of treatment and that were later made available for scientific research (so-called 'further use' of human tissue). According to the Code of Conduct for dealing with responsibly for human tissues in the context of health research (Human Tissue and Medical Research: Code of conduct for responsible use drawn up by the Federation of Dutch Medical Scientific Societies in collaboration with the Dutch Patient Consumer federation, the Federation of Parent and Patient Organizations and the Biobanking and Biomolecular Resources Research Infrastructure; https://www.federa.org/sites/default/files/digital_version_first_part_code_of_conduct_in_uk_2011_12092012.pdf) these biological materials are as such, not subject to any requirement for ethical review or consent from patients.

Availability of data and material
The gene expression datasets analyzed during the current study were derived from the Gene Expression Omnibus (http://www.ncbi.nlm.nih.gov/gds) using the R2 microarray analysis and visualization platform (http://r2.amc.nl). The gene expression datasets include GSE62452 (Hussain, n = 130), GSE28735 (Zhang, n

= 90), GSE15471 (Badea, n = 78), GSE62165 (Topal, n = 131), E-MTAB-6830 (Xin, n = 90), GSE49149 (Bailey, n = 96), TCGA-PDAC (n = 178) and GSE93326 (Olive, n = 60 epithelial samples) . The data obtained from TMAs are available upon reasonable request from the corresponding author.

REFERENCES

[1]   Li D, Xie K, Wolff R, Abbruzzese JL, Neoptolemos JP, Urrutia R, et al. Pancreatic Cancer [Internet]. Neoptolemos JP, Urrutia R, Abbruzzese JL, Büchler MW, editors. Vol. 980, Pancreatic Cancer. New York, NY: Springer New York; 2018. 1–1661 p.

[2]   Siegel RL, Miller KD, Jemal A. Cancer statistics, 2019. CA Cancer J Clin. 2019;69:7–34.

[3]   Burris HA, Moore MJ, Andersen J, Green MR, Rothenberg ML, Modiano MR, et al. Improvements in survival and clinical benefit with gemcitabine as first-line therapy for patients with advanced pancreas cancer: a randomized trial. J Clin Oncol. 1997;15:2403–13.

[4]   Conroy T, Desseigne F, Ychou M, Bouché O, Guimbaud R, Bécouarn Y, et al. FOLFIRINOX versus gemcitabine for metastatic pancreatic cancer. N Engl J Med. 2011;364:1817–25.

[5]   Von Hoff DD, Ervin T, Arena FP, Chiorean EG, Infante J, Moore M, et al. Increased Survival in Pancreatic Cancer with nab-Paclitaxel plus Gemcitabine. N Engl J Med. 2013;369:1691–703.

[6]   Porta C, Riboldi E, Totaro MG, Strauss L, Sica A, Mantovani A. Macrophages in cancer and infectious diseases: the 'good' and the 'bad.' Immunotherapy. 2011;3:1185–202.

[7]   Jadus MR, Irwin MRC, Horansky RD, Sekhon S, Pepper KA, Kohn DB, et al. Macrophages can recognize and kill tumor cells bearing the membrane isoform of macrophage colony-stimulating factor. Blood. 1996;87:5232–41.

[8]   Goswami KK, Ghosh T, Ghosh S, Sarkar M, Bose A, Baral R. Tumor promoting role of anti-tumor macrophages in tumor microenvironment. Cell Immunol. 2017;316:1–10.

[9]   Jung KY, Cho SW, Kim YA, Kim D, Oh B-C, Park DJ, et al. Cancers with Higher Density of Tumor-Associated Macrophages Were Associated with Poor Survival Rates. J Pathol Transl Med. 2015;49:318–24.

[10]   Lindsten T, Hedbrant A, Ramberg A, Wijkander J, Solterbeck A, Eriksson M, et al. Effect of macrophages on breast cancer cell proliferation, and on expression of hormone receptors, uPAR and HER-2. Int J Oncol. 2017;51:104–14.

[11]   Zhang Q wen, Liu L, Gong C yang, Shi H shan, Zeng Y hui, Wang X ze, et al. Prognostic Significance of Tumor-Associated Macrophages in Solid Tumor: A Meta-Analysis of the Literature. Hoque MO, editor. PLoS One. 2012;7:e50946.

[12]   Su S, Liu Q, Chen J, Chen J, Chen F, He C, et al. A Positive feedback loop between mesenchymal-like cancer cells and macrophages is essential to breast cancer metastasis. Cancer Cell. 2014;25:605–20.

[13]   Fan QM, Jing YY, Yu GF, Kou XR, Ye F, Gao L, et al. Tumor-associated macrophages promote cancer stem cell-like properties via transforming growth factor-beta1-induced epithelial-mesenchymal transition in hepatocellular carci-

3

noma. Cancer Lett. 2014;352:160–8.

[14]   Liu CY, Xu JY, Shi XY, Huang W, Ruan TY, Xie P, et al. M2-polarized tumor-associated macrophages promoted epithelial-mesenchymal transition in pancreatic cancer cells, partially through TLR4/IL-10 signaling pathway. Lab Invest. 2013;93:844–54.

[15]   Mitchem JB, Brennan DJ, Knolhoff BL, Belt BA, Zhu Y, Sanford DE, et al. Targeting tumor-infiltrating macrophages decreases tumor-initiating cells, relieves immunosuppression, and improves chemotherapeutic responses. Cancer Res. 2013;73:1128–41.

[16]   Weizman N, Krelin Y, Shabtay-Orbach A, Amit M, Binenbaum Y, Wong RJ, et al. Macrophages mediate gemcitabine resistance of pancreatic adenocarcinoma by upregulating cytidine deaminase. Oncogene. 2014;33:3812–9.

[17]   Adamska A, Domenichini A, Falasca M. Pancreatic Ductal Adenocarcinoma: Current and Evolving Therapies. Int J Mol Sci. 2017;18:1338.

[18]   Boire A, Covic L, Agarwal A, Jacques S, Sherifi S, Kuliopulos A. PAR1 is a matrix metalloprotease-1 receptor that promotes invasion and tumorigenesis of breast cancer cells. Cell. 2005;120:303–13.

[19]   Cisowski J, O'Callaghan K, Kuliopulos A, Yang J, Nguyen N, Deng Q, et al. Targeting protease-activated receptor-1 with cell-penetrating pepducins in lung cancer. Am J Pathol. 2011;179:513–23.

[20]   Grisaru-Granovsky S, Salah Z, Maoz M, Pruss D, Beller U, Bar-Shavit R. Differential expression of protease activated receptor 1 (Par1) and pY397FAK in benign and malignant human ovarian tissue samples. Int J Cancer. 2005;113:372–8.

[21]   Zhu L, Wang X, Wu J, Mao D, Xu Z, He Z, et al. Cooperation of protease-activated receptor 1 and integrin alphanubeta5 in thrombin-mediated lung cancer cell invasion. Oncol Rep. 2012;28:553–60.

[22]   Macfarlane SR, Seatter MJ, Kanke T, Hunter GD, Plevin R. Proteinase-Activated Receptors. Pharmacol Rev. 2001;53:245 LP – 282.

[23]   Queiroz KCS, Shi K, Duitman J, Aberson HL, Wilmink JW, Van Noesel CJM, et al. Protease-activated receptor-1 drives pancreatic cancer progression and chemoresistance. Int J Cancer. 2014;135:2294–304.

[24]   Committee for Guidelines in Research (COREON). Human Tissue and Medical Research: Code of conduct for responsible use. 2011;

[25]   Pertiwi KR, Van Der Wal AC, Pabittei DR, Mackaaij C, Van Leeuwen MB, Li X, et al. Neutrophil Extracellular Traps Participate in All Different Types of Thrombotic and Haemorrhagic Complications of Coronary Atherosclerosis. Thromb Haemost. 2018;118:1078–87.

[26]   Genin M, Clement F, Fattaccioli A, Raes M, Michiels C. M1 and M2 macrophages derived from THP-1 cells differentially modulate the response of cancer cells to etoposide. BMC Cancer. 2015;15:577.

[27]   Kumar S, Ratnikov BI, Kazanov MD, Smith JW, Cieplak P. CleavPredict:

A Platform for Reasoning about Matrix Metalloproteinases Proteolytic Events. Tsilibary EC, editor. PLoS One. 2015;10:e0127877.

[28]   Wang J, Yang S, He P, Schetter AJ, Gaedcke J, Ghadimi BM, et al. Endothelial nitric oxide synthase traffic inducer (NOSTRIN) is a negative regulator of disease aggressiveness in pancreatic cancer. Clin Cancer Res. 2016;22:5992–6001.

[29]   Zhang G, Schetter A, He P, Funamizu N, Gaedcke J, Ghadimi BM, et al. DPEP1 Inhibits Tumor Cell Invasiveness, Enhances Chemosensitivity and Predicts Clinical Outcome in Pancreatic Ductal Adenocarcinoma. El-Rifai W, editor. PLoS One. 2012;7:e31507.

[30]   Badea L, Herlea V, Dima SO, Dumitrascu T, Popescu I. Combined gene expression analysis of whole-tissue and microdissected pancreatic ductal adenocarcinoma identifies genes specifically overexpressed in tumor epithelia. Hepatogastroenterology. 2008;55:2016–27.

[31]   Raphael BJ, Hruban RH, Aguirre AJ, Moffitt RA, Yeh JJ, Stewart C, et al. Integrated Genomic Characterization of Pancreatic Ductal Adenocarcinoma. Cancer Cell. 2017;32:185-203.e13.

[32]   Dijk F, Veenstra VL, Soer EC, Dings MPG, Zhao L, Halfwerk JB, et al. Unsupervised class discovery in pancreatic ductal adenocarcinoma reveals cell-intrinsic mesenchymal features and high concordance between existing classification systems. Sci Rep. 2020;10:1–12.

[33]   Arnes L, Liu Z, Wang J, Maurer C, Sagalovskiy I, Sanchez-Martin M, et al. Comprehensive characterisation of compartment-specific long non-coding RNAs associated with pancreatic ductal adenocarcinoma. Gut. 2019;68:499–511.

[34]   Nones K, Waddell N, Song S, Patch A-MM, Miller D, Johns A, et al. Genome-wide DNA methylation patterns in pancreatic ductal adenocarcinoma reveal epigenetic deregulation of SLIT-ROBO, ITGA2 and MET signaling. Int J Cancer. 2014;135:1110–8.

[35]   Mosnier LO, Sinha RK, Burnier L, Bouwens EA, Griffin JH. Biased agonism of protease-activated receptor 1 by activated protein C caused by noncanonical cleavage at Arg46. Blood. 2012;120:5237–46.

[36]   Tekin C, Shi K, Daalhuisen JB, ten Brink MS, Bijlsma MF, Spek CA. PAR1 signaling on tumor cells limits tumor growth by maintaining a mesenchymal phenotype in pancreatic cancer. Oncotarget. 2018;9:32010–23.

[37]   Flaumenhaft R, De Ceunynck K. Targeting PAR1: Now What? Trends Pharmacol Sci. 2017;38:701–16.

[38]   Florence JM, Krupa A, Booshehri LM, Allen TC, Kurdowska AK. Metalloproteinase-9 contributes to endothelial dysfunction in atherosclerosis via protease activated receptor-1. Hribal ML, editor. PLoS One. 2017;12:e0171427.

[39]   Jaffré F, Friedman AE, Hu Z, MacKman N, Blaxall BC. β-Adrenergic receptor stimulation transactivates protease-activated receptor 1 via matrix metalloproteinase 13 in cardiac cells. Circulation. 2012;125:2993–3003.

[40]   Aiello NM, Maddipati R, Norgard RJ, Balli D, Li J, Yuan S, et al. EMT Subtype Influences Epithelial Plasticity and Mode of Cell Migration. Dev Cell. 2018;45:681-695.e4.

[41]   Kuwada K, Kagawa S, Yoshida R, Sakamoto S, Ito A, Watanabe M, et al. The epithelial-to-mesenchymal transition induced by tumor-associated macrophages confers chemoresistance in peritoneally disseminated pancreatic cancer. J Exp Clin Cancer Res. 2018;37:1–10.

[42]   Niu N, Lu P, Yang Y, He R, Zhang L, Shi J, et al. Loss of Setd2 promotes Kras-induced acinar-to-ductal metaplasia and epithelia-mesenchymal transition during pancreatic carcinogenesis. Gut. 2020;69:715–26.

[43]   Wojtukiewicz MZ, Hempel D, Sierko E, Tucker SC, Honn K V. Protease-activated receptors (PARs)—biology and role in cancer invasion and metastasis. Cancer Metastasis Rev. 2015;34:775–96.

[44]   Adams GN, Sharma BK, Rosenfeldt L, Frederick M, Flick MJ, Witte DP, et al. Protease-activated receptor-1 impedes prostate and intestinal tumor progression in mice. J Thromb Haemost. 2018;16:2258–69.

[45]   Pryczynicz A, Guzińska-Ustymowicz K, Dymicka-Piekarska V, Czyzewska J, Kemona A. Expression of matrix metalloproteinase 9 in pancreatic ductal carcinoma is associated with tumor metastasis formation. Folia Histochem Cytobiol. 2007;45:37–40.

[46]   Jakubowska K, Pryczynicz A, Januszewska J, Sidorkiewicz I, Kemona A, Niewiński A, et al. Expressions of Matrix Metalloproteinases 2, 7, and 9 in Carcinogenesis of Pancreatic Ductal Adenocarcinoma. Dis Markers. 2016;2016:1–7.

[47]   Mroczko B, Lukaszewicz-Zajac M, Wereszczynska-Siemiatkowska U, Groblewska M, Gryko M, Kedra B, et al. Clinical significance of the measurements of serum matrix metalloproteinase-9 and its inhibitor (tissue inhibitor of metalloproteinase-1) in patients with pancreatic cancer: Metalloproteinase-9 as an independent prognostic factor. Pancreas. 2009;38:613–8.

[48]   Shah MA, Starodub A, Sharma S, Berlin J, Patel M, Wainberg ZA, et al. Andecaliximab/GS-5745 alone and combined with mFOLFOX6 in advanced gastric and gastroesophageal junction adenocarcinoma: Results from a phase I study. Clin Cancer Res. 2018;24:3829–37.
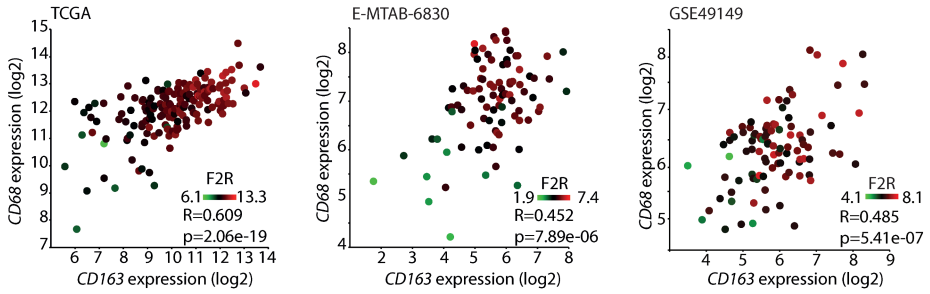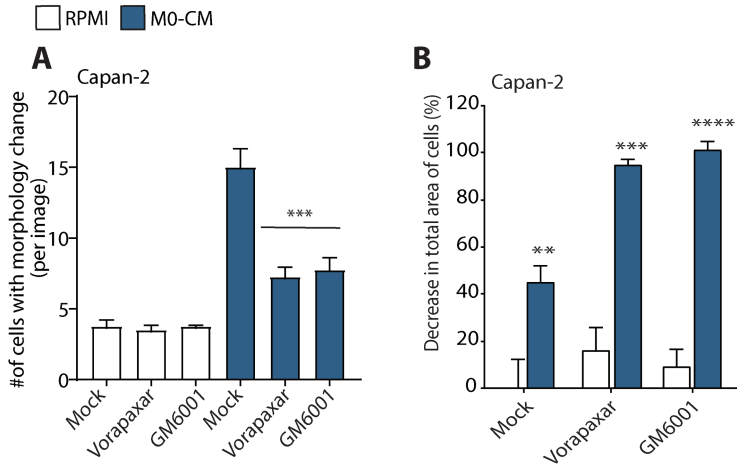
Supplementary Figure 1

Correlation of CD68 with CD163 expression (on log2 scale) in the TCGA-PDAC, E-MTAB-6830, and GSE49149 datasets. On the lower right corner of each graph, p-values and Pearson correlation coefficients (R) are shown.
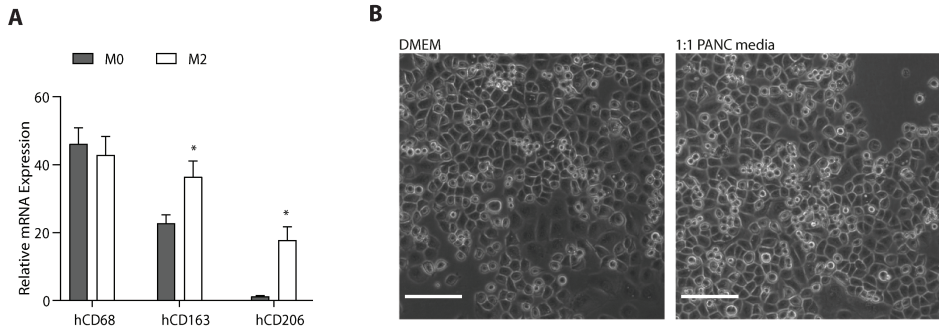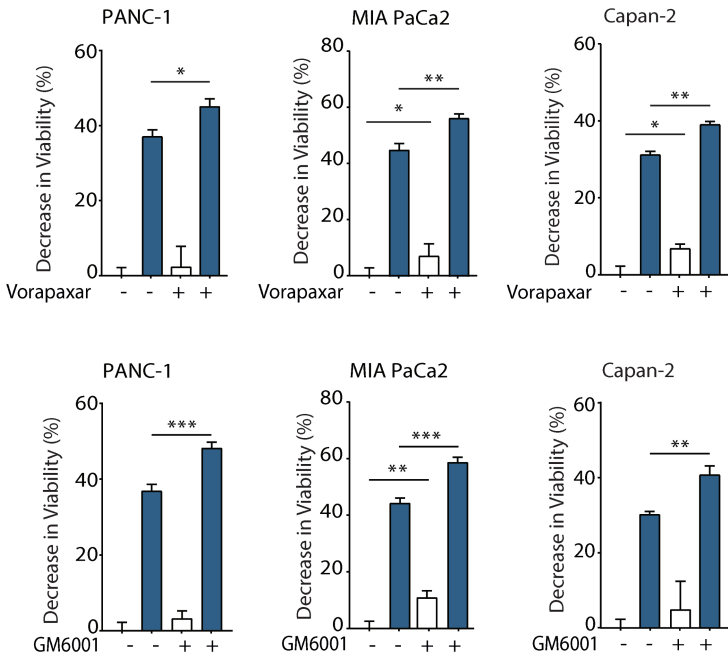

Supplementary Figure 2

(A) Relative mRNA expression of CD68, CD163, and CD206 in M0 and M2 macrophages. Shown is the mean±SEM (n=4); One-way ANOVA. Relative expression levels, as depicted in this panel, were calculated using the comparative threshold cycle (dCt method) and were normalized for expression of the reference gene TBP. (B) Phase-contrast microscope images of PANC-1 cells under RPMI and 1:1 PANC-CM treatment. Images are taken at t=72 hours. Magnification is at 10X, and scale bars indicate 100 µm.
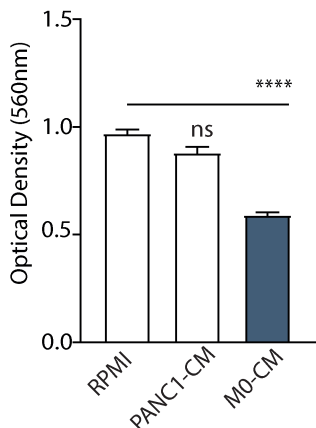
Supplementary Figure 3

(A) Quantification of morphological changes of Capan-2 cells treated with RPMI (white) or M0-CM (blue). PAR1 was inhibited by Vorapaxar (500 nM), MMP9 was inhibited by GM6001 (5 µM), and DMSO served as a mock control. Quantification is done at t=72h (images are shown in Fig. 3G). Shown is the mean±SEM (n=4); One-way ANOVA. (B) Cell numbers of Capan-2 cells after RPMI (white) or M0-CM (blue) treatment calculated based on the difference in total cell area at t=96 versus t=0 hours. PAR1 was inhibited by Vorapaxar (500 nM), MMP9 was inhibited by GM6001 (5 µM), and DMSO served as a mock control. Shown is the mean±SEM (n=3); Student´s t-test. (C) Crystal Violet assays of PANC-1, MIA PaCa-2, and Capan-2 cells treated with RPMI (white) or M0-CM (blue). Shown is the effect of PAR1 inhibition with 500 nM Vorapaxar (A) or MMP9 inhibition with 5 µM GM6001.

Supplementary Figure 4

MTT viability assays of PANC-1 cells treated with RPMI, PANC-CM, and M0-CM. Shown is the mean±SEM (n=4); One-way ANOVA.
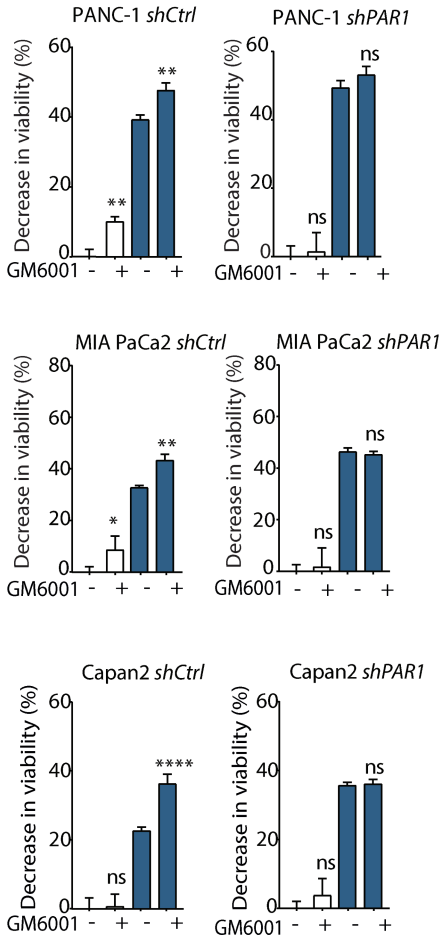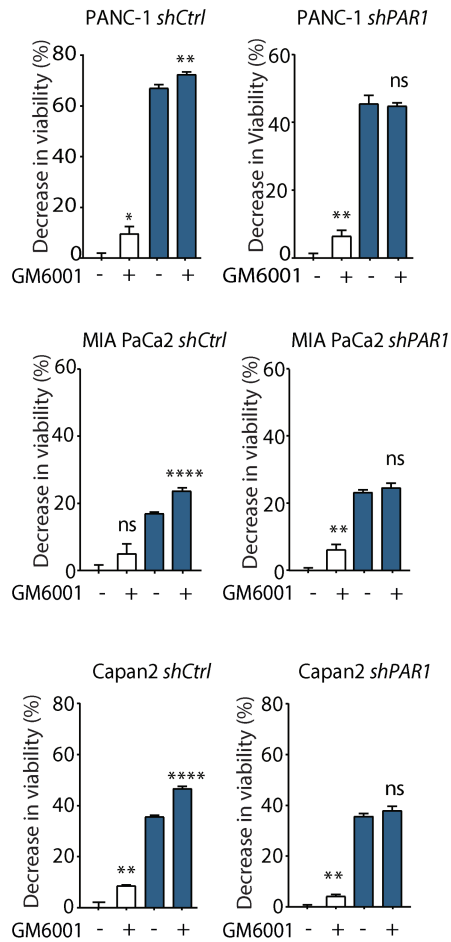
Supplementary Figure 5

MTT (A) and Crystal Violet (B) cell viability assays of PANC-1, MIA PaCa-2, and Capan-2 cells treated with RPMI (white) or M0-CM (blue). PAR1 was inhibited by Vorapaxar (500 nM), MMP9 was inhibited by GM6001 (5 µM), and DMSO served as a mock control. Shown is the mean±SEM (n=6); One-way ANOVA.
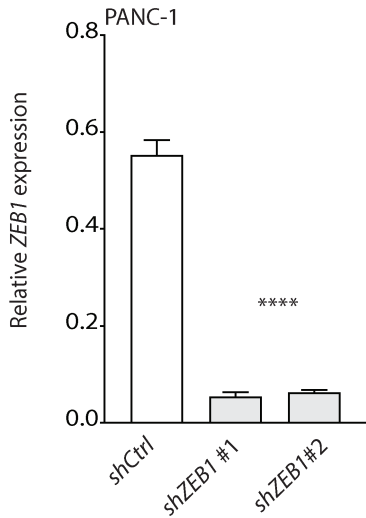
Supplementary Figure 6

Relative ZEB1 mRNA expression of control (shCtrl) and ZEB1 (shZEB1 #1 and shZEB1 #2) silenced PANC-1 cells. Shown is the mean±SEM (n=4); One-way ANOVA. Relative expression level, as depicted in this panel, was calculated using the comparative threshold cycle (dCt method) and was normalized for expression of the reference gene TBP.

Chapter 4

Early macrophage infiltrates impair pancreatic cancer cell growth by TNF-α secretion

Cansu Tekin, Hella L Aberson, Maarten F Bijlsma, C Arnold Spek

ABSTRACT

Background: Pancreatic ductal adenocarcinoma (PDAC) is a grim disease with high mortality rates. Increased macrophage influx in PDAC is a common hallmark and associated with poor prognosis. Macrophages have high cellular plasticity, which can differentiate into both anti- and pro-tumorigenic properties. Here, we investigated how naïve (M0) macrophages differ from other macrophages in their anti-tumorigenic activities.

Methods: In vitro BrdU proliferation and Annexin V cell death analyses were performed on PANC-1 and MIA PaCa-2 PDAC cell lines exposed to conditioned medium of different macrophage subsets. Macrophage secreted factors were measured by transcript analysis and ELISA. Therapeutic antibodies were used to functionally establish the impact of the identified cytokine on PDAC proliferation.

Results: Proliferation and cell death assays revealed that only M0 macrophages harbor anti-tumorigenic activities and that M1, M2, and TAMs do not. mRNA analysis and ELISA results suggested TNF-α as a potential candidate to mediate M0 macrophage induced cell death. To demonstrate the importance of TNF-α in M0 macrophage-induced cell death, PANC-1 and MIA PaCa-2 cell-lines were exposed to M0 macrophage conditioned medium in the presence of the TNF-α inhibitor Infliximab, which effectively diminished the anti-tumor activities of M0 macrophages.

Conclusion: Newly tumor-infiltrated naive M0 macrophages exert anti-tumorigenic activities via TNF-α secretion. Their subsequent differentiation into either M1, M2, or TAM subsets reduces TNF-α levels, thereby abolishing their cytotoxic activity on PDAC cells. These data suggest that reestablishing TNF-α secretion in differentiated macrophages might yield a therapeutic benefit.

INTRODUCTION

Pancreatic ductal adenocarcinoma (PDAC), the most common form of pancreatic cancer, is a highly malignant disease with very poor reported 5-year survival rates of less than 8% [1]. Despite numerous research efforts and the development of therapeutics to overcome the low overall survival in PDAC, disease progression rates and mortality have declined only marginally [2]. High therapy resistance and complex interactions with the immune system are some of the major features that limit the efficacy of current treatments against PDAC [3].

As part of the innate immune system, monocytes are recruited to damaged tissue as the initial response and are subsequently activated to become macrophages. These newly infiltrated macrophages, also known as naïve (M0) macrophages, then respond to extracellular signals in the tissue and differentiate into either classically activated macrophages (M1, also known as pro-inflammatory) or alternatively activated macrophages (M2, also known as anti-inflammatory) [4]. However, in tumor tissue, infiltrated macrophages can differentiate into a specific subset of macrophages known as tumor-associated macrophages (TAMs), which often harbor M2-like characteristics [5]. Macrophage infiltration in solid tumors is common, and despite being part of an immune response, it is often associated with poor prognosis and metastatic disease [6].

In pancreatic cancer, the role of TAMs in metastasis and chemoresistance has been studied extensively. TAMs are generally considered to be tumor-promoting members of the PDAC tumor microenvironment, which should be targeted to limit disease progression [7]. Notwithstanding, when and how the initial anti-tumor macrophage response transitions to a tumor-promoting macrophage phenotype are unclear. Given the increasingly recognized importance of the immune system in cancer and its potential for therapy development, the identification of anti-tumor macrophage responses could be an essential step forward to harness the immune responses at play in PDAC. This study demonstrates how naïve M0 macrophages differ from further differentiated macrophages in terms of anti-tumorigenic activities. We further identify M0 macrophage secreted c as a potent tumor cell-death inducer.

MATERIAL AND METHODS

Cell-lines and cell culture

Human PANC-1 and MIA PaCa2 pancreatic cancer cells (ATCC, Manassas, VA) were cultured in DMEM (Gibco, Thermo Fischer Scientific, Waltham, MA) with 4.5 g/mL glucose, and human THP-1 cells (ATCC) were cultured in RPMI-1640 (Gibco). All cell culture media were supplemented with 10% fetal bovine serum (FBS), L-glutamine (2 mM), except RPMI-1640 media for conditioned media experiments, which was supplemented with 1X GlutaMAX (Gibco), penicillin (100 units/mL) (Gibco), and streptomycin (500 μg/mL) (Lonza, Basel, Switzerland) in regular cell culture procedures. Cultures were incubated in 5% CO_2 incubators at 37oC. All cell lines were authenticated by STR profiling (Promega PowerPlex, Leiden, Netherlands) and tested for mycoplasma by PCR monthly.

Generation of M0, M1, M2, and TAM macrophages from THP-1 cells

THP-1 cells were initially treated with 150 nM phorbol 12-myristate 13-acetate (PMA, Sigma, St. Louis, MO, USA) for 24 hours in RPMI-1640 medium. Next, activated THP-1 cells were washed with fresh medium to remove PMA. Cells were cultured in refreshed, fully supplemented RPMI-1640 medium for another 24 hours, after which the medium was renewed once more. Without any other additions, macrophages were considered M0 macrophages at this stage (see Figure 1 for validation). M0 macrophages were treated with 1 ng/ml LPS (Ultrapure, Invivogen, Toulouse, France) for 24 hours to generate M1 macrophages. M0 macrophages were treated with 20 ng/ml recombinant IL-4 (Peprotech, Rocky Hill, NJ) and IL-13 (Peprotech) each for 72 hours to generate M2 macrophages. Finally, for the generation of tumor-associated macrophages (TAM), M0 macrophages were treated with a supernatant mix (collected from PANC-1 and MIA PaCa-2 cells at ~80% confluence) in a 1:1 dilution with fresh complete RPMI-1640 media for 72 hours. At the end of each incubation, macrophages were washed twice with a fully supplemented RPMI-1640 medium to remove the cytokines and other factors from the flask. Media collections were performed after 48 hours of incubation. Collected media centrifuged at 1200 rpm for 4 minutes to remove cell debris, filtered using 0.2 μm syringe filters (Corning, Corning, New York), and stored at 4oC. For experimental procedures, all conditioned media were diluted

1:1 with fresh media (DMEM) to ascertain the medium's appropriate nutrient content.

Generation of monocyte-derived macrophages from peripheral blood mononuclear cells

Peripheral blood mononuclear cells (PBMC) were obtained by Ficoll-Paque (GE Healthcare, Chicago, IL, USA) density centrifugation from whole blood collected from a single healthy volunteer (following institutional standard operating protocol and under the approval of Medical Ethics Review Committee) in lithium-heparin coated blood tubes (BD, Franklin Lakes, NJ). For monocyte isolation from PBMC, the MACS Monocyte Isolation kit with CD14+ magnetic beads was used with MACS LS Columns according to the manufacturer's manual (Miltenyi Biotec, Bergisch Gladbach, Germany). Isolated monocytes were plated in fully supplemented RPMI media and treated with either 50 ng/ml M-CSF (Prospec, Rehovot, Israel) or 50 ng/ml GM-CSF (Prospec) for six days to obtain M0 subtype monocyte-derived macrophages (MDM); media were refreshed together with the cytokines every two days. To obtain the M1 and M2 MDM subtypes, all media were removed on day six, after which the M0 macrophages were treated for 24 hours with 50 ng/ml IFN-γ (Peprotech) on the previously GM-CSF treated group or with 20 ng/ml IL-4 (Peprotech) and IL-13 (Peprotech) on the previously M-CSF treated group to obtain M1 and M2 MDMs respectively. Conditioned media from all subtypes were collected and processed as for the THP-1 derived macrophage media.

Quantitative real-time PCR

Total RNA of the samples was isolated using a NucleoSpin RNA miniprep kit with DNase treatment (Macherey Nagel, Düren, Germany), and cDNA from the samples were synthesized from total RNA (with 1000ng total RNA per sample) using M-MLV-RT (Promega, Leiden, Netherlands) and random hexamers (Qiagen, Hilden, Germany). Quantitative RT-PCR was performed to determine the mRNA levels, with Sensifast SYBR No-Rox Kit (Bioline, London, UK), measured on LightCycler 480 II (Roche, Basel, Switzerland). Relative expression levels were calculated using the comparative threshold cycle (dCt) method and further normalized to expression of the reference gene TBP. All primer sequences of the analyzed genes are shown in Supplementary Table 1.

BrdU proliferation assay

PANC-1 and MIA PaCa2 cells were seeded in black, clear-bottom 96-well plates (Corning) in DMEM without serum. The following day, macrophage conditioned media were added in a 1:1 dilution with complete DMEM. BrdU labeling solution was given to cells after 48 hours of conditioned media treatment. All experimental steps in the BrdU assay were performed according to the manufacturer's instructions (Chemiluminescent BrdU assay, Roche). Luminescence was measured on a Synergy HT Biotek Microplate Reader (Biotek Instruments, Winooski, VT). For testing the functional importance of TNF-α in M0 conditioned medium, we included human recombinant TNF-α (Sigma) in increasing concentrations from 10 pg to 10 ng and the TNF-α inhibitor Infliximab (Remicade, MSD, Kenilworth, NJ) at 25 ug/ml.

TNF-α ELISA

A commercially available ELISA kit (R&D Systems, Minneapolis, MN) was used to determine TNF-α levels from THP-1- and MDM-derived macrophage supernatants. Samples were measured in 4 biological replicates. All experimental steps were performed according to the manufacturer's instructions, and the absorbance was measured with the Synergy HT Biotek microplate reader (Biotek Instruments) at 450 and 655 nm.

Flow cytometry detection of Annexin V

Cells were treated for 48 hours with different macrophage supernatants and with a 1:1 DMEM-RPMI mix as control. Cell supernatants were collected in a tube to include non-adherent cells. Cells were detached using trypsin, and this cell fraction was pooled with the cell supernatant in a 15 mL tube. The mix was pelleted by centrifugation at 1200 rpm for 5 minutes. The pellet was re-suspended in Annexin V binding buffer (BD) and distributed to 96-well plates for staining. Each well contained 100 μl of cell mix and 1 μl Annexin V FITC (BD). The plate was incubated on ice, in the dark, for 1 hour. After incubation, the plate was washed twice with Annexin V binding buffer, and cells were re-suspended in 200 μL in the same buffer for measuring. The measurements were performed on a FACS Canto II (BD). Data were analyzed using FLOWJO v10 (FlowJo LLC, Ashland, OR). Cells were gated initially based on FCS and SSC for the main cell

population, and then on FCS-H and FCS-W to obtain single cells. FITC-positive populations were gated based on isotype antibody control samples. For quantification, Geometric Mean Fluorescent Intensity (gMFI) on FITC values were used.

Statistical Analysis

Data were presented as mean ± SEM. Statistical analyses were performed using GraphPad PRISM 7.0 (Graphpad Software Inc., La Jolla, CA). Differences were considered statistically significant at a p-value of less than 0.05. For further details of the statistical analysis, see figure legends. P-values on graphs are indicated by asterisks with * $p < 0.05$, ** $p < 0.01$, *** $p < 0.001$, and **** $p < 0.0001$.

4

RESULTS

Anti-tumor activity of macrophages is restricted to the M0 (naïve) subset

The crosstalk between newly infiltrated monocytes and other constituents of the cancer microenvironment (most notably tumor cells) leads to the differentiation of monocytes into macrophages. Subsequent tumor stimuli then induce differentiation of these macrophages into TAMs, which exhibit pro-tumorigenic properties [8]. Recent work from our group has shown that M0 (naïve) macrophages harbor cytotoxic properties against PDAC cell lines [9], but how this relates to the tumor-promoting capacities of other macrophage subsets remains unclear. We hypothesized that, as macrophages differentiate in the tumor microenvironment, their anti-tumor activities would gradually be lost, with TAMs bearing no anti-tumor activity at all. To test this hypothesis, we turned to an isogenic system to generate the four major subtypes of macrophages; M0 (PMA induced THP-1 monocytes; **Fig. 1A**), M1, M2, and TAM. Macrophage differentiation was successful, as evident from mRNA analysis of the specific markers CD68 (for all macrophages), CD163 (predominantly for TAM), CD206 (for TAM and M2), CD80 (for M1), and CD31 (to confirm monocytic lineage) **(Fig. 1B)**.
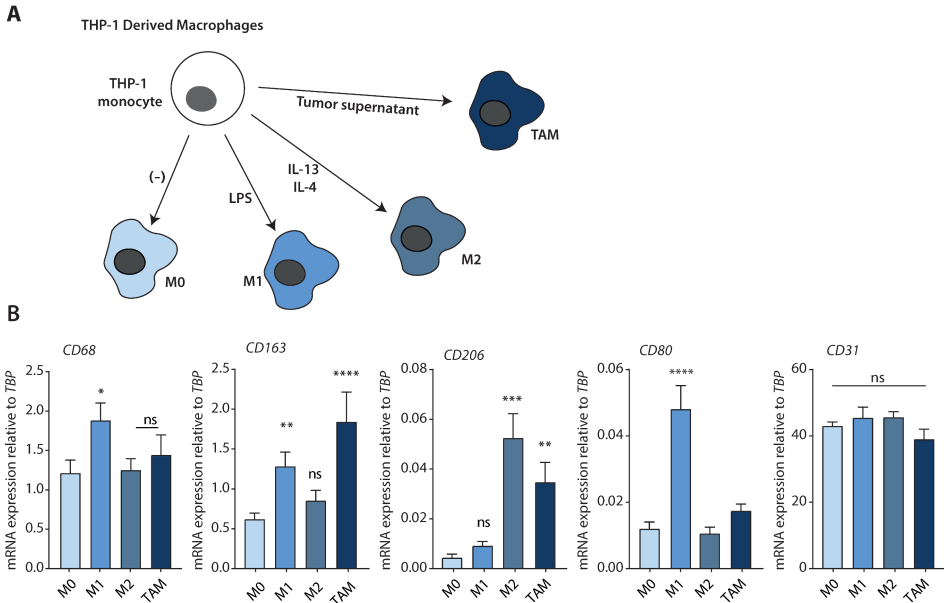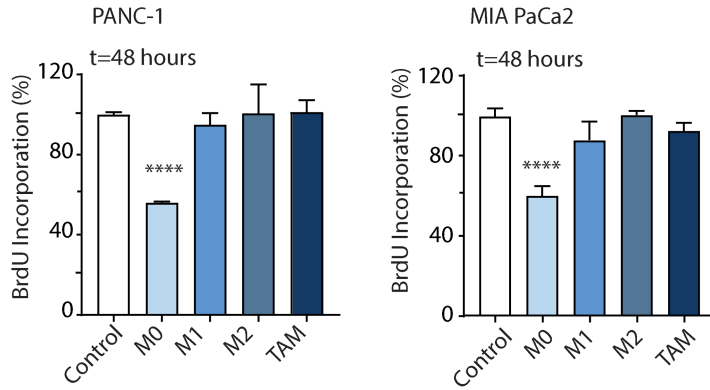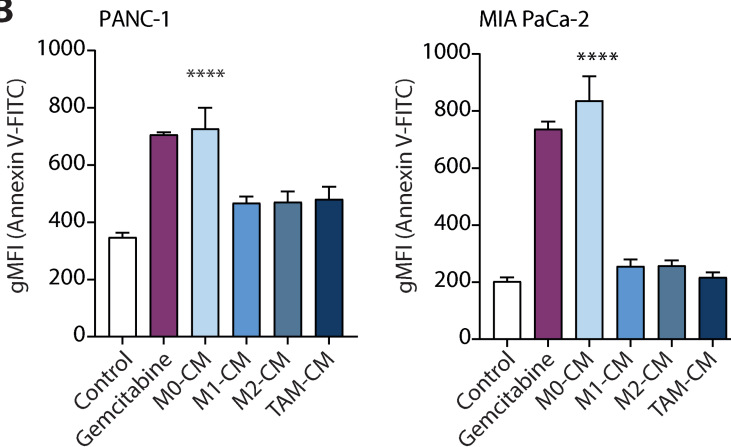
Figure 1

Macrophage subsets used in this study. (A) Schematic representation of the macro-phage differentiation procedure and the resulting macrophage subtypes. (B) Relative mRNA expression of CD68, CD163, CD206, CD80, and CD31 on the macrophage subtypes. On the figure shown is the mean ± SEM (n = 6); One-way ANOVA was used to assess statistical significance. Relative expression levels were calculated using the dCt method and normalized to the expression of the reference gene TBP.

To assess the impact of these different macrophage subtypes on cancer cell viabil-ity, we cultured PANC-1 and MIA PaCa-2 PDAC cell lines with conditioned me-dia from the different macrophage subsets. Proliferation was measured by BrdU incorporation. We found that both cell lines treated with M0-conditioned media (M0-CM) had significantly fewer proliferating cells when compared to control, and, of note, compared to all other macrophage media **(Fig. 2A)**. To test whether this observation was due to M0-CM-induced cell cycle arrest or cell death, we stained the macrophage media-treated cells with a fluorescently labeled Annexin V and measured its levels by flow cytometry. This revealed that M0-CM treated cells had markedly increased Annexin V positivity **(Fig. 2B)**, indicating that M0 macrophages induce apoptosis in PDAC cells, whereas more differentiated mac-rophage subsets do not.

M0 macrophage secreted TNF-α is essential for anti-tumorigenic activities
Next, we investigated potential key cytokines secreted by the macrophage sub-sets. We included both anti- and pro-inflammatory cytokines involved in tumor suppression such as TNF-α, IL-1β, and tumor promotion such as IL-10, CCL22, CXCL5, and TGF-β (selection of cytokines based on ref. [10,11]). Since only M0 macrophages exerted anti-tumor effects, we looked for a significantly different expression of any cytokine in this particular macrophage subset. mRNA anal-ysis of selected cytokines revealed a marked increased expression of TNFA in the M0 group **(Fig. 3A)**, whereas other cytokines exhibited either no significant differences or non-M0 specific expression. ELISA measurements of TNF-α in macrophage media further confirmed that M0 macrophages secrete significantly more TNF-α than do other macrophage subsets **(Fig. 3B)**.

Figure 2

Anti-tumorigenic activities on PDAC cells are unique to the M0 subset of macrophages. (A) BrdU proliferation assay of PANC-1 and MIA PaCa-2 cells in RPMI-1640 (negative-control) or conditioned media from different macrophage subtypes at t=48 hours. On the figure shown is the mean ± SEM (n = 4); One-way ANOVA was used to assess statistical significance. (B) Annexin V-FITC positive cells in negative-control (RPMI-1640), conditioned media from different macrophage subtypes, or Gemcitabine (as positive-control) treated PANC-1 and MIA PaCa-2 cells at t = 48 h. Plotted is the Geometric Mean Fluorescence Intensity (gMFI) on the FITC channel (Annexin V density). On the figure shown is the mean ± SEM (n = 3); One-way ANOVA was used to assess statistical significance.
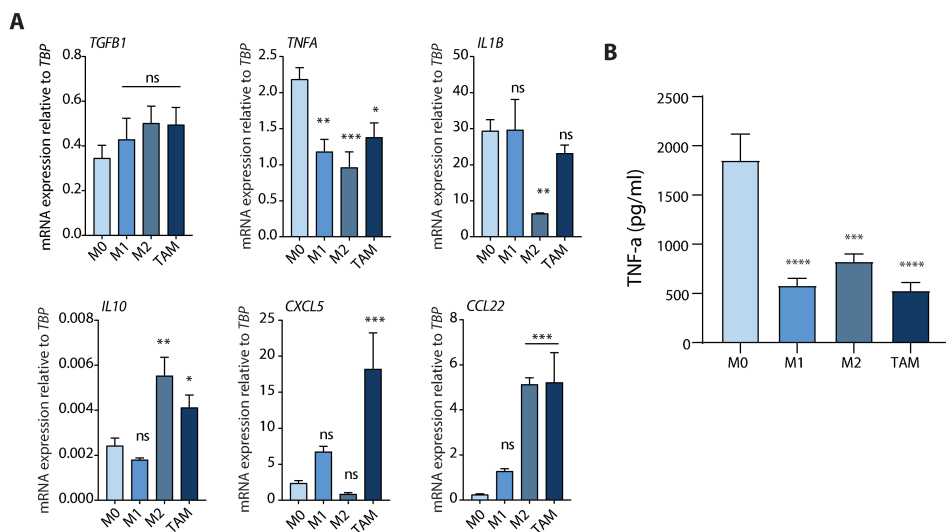
Figure 3

M0 macrophages express higher levels of TNF-α. (A) Relative mRNA expression of TGF-β, TNF-α, IL-1β, IL10, CXCL5, and CCL22 in the indicated macrophage subsets. On the figure shown is the mean ± SEM (n = 4); One-way ANOVA was used to assess statistical significance. Relative expression levels were calculated using the dCt method and normalized to the expression of TBP. (B) TNF-α levels in conditioned media from all given macrophage subsets, measured by ELISA. On the figure shown is the mean ± SEM (n = 4); One-way ANOVA was used to assess statistical significance.

The THP-1 cell line is a human monocytic cell line derived from an acute myeloid leukemia (AML) patient. Therefore, due to its cancerous nature, the cell line may exhibit differences from healthy monocytes. We aimed to confirm the role of TNF-α secretion by M0 macrophages derived from monocyte-derived macrophages (MDMs) isolated from peripheral blood mononuclear cells (PBMC). CD14+ monocytes were isolated from PBMC and further processed to yield M0 (M-CSF primed or GM-CSF primed), M1, and M2 subtypes **(Fig. 4A)**. To confirm the differentiation, phenotype analysis was done by mRNA analysis of specific surface markers (as for Fig.1); CD68, CD163, CD206, CD80, and CD31 **(Fig.4B)**. As expected, all macrophage subtypes had similar CD69 and CD31 expression, whereas CD80 was only enhanced in M1 macrophages. Importantly, similar to THP-1-derived M0 macrophages, M-CSF and GM-CSF primed MDM

M0 macrophages have significantly enhanced TNF-α secretion compared to MDM-derived M1 and M2 macrophages **(Fig. 4C)**.
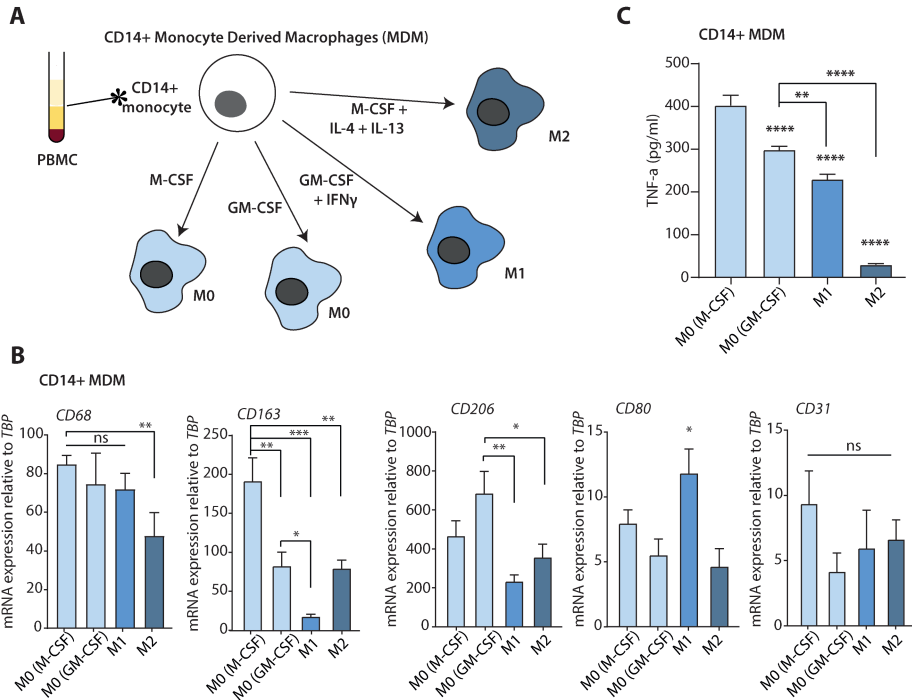
Figure 4

Isolation and TNF-α expression of CD14+ monocyte-derived macrophages (MDM). (A) Schematic representation of the macrophage differentiation procedure and the resulting macrophage subtypes. (B) Relative mRNA expression of CD68, CD163, CD206, CD80, and CD31 on the macrophage subtypes. On the figure shown is the mean ± SEM (n = 4); One-way ANOVA was used to assess statistical significance. Relative expression levels were calculated using the dCt method and normalized to the expression of the reference gene TBP. (C) TNF-α levels in conditioned media from all different macrophage subsets, measured by ELISA. On the figure, shown is the mean ± SEM (n = 4); One-way ANOVA was used to assess statistical significance

Titration curves with recombinant TNF-α show that TNF-α levels in the range as secreted by M0 macrophages induces cell death of PANC-1 cells **(Sup. Fig. 1)**. Following these findings, which strongly point to TNF-α as a critical cytokine in early-macrophage induced tumor cell death, the question arises whether TNF-α

inhibition can reverse the M0 induced cell death. To test his, we used Infliximab, a TNF-α inhibitor in clinical use against ulcerative colitis and Crohn's disease [12]. Infliximab treatment almost completely diminished the growth-inhibitory effects of THP-1-derived M0-CM on PANC-1 and MIA PaCa-2 cell-lines **(Fig. 5A)**. Likewise, treatment with Infliximab prevented THP-1-derived M0-CM induced apoptosis of both PDAC cell lines **(Fig. 5B)**. Interestingly, CM of M-CSF primed MDM-derived M0 macrophages also induced apoptosis of PDAC cells in a TNF-α dependent manner **(Fig. 5C)**. Altogether these findings suggest that M0 macrophage-secreted TNF-α is a robust anti-tumor cytokine, but that exposure of macrophages to tumor microenvironmental cues functions to convert macrophages into subsets that no longer express sufficient TNF-α to exert anti-tumor activities.
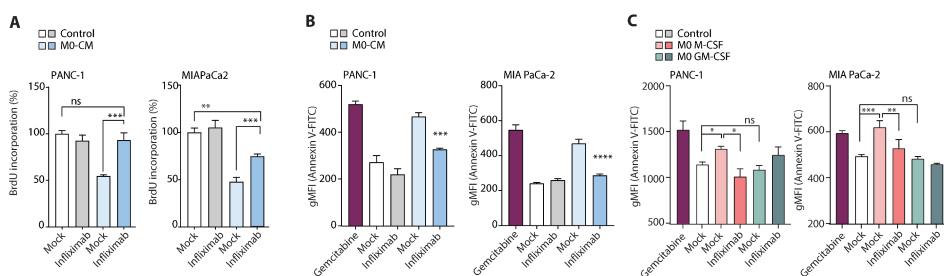
Figure 5

Infliximab inhibits the cytotoxic activity of M0 macrophages. (A) BrdU proliferation assay of PANC-1 and MIA PaCa-2 cells in RPMI-1640 (negative-control) or M0-CM with 25 µg/ml Infliximab where indicated. On the figure shown is the mean ± SEM (n = 4); One-way ANOVA was used to assess statistical significance. (B) Annexin V-FITC positive cells in control, M0-CM with or without 25 µg/ml Infliximab where indicated, or Gemcitabine (as positive control) treated PANC-1 and MIA PaCa-2 cells at t = 48 h. Plotted is the Geometric Mean Fluorescent Intensity (gMFI) on the FITC channel (Annexin V density). On the figure shown is the mean ± SEM (n = 3); One-way ANOVA was used to assess the significance. (C) Annexin V-FITC positive cells in control, M0 M-CSF, or M0 GM-CSF with or without 25 µg/ml Infliximab where indicated, or Gemcitabine (as positive-control) treated PANC-1 and MIA PaCa-2 cells at t = 48 h. Plotted is the Geometric Mean Fluorescent Intensity (gMFI) on the FITC channel (Annexin V density). On the figure shown is the mean ± SEM (n = 3); One-way ANOVA was used to assess the significance.

DISCUSSION

Increased inflammation and enhanced macrophage influx in cancer tissue are associated with poor prognosis and increased risk of developing therapy resistance and metastasis [13]. Numerous studies in murine PDAC models have shown that macrophage influx into the tumor is accompanied by gemcitabine resistance and metastatic burden [14–16]. Despite these tumor-promoting effects [17–19], our group has previously shown that early macrophage infiltrates instead initially exert cytotoxic effects on PDAC cells. However, factors secreted by infiltrated macrophages, such as MMP9, induce epithelial to mesenchymal transition (EMT) of PDAC cells [9]. This EMT enables PDAC cells to escape cytotoxicity, also that induced by macrophages, further underscoring the dual contributions of macrophages to tumor progression [9]. An abundance of studies has reported tumor-associated macrophages (TAMs; M2-like differentiated macrophages) to be associated with increased tumor growth and therapy resistance [20], which has led to the notion that macrophage entry into the tumor should be prevented. However, clinical trials aimed to block monocyte recruitment to reduce TAM content did not yield promising results [21]. Consequently, the majority of subsequent trials have focused on reprogramming TAMs into anti-tumorigenic macrophages [21]. Our results suggest that this latter approach is most promising, as early infiltrated macrophages exert strong anti-tumor effects, and their influx should not be hampered. Ideally, the differentiation of naïve M0 macrophages should be blocked. However, a complicating factor for the development of therapies that target monocyte infiltration into the PDAC tumor tissue (or prevent early differentiation events) is that at the moment of diagnosis, the tumor microenvironment is at least several years old, and the window of opportunity to retain or boost M0 activity is likely lost.

Although the immune regulation in the tumor microenvironment is a complex phenomenon, it is known that tumor cells induce the downregulation of pro-inflammatory cytokines during TAM differentiation [22]. Bearing in mind that, M0 macrophages to be naïve macrophages that have not been exposed to any tumor tissue (unlike the other more differentiated macrophage subsets), this study supports the notion that the tumor environment actively instructs macrophages to be less detrimental to tumor growth. We propose that it is unlikely that the complex

mixture of cues from the tumor microenvironment that instruct macrophages can be adequately targeted, and instead posit that the macrophage-intrinsic mechanisms that suppress TNF-α secretion should be studied. This could preserve macrophage-mediated cell-death in the tumor. For instance, IL-1 Receptor Associated Kinase-M (IRAK-M) activity is known to be upregulated in tumor-exposed macrophages with significantly high expression in TAMs, which in return, suppresses TNF-α secretion [23]. Reprogramming TAMs to secrete increased amounts TNF-α for instance, by exposure to (yet unknown) ligands, could be an interesting avenue to pursue.

We would like to point out several limitations of our study. In part, these are technical in nature; a publicly available lymphoma-derived monocyte cell line (THP-1), and single-donor PBMC isolated monocyte-derived macrophages (MDM) as a primary monocyte cell culture, were used as in vitro proxies for macrophage subsets. One of the technical limitations of using healthy primary monocytes is that obtaining tumor-associated macrophages (TAM) is not possible. Moreover, although M-CSF and GM-CSF treated MDMs may be considered as naïve M0 macrophages, they are already primed towards M2 (M-CSF) or M1 (GM-CSF) subtypes [24]. Indeed, both cell-surface markers (Fig 4 and [24]) and TNF-α secretion suggest that especially the GM-CSF-primed MDM-derived M0 macrophages are less naïve as THP-1 derived M0 macrophages. In line with this notion, M-CSF-primed MDM-derived M0 macrophages mimic the results of THP-1-derived M0 macrophages, whereas GM-CSF-primed MDMs do not. Most likely, this is due to the fact that GM-CSF-primed MDMs secrete less TNF-α as compared to M-CSF-primed MDM-derived M0 macrophages (Fig 4c). Another limitation of our study is that no in vivo experiments were performed to determine the contributions of M0 macrophages to tumor growth and the effects of TNF-α inhibition in such a setting. Finally, an issue that urges clarification in future studies is the discrepancy between the large difference in cell killing by M0 macrophages and the complete reliance on TNF-α on the one hand and the relatively modest difference in TNF-α levels in the macrophage subsets found by ELISA on the other. This suggests that other cytokines can be at play but that TNF-α levels determine how the balance of the tumor-promoting and –limiting contributions of these cytokines add up.

4

A more fundamental question arises from the efficacy with which Infliximab appears to inhibit macrophage-mediated cytotoxicity. If indeed this antibody prevents the tumor inhibitory effects of early macrophage infiltrates in cancers (amongst which PDAC), one would expect this to have become apparent from clinical data and longitudinal studies following the approval of this drug 20 years ago. One argument to explain this discrepant notion is that for PDAC, it is now recognized that the progress from premalignant cell-of-origin to full-blown carcinoma takes several decades [25]. This implies that any tumor-promoting effects of TNF-α inhibition may become apparent from epidemiological analyses in the years to come.

CONCLUSION

Early macrophage infiltrates in the tumor microenvironment are intrinsically anti-tumorigenic, but this is quickly thwarted by differentiation into TAMs that harbor pro-tumorigenic activities. The current therapeutic focus has been to block macrophage entry and thereby TAM content. In this study, we identify TNF-α as a potent cytokine in early macrophages, which is downregulated following further macrophage differentiation. Altogether these findings suggest that restoring TNF-α expression in TAMs might reverse their pro-tumorigenic potential and that this could be a more promising strategy than preventing macrophage influx.

List of abbreviations

TNF-α: Tumor necrosis factor-α; PDAC: pancreatic ductal adenocarcinoma; MDM; monocyte-derived macrophages; PBMC: peripheral blood mononuclear cells; TAM: tumor-associated macrophages; IL: Interleukin; CCL22: C-C motif chemokine 22; CXCL5: C-X-C motif chemokine 5; TGF-β: Transforming growth factor-β; PMA: phorbol 12-myristate 13-acetate; EMT: epithelial-to-mesenchymal transition; M-MLV-RT: Moloney murine leukemia virus reverse-transcriptase; ELISA: enzyme-linked immunosorbent assay; RT-PCR: reverse-transcriptase polymerase chain reaction; CM: conditioned medium; cDNA: complementary DNA.

DECLARATIONS

Ethics approval and consent to participate

Availability of data and materials

Consent for publication

Not applicable.

Competing interests

Funding

Authors' contributions

CT, MFB, and CAS, designed the project, interpreted the data, and wrote the manuscript. CT and HLA acquired the data, performed the experiments and the analyses. All authors have read and approved the manuscript.

Acknowledgments

4

REFERENCES

[1]   Ducreux M, Cuhna AS, Caramella C, Hollebecque A, Burtin P, Goéré D, et al. Cancer of the pancreas: ESMO Clinical Practice Guidelines for diagnosis, treatment and follow-up. Ann Oncol. 2015;26:v56–68.

[2]   Siegel RL, Miller KD, Jemal A. Cancer statistics, 2019. CA Cancer J Clin. 2019;69:7–34.

[3]   Gaianigo N, Melisi D, Carbone C. EMT and Treatment Resistance in Pancreatic Cancer. Cancers (Basel). 2017;9:122.

[4]   Mosser DM, Edwards JP. Exploring the full spectrum of macrophage activation. Nat Rev Immunol. 2008;8:958–69.

[5]   Mantovani A, Schioppa T, Porta C, Allavena P, Sica A. Role of tumor-associated macrophages in tumor progression and invasion. Cancer Metastasis Rev. 2006;25:315–22.

[6]   Pollard JW. Tumour-educated macrophages promote tumour progression and metastasis. Nat Rev Cancer. 2004;4:71–8.

[7]   Ruffell B, Coussens LM. Macrophages and therapeutic resistance in cancer. Cancer Cell. 2015;27:462–72.

[8]   Qian B-Z, Pollard JW. Macrophage Diversity Enhances Tumor Progression and Metastasis. Cell. 2010;141:39–51.

[9]   Tekin C, Aberson HL, Waasdorp C, Hooijer GKJ, de Boer OJ, Dijk F, et al. Macrophage-secreted MMP9 induces mesenchymal transition in pancreatic cancer cells via PAR1 activation. Cell Oncol. 2020;

[10]   Balkwill FR, Mantovani A. Cancer-related inflammation: Common themes and therapeutic opportunities. Semin Cancer Biol. 2012;22:33–40.

[11]   Arango Duque G, Descoteaux A. Macrophage Cytokines: Involvement in Immunity and Infectious Diseases. Front Immunol. 2014;5:1–12.

[12]   Vos ACW, Wildenberg ME, Arijs I, Duijvestein M, Verhaar AP, De Hertogh G, et al. Regulatory macrophages induced by infliximab are involved in healing in vivo and in vitro. Inflamm Bowel Dis. 2012;18:401–8.

[13]   Stone ML, Beatty GL. Cellular determinants and therapeutic implications of inflammation in pancreatic cancer. Pharmacol Ther. 2019;201:202–13.

[14]   Queiroz KCS, Shi K, Duitman J, Aberson HL, Wilmink JW, Van Noesel CJM, et al. Protease-activated receptor-1 drives pancreatic cancer progression and chemoresistance. Int J Cancer. 2014;135:2294–304.

[15]   Sanford DE, Belt BA, Panni RZ, Mayer A, Deshpande AD, Carpenter D, et al. Inflammatory monocyte mobilization decreases patient survival in pancreatic cancer: A role for targeting the CCL2/CCR2 axis. Clin Cancer Res. 2013;19:3404–15.

[16]   Mitchem JB, Brennan DJ, Knolhoff BL, Belt BA, Zhu Y, Sanford DE, et al. Targeting tumor-infiltrating macrophages decreases tumor-initiating cells, relieves immunosuppression, and improves chemotherapeutic responses. Cancer

Res. 2013;73:1128–41.

[17]   Jung KY, Cho SW, Kim YA, Kim D, Oh B-C, Park DJ, et al. Cancers with Higher Density of Tumor-Associated Macrophages Were Associated with Poor Survival Rates. J Pathol Transl Med. 2015;49:318–24.

[18]   Lindsten T, Hedbrant A, Ramberg A, Wijkander J, Solterbeck A, Eriksson M, et al. Effect of macrophages on breast cancer cell proliferation, and on expression of hormone receptors, uPAR and HER-2. Int J Oncol. 2017;51:104–14.

[19]   Zhang Q wen, Liu L, Gong C yang, Shi H shan, Zeng Y hui, Wang X ze, et al. Prognostic Significance of Tumor-Associated Macrophages in Solid Tumor: A Meta-Analysis of the Literature. Hoque MO, editor. PLoS One. 2012;7:e50946.

[20]   Habtezion A, Edderkaoui M, Pandol SJ. Macrophages and pancreatic ductal adenocarcinoma. Cancer Lett. 2016;381:211–6.

[21]   Cassetta L, Pollard JW. Targeting macrophages: therapeutic approaches in cancer. Nat Rev Drug Discov. 2018;17:887–904.

[22]   Standiford TJ, Kuick R, Bhan U, Chen J, Newstead M, Keshamouni VG. TGF-B-induced IRAK-M expression in tumor-associated macrophages regulates lung tumor growth. Oncogene. 2011;30:2475–84.

[23]   del Fresno C, Otero K, Gómez-García L, González-León MC, Soler-Ranger L, Fuentes-Prior P, et al. Tumor Cells Deactivate Human Monocytes by Up-Regulating IL-1 Receptor Associated Kinase-M Expression via CD44 and TLR4. J Immunol. 2005;174:3032–40.

[24]   Lescoat A, Ballerie A, Augagneur Y, Morzadec C, Vernhet L, Fardel O, et al. Distinct Properties of Human M-CSF and GM-CSF Monocyte-Derived Macrophages to Simulate Pathological Lung Conditions In Vitro: Application to Systemic and Inflammatory Disorders with Pulmonary Involvement. Int J Mol Sci. 2018;19:894.

[25]   Yachida S, Jones S, Bozic I, Antal T, Leary R, Fu B, et al. Distant metastasis occurs late during the genetic evolution of pancreatic cancer. Nature. 2010;467:1114–7.

4
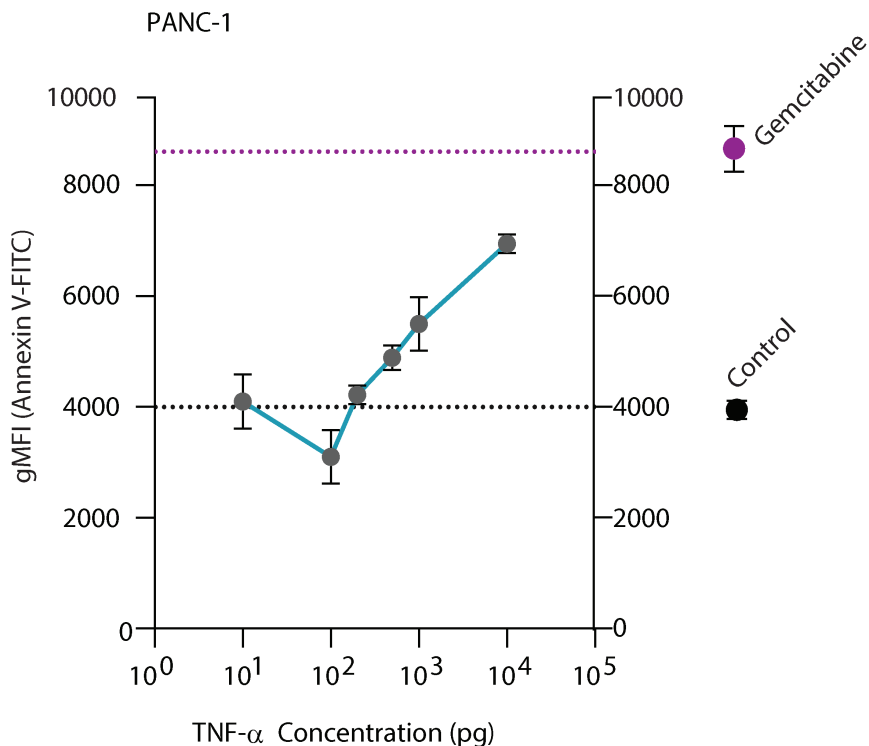
PANC-1

Supplementary Figure 1

Cytotoxicity of human recombinant TNF-α on PANC-1 cell-line is dose-dependent. PANC-1 cells were treated with human recombinant TNF-α in increasing concentrations (10 ng to 10 pg). Annexin V-FITC positive cells in control media (black dashed line given as baseline), or Gemcitabine (as the positive control, purple dash bar given as cell-death comparison) treated PANC-1 cells at t = 48 h. Plotted is the Geometric Mean Fluorescent Intensity (gMFI) on the FITC channel (Annexin V density), and decreasing concentration is plotted on Y-axis. On the figure shown is the mean ± SEM (n = 2).

Chapter 5

PAR1 drives and maintains ductal cell-fates
in the premalignant pancreas
and ductal adenocarcinoma

Cansu Tekin, Brendon P. Scicluna, Sophie C. Lodestijn, Kun Shi,
Maarten F. Bijlsma, C. Arnold Spek

ABSTRACT

Pancreatic acinar cells have high plasticity and can transdifferentiate into ductal-like cells. This acinar-to-ductal metaplasia (ADM) contributes to tissue maintenance but may also contribute to the premalignant transformation that can eventually progress to pancreatic ductal adenocarcinoma (PDAC). Macrophages are key players in ADM, and macrophage secreted matrix metalloproteinase (MMP)-9 induces ADM through yet unknown mechanisms. As we previously identified MMP9 as a novel agonist of protease-activated receptor 1 (PAR1), a receptor that is known to orchestrate the cross-talk between macrophages and tumor cells in PDAC, we here assessed the contribution of PAR1 to pancreatic cell fates. We found that genetic deficiency for PAR1 increases acinar gene expression programs in the healthy pancreas and that PAR1 deficiency limits ductal transdifferentiation in experimental systems for ADM. Moreover, PAR1 silencing in PDAC cells increases acinar marker expression. Changes in PDAC cell lines were associated with a downregulation of known Myc-target genes, and Myc inhibition mimics PAR1 deficiency in enhancing acinar programs in healthy organoids and PDAC cells. Overall, we identify the PAR1-Myc axis as a driver of ductal cell fates in premalignant pancreas and PDAC. Moreover, we show that cellular plasticity is not unique to acinar cells and that ductal regeneration into acinar-like cells is possible even in the context of oncogenic KRAS activation.

INTRODUCTION

Pancreatic ductal adenocarcinoma (PDAC) is the most common type of pancreatic cancer [1]. Five-year survival rates of PDAC are around 9%, and despite intense research efforts to improve the poor outcome, there has been little improvement in the last decades [1,2]. Several features of PDAC contribute to the dismal prognosis, including the late stage at which the disease is typically diagnosed [3] and high intrinsic resistance against chemotherapeutics.

In the exocrine pancreas, which facilitates food digestion, two main cell types exist; acinar cells that produce digestive enzymes and epithelial cells that line the ducts through which these enzymes are transported to the duodenum. Despite the strong ductal characteristics and nomenclature of PDAC, the cell of origin of PDAC development remains the subject of debate. In fact, both acinar and ductal cells may give rise to neoplasia leading up to cancerous lesions; nevertheless, acinar cells are reported to be more susceptible to rapid transdifferentiation and neoplasm formation, especially during inflammation (i.e., pancreatitis) [4–7]. During inflammatory circumstances, the acinar cell state is plastic, and mature acinar cells can de-differentiate into progenitor cells and subsequently differentiate into duct-like cells [8]. This acinar-to-ductal metaplasia (ADM) contributes to the homeostasis of the pancreas. However, oncogenic activations in acinar cells (typically activating mutations in KRAS) and inflammation of the pancreas (pancreatitis) can trigger ADM and give rise to pancreatic intraepithelial neoplasias (PanIN). Additional oncogenic mutations can accumulate in PanIN lesions, which may then progress to PDAC [9]. Studies on genetically modified mouse models have shown TGF-α expression and KRAS mutations as drivers of ADM and PanIN formation [10]. Additionally, mouse models of cerulein-induced pancreatitis have shown that inflammation contributes to PDAC development [7]. Furthermore, KRAS mutations can cooperate with the inflammatory cascade to accelerate the formation of malignant lesions [11]. Given the importance of maintaining the appropriate cell fates and lineages for homeostasis and preventing premalignant transformation, acinar differentiation processes are subject to strict regulation. This has typically been attributed to transcription factors with activity in distinct cell populations and (developmental) compartments, but the role of

G-protein coupled receptor (GPCR) signaling known to be important in embryonic development remains underexplored.

Protease-activated receptor-1 (PAR1) is a GPCR family member that is widely expressed in various tissues in both healthy and disease states. It is activated by proteolytic cleavage of the N-terminal arm, which liberates a tethered agonist that binds to its activation domain, thereby initiating intracellular signaling. PAR1 was initially described to be activated by the coagulation factor thrombin, but other agonists like MMP1, MMP13, activated protein C, and kallikreins have now been characterized [12]. Increased PAR1 expression is associated with tumor progression and poor prognosis in, amongst others, breast, lung, and pancreatic cancer [13–16]. In PDAC, an orthotopic xenograft study revealed that tumor growth is stalled in PAR1 deficient animals [16]. Interestingly, this reduced tumor growth was accompanied by a significant reduction of macrophage influx into the tumor microenvironment, suggesting a functional link between PAR1, macrophages, and PDAC growth [16].

Macrophages that infiltrate the pancreas are critical players in ADM, and macrophage depletion limits the formation of cerulein-induced PanIN lesions [17]. Infiltrated macrophages secrete matrix metalloproteinase-9 (MMP9) that targets acinar cells leading to transdifferentiation into ductal cells. This is particularly interesting as we recently identified macrophage secreted MMP9 as a novel PAR1 agonist in the setting of PDAC [18]. In the current manuscript, we address the hypothesis that PAR1 plays a more central role in cellular differentiation and that its activation balances acinar and ductal cell fates in the healthy and premalignant pancreas and PDAC.

MATERIALS AND METHODS

Reagents

Collagenase type IA (Sigma, St. Louis, MO, St. Louis, MO), Collagen I from rat tail (Corning, Corning, NY), Trypsin Inhibitor (Gibco, Thermo Fisher Scientific, Waltham, MA), IMDM (Gibco, Thermo Fisher Scientific, Waltham, MA), fetal bovine serum (#F7524, Sigma), pre-activated recombinant MMP9 (Sigma, St. Louis, MO), murine EGF (PeproTech, Rocky Hill, NJ), Vorapaxar (Adooq Bioscience, Irvine, CA), p1pal-12 (palmitate-RCLSSSAVANRS-NH2; GL Biochem Shanghai, China), 10058-F4 (c-Myc inhibitor; Selleck Chemicals, Houston, TX), ActinGreen 488 ReadyProbes Reagent (Thermo Fisher Scientific), Dolichos Biflorus Agglutinin (DBA)-rhodamine (RL-1032, Vector Laboratories, Burlingame, CA).

Animal Studies and Ethics approval

C57BL/6 mice (Charles River Laboratories) were housed at the animal facility of the Academic Medical Center of Amsterdam. All mice had access to food and water ad libitum. Institutional Animal Care and Use Committee of Academic Medical Center approved all animal experiments according to protocol number DIX107AA.

Isolation of Mouse Pancreatic Acinar cells

Pancreata from wildtype and PAR1 deficient C57BL/6 mice were dissected and washed twice with Hank's Buffered Saline Solution (HBSS, Gibco, Thermo Fisher Scientific). Pancreata were cut with a scalpel to 3-5 mm pieces, after which acinar cells were isolated, mostly as described before [19]. In detail, the pancreas pieces were centrifuged at 500 g for 2 minutes to remove debris and supernatant. For dissociation of cells, pancreas pieces were next treated with collagenase IA solution (200 U/ml collagenase IA, 10 mM HEPES, and 0.25 mg/ml trypsin inhibitor in HBSS) for 30 minutes. Dissociated cells were centrifuged at 500 g for 2 minutes and washed twice with wash solution (HBSS supplemented with 5 % Fetal Bovine Serum (FBS) and 10 mM HEPES) to stop the collagenase reaction. The cell pellet was resuspended in 1 ml seeding medium (IMDM containing 1% FBS, 0.1 mg/ml trypsin inhibitor, and 1 µg/ml dexamethasone), passed through a 100 µm cell strainer, collected in 5% FCS-IMDM medium, seeded in 6-well

plates and incubated for 24 hours to separate non-adherent acinar cells from adherent epithelial and other contaminant cells. The following day, cells in suspension were centrifuged at 500 g for 2 minutes and embedded in a collagen mixture (1 mg/ml collagen, 1X PBS, 0.1 M HEPES, 0.75% Sodium Bicarbonate, 0.1 M NaOH) in 6-well plates with a double 3D layer of 1 mg/ml collagen (bottom layer without cells, set prior to seeding).

Viability assessment of acinar spheroids

To assess the viability of collagen embedded acini, 2 different methods were used. First, cells were stained with propidium iodide (PI) at 20µg/ml (final concentration). After 20 minutes of incubation phase-contrast images depicting the explanted acinar cells and TxRed channel images identifying PI positive dead cells were taken. As positive control for cell death, 0.5 mM NaN3 (sodium azide) treated spheroids were used. In our second approach, we performed a resazurin to resofurin reduction (CellTiter Blue) experiment to determine the cells' metabolic activity. In viable cells, resazurin (blue) is converted to resofurin (pink) through reductase activity in the mitochondria. The collagen in which the cells are embedded precluded efficient fluorescence read-out, and we have used imaging instead to reveal color conversion in the viable cells. In this case,0.5 mM NaN3 (sodium azide) treated spheroids were used as a negative control. Images were taken in the color mode of phase-contrast imaging. In both methods, pictures were taken with the EVOS FL cell imaging system (Thermo Fisher Scientific) at 4X, 10X, and 20X magnification.

Induction of ADM in acinar spheroids

Collagen embedded acinar cells were cultured in IMDM containing 1% FBS, 0.1 mg/ml trypsin inhibitor, and 1 µg/ml dexamethasone. According to a previously described protocol for ADM [17], acinar cells were treated with 50 ng/ml murine EGF (PeproTech) or 1 ng/ml recombinant MMP9 for 5 days. At the end of the experiment, one batch of cells was visualized with the phase contrast channel of the EVOS FL cell imaging system (Thermo Fisher Scientific) at 20X magnification, after which cells were used to isolate RNA. The other batch of cells was fixed with 4% formalin and permeabilized with 0.2% Triton-X (Sigma). For fluorescence imaging, F-actin was stained with Alexa488 conjugated phalloidin (ActinGreen 488 ReadyProbes Reagent, Thermo Fischer Scientific), and ductal

structures were stained using rhodamine linked DBA (Dolichos Biflorus Agglutinin; Vector Laboratories). After staining, cells were washed with PBS and imaged with the Yellow Fluorescence (YFP) and Texas-Red channels of the EVOS FL cell imaging system (Thermo Fisher Scientific) at 20X magnification.

Cell culture

Human PANC-1, MIA PaCa-2, and Capan-2 PDAC cell lines (all obtained from ATCC, Manassas, VA) and primary PDAC cells (i.e., AMC-PDAC-096 cells generated from patient-derived xenografts as described previously [20]) were cultured in high glucose (4.5g/mL) containing DMEM (Gibco, Thermo Fisher). All media were supplemented with 10% fetal bovine serum (FBS, #F7524, Sigma), L-glutamine (2 mM), penicillin (100 units/mL), and streptomycin (500 μg/mL) (all Lonza, Basel, Switzerland) according to routine cell culture procedures. Cells were incubated in 5% CO2 incubators at 37oC. All PDAC cell-lines were authenticated by STR profiling (Promega PowerPlex, Leiden, Netherlands) and tested for mycoplasma by PCR monthly.

Immunohistochemistry on Paraffin-Embedded Material

Orthotopic KP tumors, isolated murine healthy pancreata, and murine organoids were fixed in formalin, embedded in paraffin, and 4-μm-thick slides were subsequently deparaffinized, rehydrated, and washed in deionized water. Slides were stained with hematoxylin and eosin (H&E) according to routine procedures. For immunohistochemistry, endogenous peroxidase activity was quenched with 0.3% hydrogen peroxide for 15 min at room temperature, with antigen retrieval for 10 min at 100°C in 10 mM sodium citrate buffer, pH 7.4. Slides were blocked for 10 min with Ultra V block (Thermo Fisher Scientific). Primary antibodies against Cytokeratin 19 (SAB4501670, Sigma) and Amylase (A8273, Sigma) were added (1:1600 dilution) for overnight incubation at 4°C. Slides were subsequently incubated with appropriate HRP-conjugated goat anti-rabbit IgG (Brightvision, Immunologic, VWR, Radnor, PA), after which DAB (Brightvision, Immunologic, VWR) staining was used to visualize peroxidase activity. Slides were photographed with a microscope equipped with a digital camera (Leica CTR500, Leica Microsystems, Wetzlar, Germany).

5

RNA-Seq

Total RNA was isolated from shCtrl PANC-1 and shPAR1 PANC-1 cells using the NucleoSpin RNA miniprep kit (Macherey Nagel, Düren, Germany). Yield and purity (260 nm:280 nm) were determined by a Nanodrop ND-1000 (Thermo Fisher Scientific). The integrity (RNA integrity number (RIN) >9.0) of the resuspended total RNA was determined by using the RNA Nano Chip Kit on the Bioanalyzer 2100 and the 2100 Expert software (Agilent, Amstelveen, the Netherlands). RNA-sequencing libraries were prepared from 250 ng total RNA using KAPA RNA HyperPrep with RiboErase (HMR) kits (Roche, Basel, Switzerland). Libraries were sequenced using the Illumina HiSeq4000 instrument (Illumina) to generate single reads (50bp). The sequencing depth was approximately 40 million reads per sample. Read quality was assessed by means of the FastQC method (v0.11.5; http://www.bioinformatics.babraham.ac.uk/projects/fastqc/). Trimmomatic version 0.36 [21] was used to trim Illumina adapters and poor-quality bases (trimmomatic parameters: leading=3, trailing=3, sliding window=4:15, minimum length=40). The remaining high-quality reads were used to align against the Genome Reference Consortium human genome build 38 (GRCh38) [22]. Mapping was performed by HISAT2 version 2.1.0 [23] with parameters as default. Count data were generated by means of the HTSeq method [24]and analyzed using the DESeq2 method [25] in the R statistical computing environment [26] (R Core Team 2014. R: A language and environment for statistical computing. R Foundation for Statistical Computing, Vienna, Austria). Statistically significant differences were defined by Benjamini & Hochberg adjusted probabilities < 0.05. Gene expression extraction was performed via the R2 microarray analysis and visualization platform (http://r2.amc.nl). Sequence libraries are publicly available through the National Center for Biotechnology Information (NCBI) gene expression omnibus (GEO) under the following accession numbers: GSE155010

Murine healthy ductal organoids

Murine pancreatic ductal organoids were cultured according to the previously described methodology [27]. Organoid media consisted of Advanced DMEM/F-12 (Gibco, Thermo Fisher Scientific) supplemented with B-27 supplement (Invitrogen, Carlsbad, CA), N-Acetylcysteine (Sigma), Nicotinamide (Sigma), Gastrin (PeproTech), FGF10 (PeproTech), mEGF (PeproTech), and in-house produced Noggin and RSPO1 (Supplementary Table 1). Media were refreshed twice week-

ly with murine organoid media, and passages were performed weekly with a 1:4 ratio with fresh Matrigel (Corning).

Quantitative Real-Time PCR
Total RNA was isolated with the NucleoSpin RNA miniprep kit (Macherey Nagel). cDNA was synthesized from DNase-treated total RNA with M-MLV-RT (Promega) and random hexamers (Qiagen, Hilden, Germany). Real-time quantitative RT-PCR was performed using the Sensifast SYBR No-Rox Kit (Bioline, London, UK) on a LightCycler 480 II (Roche). Relative expression levels were calculated using the comparative threshold cycle (dCt) method and normalized for expression of the reference gene TBP. Primer sequences of the analyzed genes are shown in Supplementary Table 2.

Lentiviral Gene Silencing
PAR1 silenced KP, PANC-1, MIA PaCa-2, and Capan-2 cells were established with knockdown efficiencies of around 70% for KP, PANC-1, and Capan-2 and around 50% for MIA PaCa-2 cells [28]. The knockdown efficiency of the primary AMC-PDAC-096 cell line was around 50% (Sup. Fig.2). For lentiviral silencing of F2R in the human PDAC cells, MISSION shRNA library (Sigma-Aldrich, St. Louis, MO) clone TRCN0000003690 was used, and for the murine KP cells, we used MISSION library clone TRCN0000026806. Clone shc004 was used as control. Lentivirus was produced by transfecting HEK293T cells (ATCC) with 3rd generation transfer and packaging plasmids pVSV, pMDL, and pRES using Lipofectamine 2000 (Thermo Fisher Scientific). Forty-eight and 72 hours after transfection, the supernatant was harvested and 0.45 μm filtered (Millipore, Billerica, MA, USA). Transduced cells were selected with 2 μg/ml puromycin (Sigma, St. Louis, MO) for 72 hours, after which the transduction efficiency was analyzed by qRT-PCR.

Gene Set Enrichment Analysis
Datasets used were the tumor expression datasets GSE15471 [29], GSE62452 [30], GSE16515 [31], GSE28735 [32], GSE49149 [33,34], GSE36924 [33,35–37] and TCGA-PDAC [38]. GSEA software (Broad Institute, Cambridge, MA, USA) was downloaded from the Broad Institute website (http://www.broad.mit.edu/gsea/). Acinar and ductal gene signatures were curated based on single-cell

expression profiling of the human pancreas [39]. Expression datasets were compiled with annotated gene names (.gct), samples were segmented for median PAR1/F2R expression (i.e., high and low) as phenotype label files (.cls), and signature sets were assembled (.grp). One thousand permutations were run on the phenotype. Datasets were not collapsed to gene symbols (collapse to gene symbols=false) in the GSEA software.

Statistical Analysis

Data were presented as mean ± SEM. Statistical analyses were performed using GraphPad PRISM 8.0 (Graphpad Software Inc., La Jolla, CA). Statistically significant differences were considered with a p-value of less than 0.05. For further details of the statistical analysis, see figure legends. P-values are indicated by asterisks with * p<0.05, ** p< 0.01, *** p< 0.001, and **** p<0.0001.

RESULTS

PAR1 deficiency promotes acinar gene expression programs in the pancreas
In light of the recent identification of macrophage-secreted MMP9 as a driver of ADM [17] and our data pointing to MMP9 as a novel PAR1 agonist [18], we hypothesized that PAR1 is the receptor that mediates macrophage-induced ADM. To test this, we first ascertained whether PAR1 deficiency results in altered cell fates in the pancreas. Expression levels of known acinar and ductal markers were measured in pancreata of wildtype and F2R/PAR1 deficient (PAR1-KO) mice. Expression levels of the acinar cell marker carboxypeptidase A1 (Cpa1) and acinar cell-fate transcription factors Ptf1a, Nr5a2, and Mist1 were strongly increased in PAR1-deficient pancreata compared to wildtype controls **(Fig 1A)**. The expression of ductal and centroacinar markers was not different **(Fig 1B)**. To corroborate the findings in a human setting, we next assessed the association of PAR1 with acinar and ductal gene sets in human (non-tumor) pancreas gene expression datasets. Samples were dichotomized for median PAR1 expression (i.e., PAR1-high versus PAR1-low), and gene set enrichment analysis (GSEA) revealed that PAR1 expression negatively correlates with acinar signatures and positively correlates with ductal signatures **(Fig. 1C)**.

5

ADM requires PAR1 activity in vitro
To evaluate the contribution of PAR1 to exocrine pancreatic cell fate, we isolated acinar cells from wildtype and PAR1-deficient mice and determined expression levels of acinar **(Fig. 2A)** and ductal **(Fig. 2B)** markers. Among all markers tested, only Cpa1 expression was significantly increased in PAR1 deficient acinar cells compared to wildtype cells. This suggests that at steady-state and in isolated cell populations, PAR1 deficiency does not result in an overt phenotype and indicates that additional interactions (as present in vivo such as in **Fig. 1C**) or cues are required to reveal the contribution of PAR1 to cell fates.
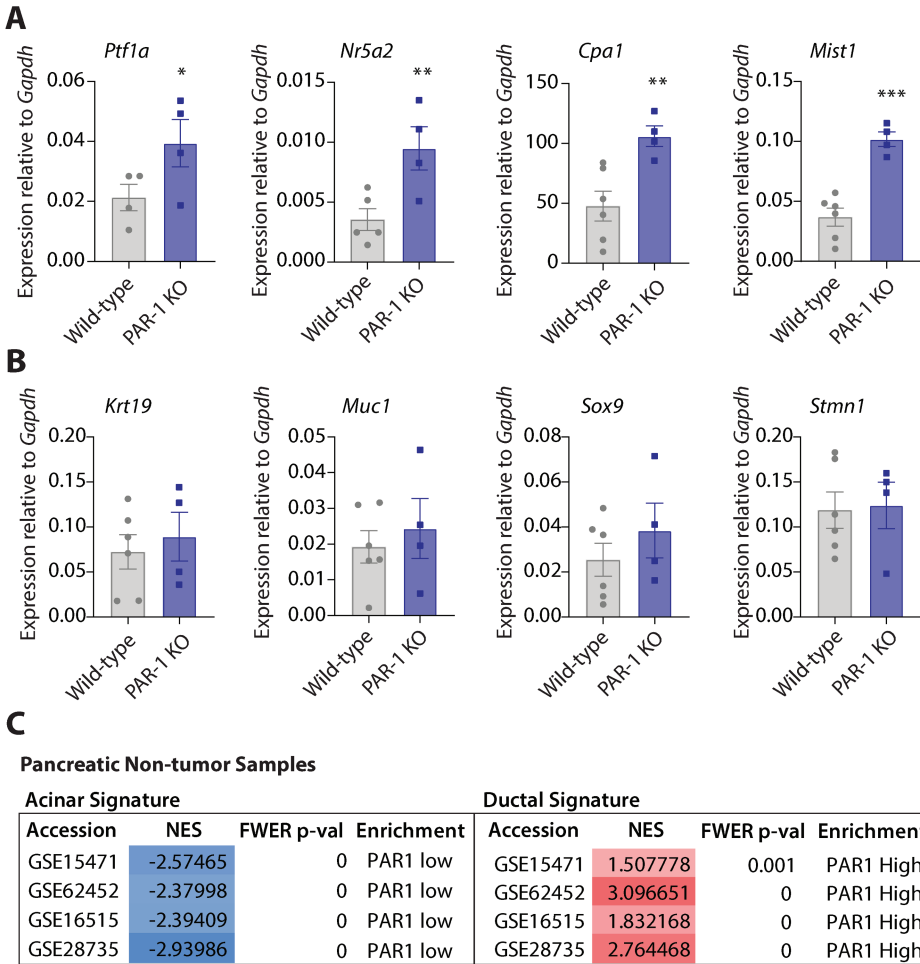
A

Ptf1a | Nr5a2 | Cpa1 | Mist1 (bar graphs comparing Wild-type vs PAR-1 KO; Expression relative to *Gapdh*)

B

Krt19 | Muc1 | Sox9 | Stmn1 (bar graphs comparing Wild-type vs PAR-1 KO; Expression relative to *Gapdh*)

C

Pancreatic Non-tumor Samples

Acinar Signature				Ductal Signature			
Accession	NES	FWER p-val	Enrichment	Accession	NES	FWER p-val	Enrichment
GSE15471	-2.57465	0	PAR1 low	GSE15471	1.507778	0.001	PAR1 High
GSE62452	-2.37998	0	PAR1 low	GSE62452	3.096651	0	PAR1 High
GSE16515	-2.39409	0	PAR1 low	GSE16515	1.832168	0	PAR1 High
GSE28735	-2.93986	0	PAR1 low	GSE28735	2.764468	0	PAR1 High

Figure 1

PAR1 deficiency in the pancreas increases acinar-related gene expression. A-B) Relative mRNA expression in whole pancreata isolated from wildtype (gray) and PAR1 deficient (PAR1-KO; purple) mice. Shown is the mean±SEM (wildtype n=4-6, PAR1-KO n=4); * $p<0.05$; **<0.01; ***<0.001, Student´s t-test. A) Acinar-related marker expression (Ptf1a, Nr5a2, Cpa1, and Mist1). Note that samples with poor/missing melt-curve were excluded from the analysis. B) Ductal-related marker expression (Krt19, Muc1, Sox9) and centroacinar marker expression (Stmn1). C) Gene Set Enrichment Analysis (GSEA) results for human non-tumor pancreatic expression sets (dichotomized for median PAR1 expression) with curated acinar (left) and ductal (right) gene signatures. Normalized Enrichment Score (NES) and Family-Wise Error Rate (FWER) p-values are shown for each tested gene expression set.

To assess whether PAR1 impacts on ADM, we utilized the same acinar cell isolates using recombinant MMP9 or EGF as positive controls for ADM induction [17]. After 5 days of culturing wildtype acinar spheroids (viability tested, shown in **Sup. Fig.1**) in collagen embedded cultures, clusters of acinar cells gave rise to duct-like budding structures **(Fig. 2C)**. The occurrence of these structures markedly increased following the exposure to MMP9 and EGF. To ascertain the ductal identity of these structures, cultures were stained with DBA [40], and additionally, F-actin was stained to reveal cell mass. Indeed, DBA staining is markedly enhanced in MMP9 and EGF-treated cultures. Importantly, in Par1-KO and in vorapaxar treated wildtype spheroids, there was no visible ductal structure formation (also in the presence of MMP9 or EGF; **Sup. Fig. 2A**), and these acinar spheroids were negative for DBA staining **(Fig. 2D and Sub. Fig.2B)**. Subsequent transcript analysis revealed that, after 5 days of ADM induction, expression levels of acinar specific transcription factors Ptf1a, Nr5a2, and Mist1 and of the acinar marker Cpa1 were decreased in wildtype acinar cells, whereas their levels remained unchanged in PAR1-deficient acinar cells **(Fig. 2E)**. In line with changes in acinar-related genes, MMP9 and EGF treatment of wildtype acinar cells led to increased expression levels of the ductal markers Krt19, Muc1, and Sox9 and the centroacinar marker Stmn1 **(Fig. 2F)**. Interestingly, under these culture conditions, the expression of the acinar-specific markers Nr5a2 and Cpa1 and the ductal-specific transcription factor Sox9 significantly differed between the two genotypes in the absence of additional ADM cues **(Fig. 2E, F)**. Altogether these data suggest that PAR1 contributes to ductal transdifferentiation of acinar cells in response to macrophage secreted MMP9.
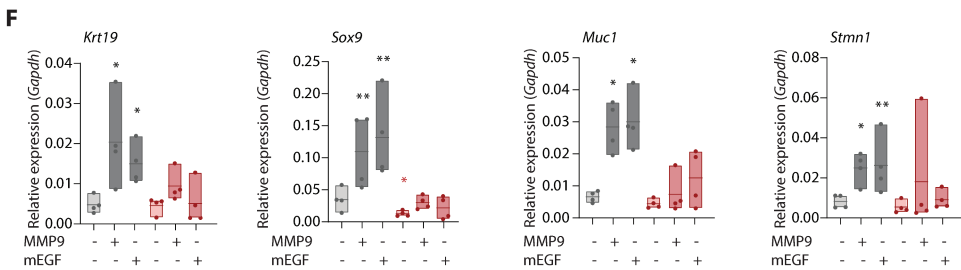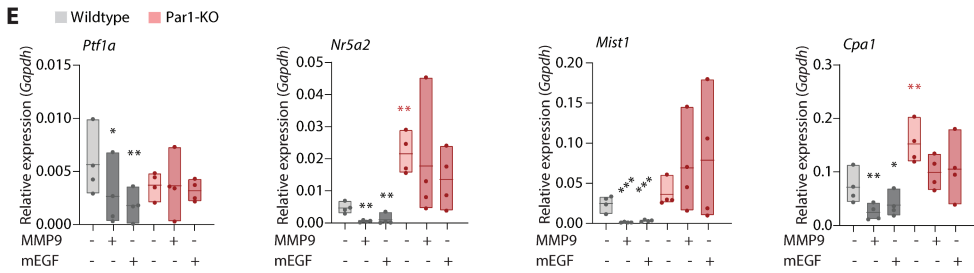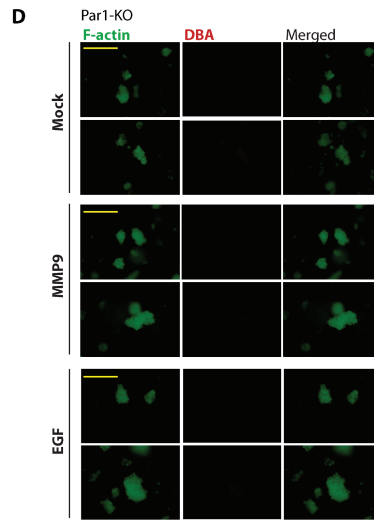
5

A

Ptf1a — Relative expression (*Gapdh*): WT, Par1-KO

Nr5a2 — Relative expression (*Gapdh*): WT, Par1-KO

Cpa1 — Relative expression (*Gapdh*): WT, Par1-KO *

Mist1 — Relative expression (*Gapdh*): WT, Par1-KO

B

Krt19 — Relative expression (*Gapdh*): WT, Par1-KO

Sox9 — Relative expression (*Gapdh*): WT, Par1-KO

Muc1 — Relative expression (*Gapdh*): WT, Par1-KO

Stmn1 — Relative expression (*Gapdh*): WT, Par1-KO

C Wildtype — F-actin, DBA, Merged — Mock, MMP9, EGF

D Par1-KO — F-actin, DBA, Merged — Mock, MMP9, EGF

E ▢ Wildtype ▢ Par1-KO

Ptf1a — Relative expression (*Gapdh*) — MMP9 / mEGF

Nr5a2 — Relative expression (*Gapdh*) — MMP9 / mEGF

Mist1 — Relative expression (*Gapdh*) — MMP9 / mEGF

Cpa1 — Relative expression (*Gapdh*) — MMP9 / mEGF

F

Krt19 — Relative expression (*Gapdh*) — MMP9 / mEGF

Sox9 — Relative expression (*Gapdh*) — MMP9 / mEGF

Muc1 — Relative expression (*Gapdh*) — MMP9 / mEGF

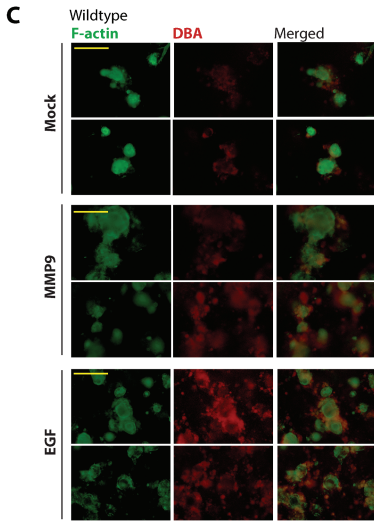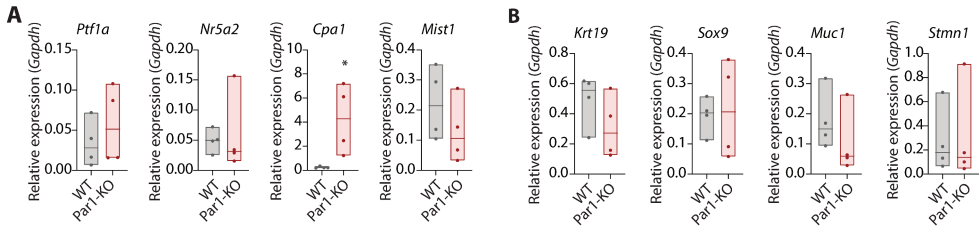*Stmn1* — Relative expression (*Gapdh*) — MMP9 / mEGF

132

Figure 2

PAR1 deficiency impairs ADM. A-B) Relative mRNA expression analysis of isolated acinar cells from wildtype (gray) and PAR1-deficient (PAR1-KO; red) mice. Shown is the mean±SEM (n=4); * p<0.05, Student´s t-test. A) Acinar-related marker expression (Ptf1a, Nr5a2, Cpa1, and Mist1). B) Ductal-related marker expression (Krt19, Muc1, Sox9) and centroacinar marker expression (Stmn1). C-D) Epifluorescence images of 3D collagen embedded acinar cells from wildtype (C) and PAR1-deficient (D) acinar cells. Acinar cells were treated with DMSO as mock and with 1 ng/ml MMP9, or 50 ng/ml EGF for 5 days. Scale bars indicate 200 μm. Image acquisition was performed on day 5 at 20X magnification with EVOS FL cell imaging system with YFP and Tx-Red channels. YFP and Tx-Red channels were merged on ImageJ. E-F) Relative mRNA expression analysis of 3D collagen embedded acinar cells from wildtype and PAR1 deficient (PAR1-KO) pancreas cells. Acinar cells were treated with DMSO (mock) or with 1 ng/ml MMP9 and 50 ng/ml EGF for 5 days. Shown is the mean ± SEM (n=4); * p<0.05; **<0.01; ***<0.001, One-way ANOVA. E) Acinar-related marker expression (Ptf1a, Nr5a2, Cpa1, and Mist1). F) Ductal-related marker expression (Krt19, Muc1, Sox9) and centroacinar marker expression (Stmn1).

PAR1 is associated with ductal characteristics in PDAC

The observation that ADM appears to depend on PAR1 activity in vitro raises the question of whether PAR1 also drives or maintains ductal cell fates in PDAC. To investigate this, we dichotomized 8 public PDAC gene expression datasets for PAR1 expression and applied the abovementioned acinar and ductal gene signatures. GSEA analysis showed increased expression of acinar signatures in most PAR1-low groups, and all sets showed enhanced ductal signatures in the PAR1-high group **(Fig. 3A)**. To substantiate these findings, we performed RNA-Seq and GSEA of previously established shRNA-mediated PAR1 deficient (shPAR1) PANC-1 cells (knockdown efficiency 70%, see ref [28]). Acinar signatures were significantly enhanced in shPAR1 PANC-1 cells, and a trend towards a reduced ductal signature was observed in the PAR1 deficient cells **(Fig. 3B, C)**. Next, we compared expression levels of key acinar- and ductal-related transcription factors and markers **(Fig. 3D, E)**. Expression levels of acinar cell-fate driving transcription factors NR5A2, MIST1, and GATA4 were significantly increased, whereas the ductal transcription factor SOX9 was markedly decreased in shPAR1 PANC-1 cells.
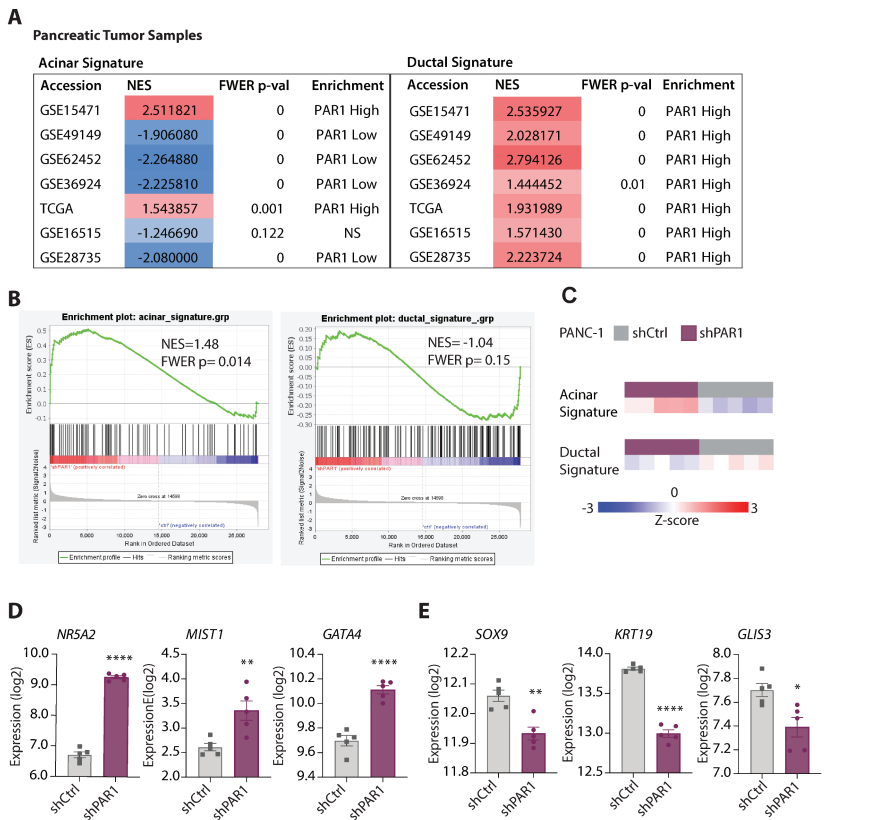
A

Pancreatic Tumor Samples

Acinar Signature				Ductal Signature			
Accession	NES	FWER p-val	Enrichment	Accession	NES	FWER p-val	Enrichment
GSE15471	2.511821	0	PAR1 High	GSE15471	2.535927	0	PAR1 High
GSE49149	-1.906080	0	PAR1 Low	GSE49149	2.028171	0	PAR1 High
GSE62452	-2.264880	0	PAR1 Low	GSE62452	2.794126	0	PAR1 High
GSE36924	-2.225810	0	PAR1 Low	GSE36924	1.444452	0.01	PAR1 High
TCGA	1.543857	0.001	PAR1 High	TCGA	1.931989	0	PAR1 High
GSE16515	-1.246690	0.122	NS	GSE16515	1.571430	0	PAR1 High
GSE28735	-2.080000	0	PAR1 Low	GSE28735	2.223724	0	PAR1 High

Figure 3

PAR1 expression in ductal tumors is associated with increased ductal marker expression. A) GSEA results for human PDAC expression sets (dichotomized for median PAR1 expression) with curated acinar (left) and ductal (right) gene signatures. Normalized Enrichment Score (NES) and Family-Wise Error Rate (FWER) p-value are shown for each tested gene expression set. B) Enrichment plots (on GSEA) for shCtrl PANC-1 and shPAR1 PANC-1cells with curated acinar (left) and ductal (right) gene signatures. Normalized Enrichment Score (NES) and Family-Wise Error Rate (FWER) p-values are shown together with the plots. C) Z-score expression difference analysis on shCtrl PANC-1 and shPAR1 PANC-1 cells with curated acinar (upper) and ductal (lower) gene signatures. Columns indicate data from individual patients. D-E) Normalized expression levels of acinar-related genes NR5A2, MIST1, and GATA4 (D) and ductal-related genes SOX9, KRT19, and GLIS3 (E) in shCtrl and shPAR1 PANC-1 cells. Shown is the mean ± SEM (n=5); * p<0.05, ** p<0.01, *** p<0.001, and **** p<0.0001 (Student's t-test).
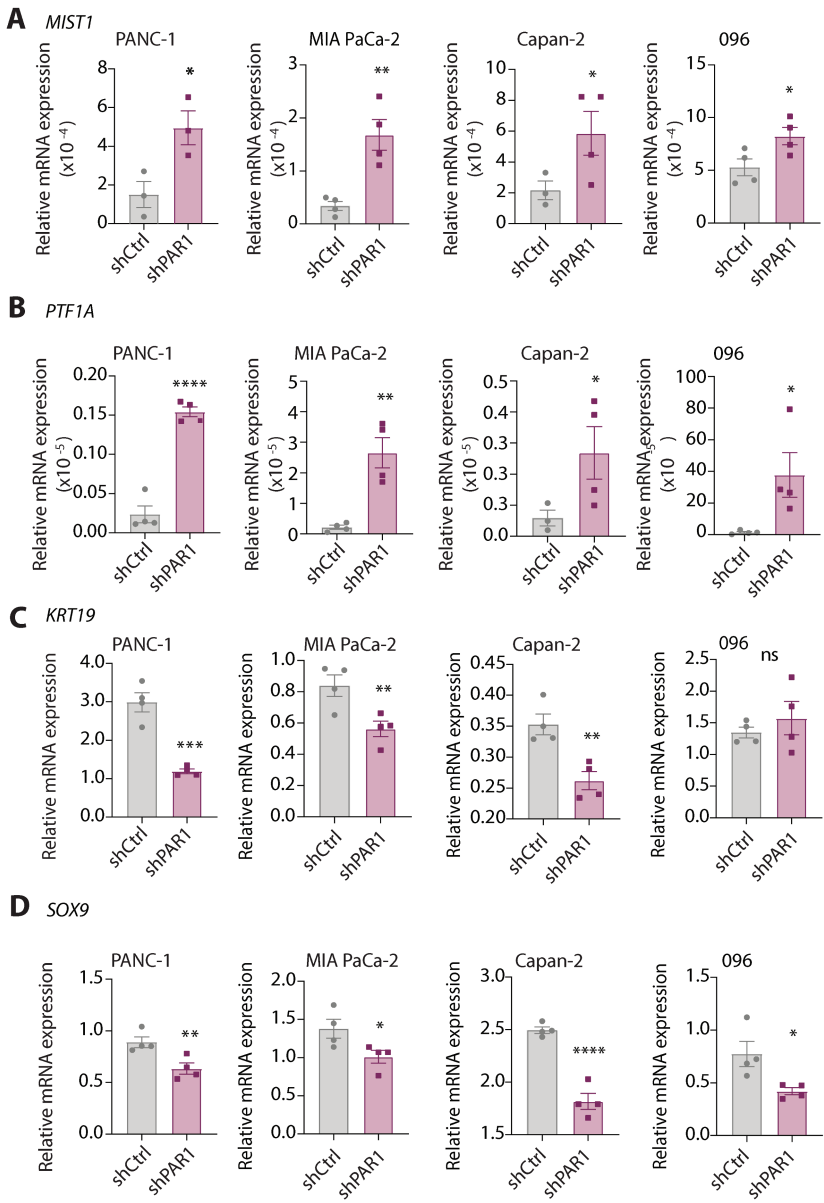
Figure 4

PAR1 downregulation in PDAC cells increases acinar marker expression. A-D) Relative mRNA expression analysis of MIST1 (A), PTF1A (B), KRT19 (C), and SOX9 (D) in shCtrl and shPAR1 PANC-1, MIA PaCa-2, Capan-2, and 096 PDAC cells. Shown is the mean ± SEM (n=4); * p<0.05, ** p<0.01, *** p<0.001, and **** p<0.0001, (Student´s t-test). E-F).

This was confirmed by shRNA silencing of PAR1 in two additional routinely used PDAC cell lines (MIA PaCa-2 and Capan-2) and one patient-derived primary line (AMC-PDAC-096; 096 in short; knockdown efficiency of PAR1 in the 096 shPAR1 cell line shown in **Sup. Fig. 3**). Transcript analysis of acinar-specific transcription factors MIST1 and PTF1A showed a significant increase in all PAR1-deficient PDAC cell lines **(Fig. 4A, B)**. Moreover, expression of the ductal marker KRT19 and of the transcription factor SOX9 was significantly decreased in all shPAR1 cell-lines **(Fig. 4C, D)**, with the exception of KRT19 in the 096 line. These data not only confirm that PAR1 is instrumental in the maintenance of ductal cell fates in cancer but also suggest that loss of its activity can re-establish acinar cell fates in this context.

We next evaluated KRT19 and amylase expression by immunohistochemistry in orthotopic tumor cell grafts grown from control or shPAR1-transduced mouse KRASG12D/TRP53flox/flox (KP) tumor cells [28] **(Fig. 5)**. In shPAR1 tumors, KRT19 expression was decreased compared to control silenced tumors (shCtrl). Interestingly, we observed numerous amylase-positive cell clusters in shPAR1 tumors, which were (largely) absent in PAR1-proficient (shCtrl) tumors (Fig. 5 with quantification shown in **Sup. Fig. 4**). This confirms that PAR1 not only contributes to ductal cell fates but that its absence partly re-establishes acinar cell identities.
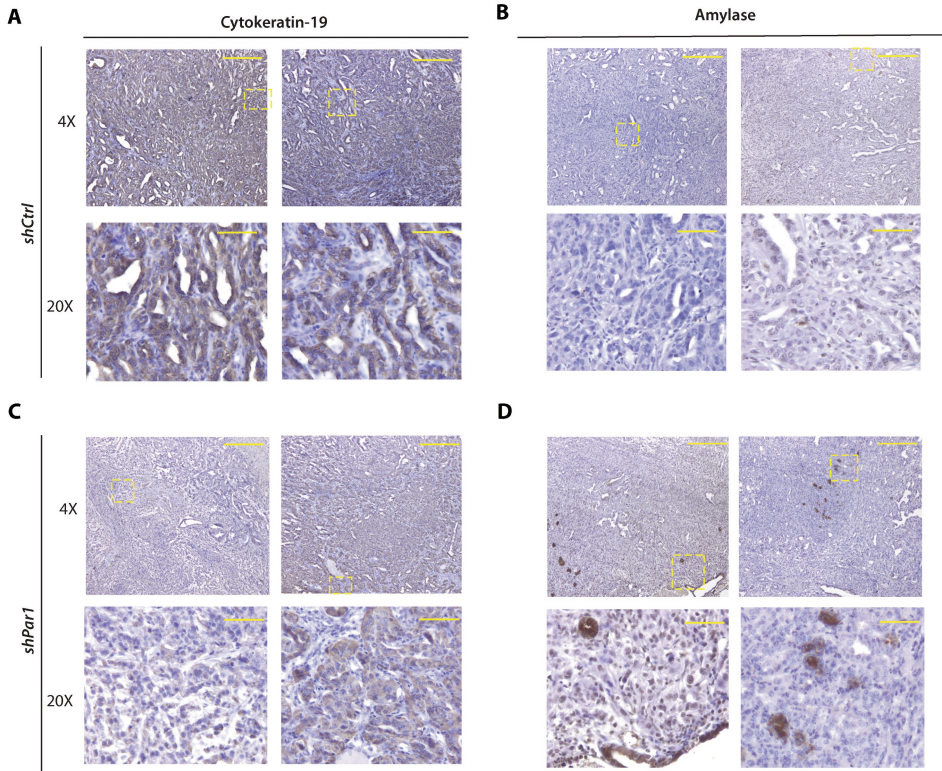
Figure 5

PAR1 silencing in murine PDAC grafts increases acinar marker expression. Immuno-histochemistry (IHC) for cytokeratin-19 (A, C) and amylase (B, D) was performed on orthotopically inoculated shCtrl (A, B) and shPAR1 (C, D) murine KP tumor sections. Image acquisition was performed at 4X and 20X magnification on a Leica CTR500 microscope. Scale bars indicate on 4x magnification 100 μm and on 20x magnification 500 μm.

PAR1 drives ductal cell fates through Myc activity

To elucidate the pathways downstream of PAR1 that govern cell fates, we performed GSEA analysis with the Hallmark Gene Sets [41] on RNA-Seq data from shPAR1 and shCtrl PANC-1 cells **(Fig. 6A)**. This analysis revealed a substantial decrease in Myc target genes in shPAR1 cells. This is particularly interesting, given that Myc overexpression in acinar cells has been shown to drive ADM [42]. Consequently, we next assessed whether inhibition of Myc activity impacted on acinar and ductal cell fates. PTF1A, MIST1, KRT19, SOX9 expression levels in different (i.e., PANC-1, MIA PaCa-2, Capan-2, and 096) PDAC cell lines were measured after treatment with a c-Myc-inhibitor (10058-F4)[43]. This revealed that expression levels of acinar-specific transcription factors were significantly increased following Myc inhibition **(Fig. 6B, C)**. In line with these changes, Myc inhibition led to a decrease in ductal marker expression **(Fig. 6D, E)**.

To establish whether Myc functions downstream of PAR1 in the maintenance of ductal cell fates, we tested Myc inhibition on control and shPAR1 PANC-1 and MIA PaCa-2 cell lines. In control silenced cell lines, Myc inhibition resulted in decreased ductal and increased acinar marker expression (dark grey bars in **Fig. 6F–I**). However, Myc inhibition did not affect the expression levels of these markers in shPAR1 cell lines (compare purple bars to pink bars). Collectively these findings suggest that PAR1 activity drives ADM and maintains a ductal phenotype through the activity of Myc.

Inhibition of PAR1 and Myc enhances acinar cell fates in murine ductal organoids

In tumor contexts, loss or inhibition of PAR1 was able to partially reverse the ductal phenotype of PDAC cells. To further determine whether PAR1 deficiency has a similar impact on ductal maintenance or acinar reprogramming in healthy (non-tumor) ductal cells, we utilized murine ductal organoids. Ductal organoids were cultured in the presence of the PAR1 inhibitors Vorapaxar or P1-pal12 and the Myc inhibitor 10058-F4. The expression of acinar markers Ptf1a, Nr5a2, Mist1, and Cpa1, and ductal-specific markers Krt19, Muc1, and Sox9, and centroacinar marker Stmn1 were measured. Both PAR1 and c-Myc inhibition led
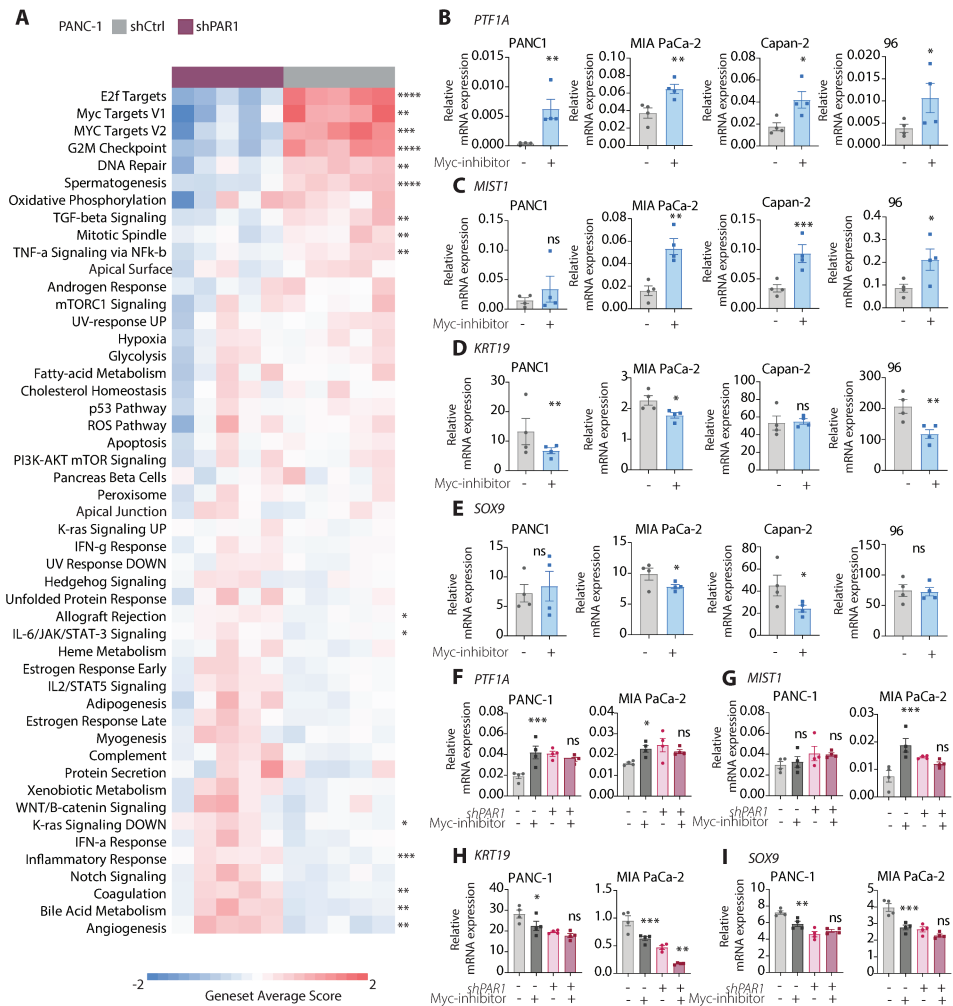
Figure 6

PAR1 drives changes in acinar and ductal related gene expression via Myc. A) Gene Set Map analysis of Hallmark Gene Signatures on shCtrl and shPAR1 PANC-1 cells. * p<0.05, ** p<0.01, *** p<0.001, and **** p<0.0001, Student´s t-test. B-E) Relative mRNA expression analysis of Ptf1a (B), Mist1 (C), Krt19 (D), and Sox9 (E) in DMSO (control) or 50 µM Myc inhibitor (10058-F4) treated PANC-1, MIA PaCa-2, Capan-2 and 096 PDAC cells. RNA was collected 48 hours after treatment. Shown is the mean±SEM (n=4); * p<0.05, ** p<0.01, *** p<0.001, and **** p<0.0001, Student´s t-test. F-I) Relative mRNA expression analysis of PTF1A (F), MIST1 (G), Krt19 (H), and Sox9 (I) in shCtrl and shPAR1 PANC-1 and MIA PaCa-2 cells after treatment with DMSO (control) or 50 µM Myc inhibitor (10058-F4). RNA was collected 48 hours after treatment. Shown is the mean±SEM (n=4); * p<0.05, ** p<0.01, *** p<0.001, and **** p<0.0001, Student´s t-test.

to an increase in acinar markers during the course of several weeks of treatment **(Fig. 7A)**. Correspondingly, expression levels of ductal markers gradually decreased over time **(Fig. 7B)**. Overall, these results show that PAR1 activation drives ductal differentiation in acinar cells **(Fig.7C)** and, more importantly, PAR1 inactivation or Myc inhibition can re-establish acinar cell identities in ductal cells and shows that such plasticity is not unique to acinar cells.
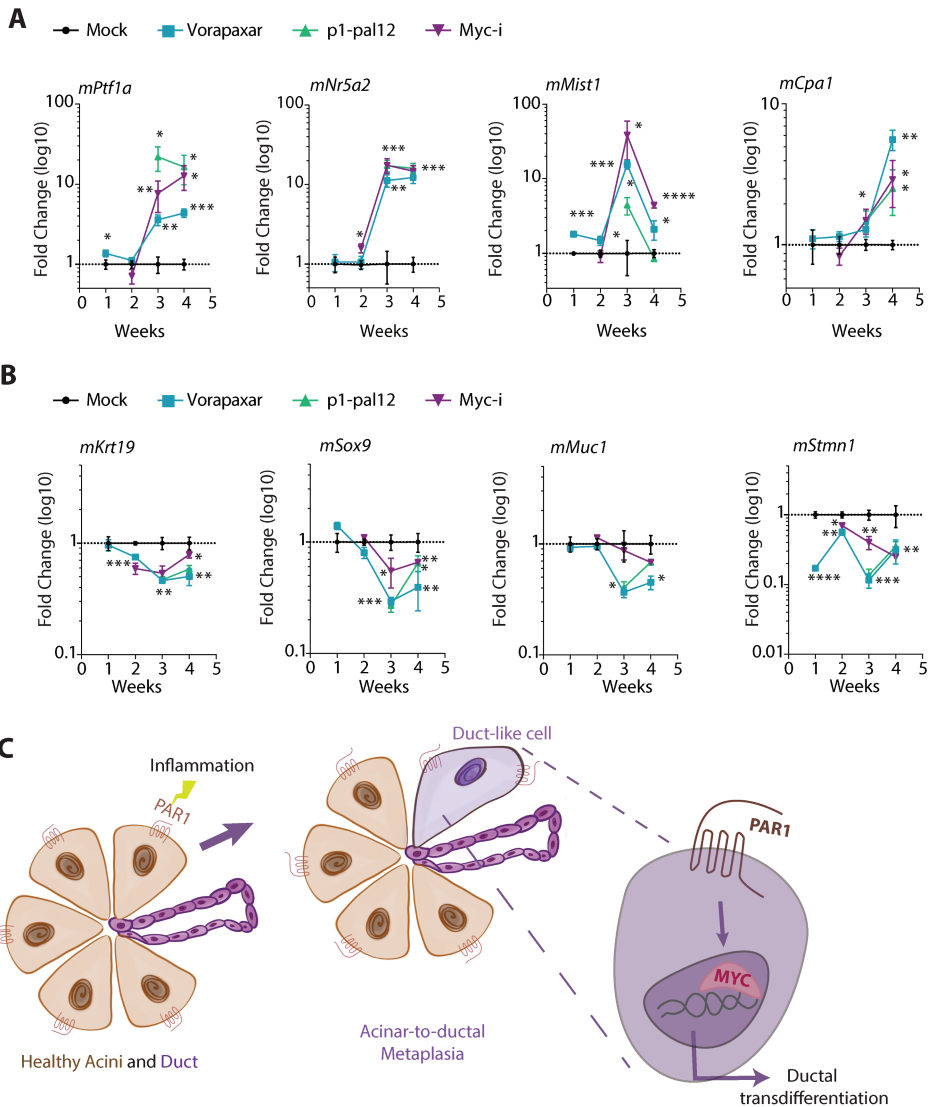
Figure 7

Inhibition of PAR1 and Myc enhances acinar regeneration in healthy murine ductal organoids. A-B) Relative mRNA expression of A) Acinar-related marker expression (Ptf1a, Nr5a2, Cpa1, and Mist1). B) Ductal-related marker expression (Krt19, Muc1, Sox9) and centroacinar marker expression (Stmn1) in murine ductal organoids after treatment with the PAR1 inhibitors Vorapaxar (1 µM) and p1pal-12 (2 µM) or the Myc inhibitor 10058-F4 (25µM). DMSO was used as a mock treatment. At each passage (i.e., each week), new inhibitors were added, and RNA was collected from a subset of cells. Fold changes at each time point were calculated based on the expression of the given marker after mock treatment. Shown is the mean±SEM (n=4); * $p < 0.05$, ** $p < 0.01$, *** $p < 0.001$, and **** $p < 0.0001$, One-way ANOVA. A) Acinar-related marker expression (Ptf1a, Nr5a2, Cpa1, and Mist1). B) Ductal-related marker expression (Krt19, Muc1, Sox9) and centroacinar marker expression (Stmn1). C) Schematic representation of the PAR1-Myc axis in ADM.

DISCUSSION

Transdifferantiation of acinar cells to ductal cells is thought to contribute to tissue regeneration after injury in the pancreas [17,44]. However, aberrant transdifferentiation of acinar cells into ductal cells during ADM is considered a prerequisite for malignant transformation [45]. ADM critically depends on macrophage secreted MMP9 and subsequent NF-κB activation in acinar cells [17]. However, the cellular receptor on acinar cells through which MMP9 activates the NF-κB pathway and subsequent ADM has not yet been identified. In the current manuscript, we addressed the hypothesis that PAR1 acts as a key cellular receptor driving cell fate programs in the exocrine pancreas. This hypothesis is based on previous work that highlights PAR1 as the orchestrating receptor of macrophage-tumor cell interactions in PDAC and on the fact that MMP9 has recently been identified as a novel PAR1 agonist [18]. In line with former findings and with our current hypothesis, we show that genetic ablation of PAR1 increases acinar-related gene expression in the healthy pancreas and that PAR1 deficiency limits ductal transdifferentiation in experimental models for ADM. Moreover, silencing PAR1 in PDAC cells re-establishes acinar cell identities in these ductal cells. Overall, here we identify PAR1 as a novel cellular receptor to orchestrate ADM, and we show that PAR1 governs cellular identity in the (pre)malignant transformed pancreas.

Acinar cells are thought to have the highest plasticity of all pancreatic cell types and, indeed, rather easily de-differentiate into a progenitor phenotype, after which they further differentiate into duct-like cells. Acinar (de)differentiation under benign conditions is reversible, but oncogenic KRAS activation renders this mechanism irreversible and thereby drives ductal metaplasia [8,46]. KRAS silences the acinar transcription factors MIST1 and PTF1A while it concurrently induces expression of the ductal transcription factor SOX9 [17,47]. Silencing the acinar transcription factors predisposes acinar cells to ductal differentiation [48] and accelerates ADM [49]. In the current manuscript, we identify PAR1 as a novel player in acinar (de)differentiation in health and disease. We show that PAR1 inactivation leads to increased expression levels of PTF1A and MIST1, whereas expression levels of SOX9 and KRT19 decrease. Importantly, this PAR1-dependent shift towards an acinar phenotype is not only evident in healthy acinar cells, as PAR1 silencing also increases acinar gene expression in cells from established

PDAC. This suggests that also ductal cells are plastic and able to regenerate into acinar-like cells, even in the presence of oncogenic KRAS activation. Based on these findings, we suggest that PAR1 is critical in ADM and that PAR1 inhibition may prevent malignant progression.

An intriguing finding in our manuscript is the identification of Myc as a downstream factor of the PAR1 driven cellular differentiation program. Myc inhibition in PDAC cells mimics PAR1 inhibition in re-activating the expression of acinar transcription factors (PTF1A, MIST1, and NR5A2). Interestingly, Myc activation is known to drive acinar transdifferentiation. Indeed, acinar-specific Myc over-expression has been described to enhance ductal metaplasia and induce the formation of neoplasms that display both acinar-like neoplastic cells and duct-like neoplastic cells [42]. In addition to affecting acinar-ductal tissue homeostasis, our data show that Myc inhibition leads to the re-expression of acinar-specific genes in both PDAC and healthy ductal cells. Surprisingly, acinar cell transdifferentiation has not been reported in the range of ductal plasticity in the pancreas [46]. Our findings here suggest that the PAR1-Myc axis may be a key driver that prevents transdifferentiation of ductal cells back into acinar-like cells.

5

Another interesting, and at first glance, surprising finding of our study is that PAR1 deficiency (either by genetic ablation or by pharmacological inhibition) also limits ADM formation by EGF. However, PAR1 is known to transactivate the epidermal growth factor receptor (EGFR) in various experimental contexts. For instance, PAR1 transactivates EGFR in invasive breast carcinoma, thereby promoting cellular invasion [50]. PAR1-dependent intracellular phosphorylation of EGFR also induces proliferation of vascular smooth muscle cells [51], whereas PAR1 also promotes human colon cancer proliferation through EGFR transactivation [52]. Our data underscore the importance of EGFR–PAR1 cross-talk in cell fate decisions.

PAR1 expression levels are known to correlate with cancer progression and overall survival in different tumor types of epithelial origin [53,54]. Consistent with such clinical data suggesting a tumor-promoting role of PAR1, experimental studies provide solid evidence for PAR-1 as a driver of cancer progression. PAR1 induces proliferation, migration, and invasion of cancer cells in in vitro experiments

[54,55], whereas tumor cell-specific PAR1 overexpression drives tumor growth in preclinical animal models of breast and prostate cancer [56]. Inline, inhibition of tumor cell PAR1 [57,58], stromal PAR1 depletion [16,59], or pharmacological PAR1 inhibition [14] consistently suppresses tumor growth in experimental animal models. In the current manuscript, we extend this notion by showing that PAR1 not only drives tumor growth but also contributes to the pre-malignant stages of PDAC. Of note, this effect of PAR1 may be context-dependent and could be specific for PDAC. Indeed, an elegant prior study showed that PAR1 deficiency in Transgenic Adenocarcinoma of the Mouse Prostate (TRAMP) mice results in diminished apoptosis in transformed epithelia with subsequent larger and more aggressive prostate tumors [60]. Similarly, PAR1 deficiency on the Adenomatous Polyposis Coli mutant (APC Min) background resulted in more and larger adenomas suggesting that PAR1 limits pre-malignant transformation in prostate and intestinal tumors. In breast cancer, PAR1 deficiency does not seem to modify spontaneous tumor formation [61], further strengthening the notion that PAR1 plays a context-dependent role in premalignant transformation.

CONCLUSION

A picture emerges in which PAR1 is a cellular receptor that governs ductal cell identity. Its perturbation reveals remarkable cellular plasticity in ductal cells. Furthermore, PAR1 represses acinar transcriptional programs to allow regeneration after injury. PAR1 activates the Myc pathway that enhances ADM and locks differentiated acinar cells in a ductal cell state. Downregulating the PAR1-Myc axis, in part, destabilizes the ductal phenotype leading to the transdifferentiation of PDAC cells. Overall, we identify the PAR1-Myc axis as a driver of ductal cell-fates in healthy, premalignant pancreas and PDAC.

DECLARATIONS

5

REFERENCES

[1]   Ducreux M, Cuhna AS, Caramella C, Hollebecque A, Burtin P, Goéré D, et al. Cancer of the pancreas: ESMO Clinical Practice Guidelines for diagnosis, treatment and follow-up. Ann Oncol. 2015;26:v56–68.

[2]   Siegel RL, Miller KD, Jemal A. Cancer statistics, 2019. CA Cancer J Clin. 2019;69:7–34.

[3]   Arnold M, Rutherford MJ, Bardot A, Ferlay J, Andersson TML, Myklebust TÅ, et al. Progress in cancer survival, mortality, and incidence in seven high-income countries 1995–2014 (ICBP SURVMARK-2): a population-based study. Lancet Oncol. 2019;20:1493–505.

[4]   Hruban RH, Goggins M, Parsons J, Kern SE. Progression model for pancreatic cancer. Clin Cancer Res. 2000;6:2969–72.

[5]   Kopp JL, Dubois CL, Schaeffer DF, Samani A, Taghizadeh F, Cowan RW, et al. Loss of Pten and Activation of Kras Synergistically Induce Formation of Intraductal Papillary Mucinous Neoplasia From Pancreatic Ductal Cells in Mice. Gastroenterology. 2018;154:1509-1523.e5.

[6]   Kopp JL, von Figura G, Mayes E, Liu F-F, Dubois CL, Morris JP, et al. Identification of Sox9-Dependent Acinar-to-Ductal Reprogramming as the Principal Mechanism for Initiation of Pancreatic Ductal Adenocarcinoma. Cancer Cell. 2012;22:737–50.

[7]   Guerra C, Schuhmacher AJ, Cañamero M, Grippo PJ, Verdaguer L, Pérez-Gallego L, et al. Chronic Pancreatitis Is Essential for Induction of Pancreatic Ductal Adenocarcinoma by K-Ras Oncogenes in Adult Mice. Cancer Cell. 2007;11:291–302.

[8]   Storz P. Acinar cell plasticity and development of pancreatic ductal adenocarcinoma. Nat Rev Gastroenterol Hepatol. 2017;14:296–304.

[9]   Feldmann G, Beaty R, Hruban RH, Maitra A. Molecular genetics of pancreatic intraepithelial neoplasia. J Hepatobiliary Pancreat Surg. 2007;14:224–32.

[10]   Morris JP, Wang SC, Hebrok M. KRAS, Hedgehog, Wnt and the twisted developmental biology of pancreatic ductal adenocarcinoma. Nat Rev Cancer. 2010;10:683–95.

[11]   Gruber R, Panayiotou R, Nye E, Spencer-Dene B, Stamp G, Behrens A. YAP1 and TAZ Control Pancreatic Cancer Initiation in Mice by Direct Up-regulation of JAK–STAT3 Signaling. Gastroenterology. 2016;151:526–39.

[12]   Flaumenhaft R, De Ceunynck K. Targeting PAR1: Now What? Trends Pharmacol Sci. 2017;38:701–16.

[13]   Boire A, Covic L, Agarwal A, Jacques S, Sherifi S, Kuliopulos A. PAR1 is a matrix metalloprotease-1 receptor that promotes invasion and tumorigenesis of breast cancer cells. Cell. 2005;120:303–13.

[14]   Cisowski J, O'Callaghan K, Kuliopulos A, Yang J, Nguyen N, Deng Q, et al. Targeting protease-activated receptor-1 with cell-penetrating pepducins in

lung cancer. Am J Pathol. 2011;179:513–23.

[15]   Grisaru-Granovsky S, Salah Z, Maoz M, Pruss D, Beller U, Bar-Shavit R. Differential expression of protease activated receptor 1 (Par1) and pY397FAK in benign and malignant human ovarian tissue samples. Int J Cancer. 2005;113:372–8.

[16]   Queiroz KCS, Shi K, Duitman J, Aberson HL, Wilmink JW, Van Noesel CJM, et al. Protease-activated receptor-1 drives pancreatic cancer progression and chemoresistance. Int J Cancer. 2014;135:2294–304.

[17]   Liou GY, Döppler H, Necela B, Krishna M, Crawford HC, Raimondo M, et al. Macrophage-secreted cytokines drive pancreatic acinar-to-ductal metaplasia through NF-KB and MMPs. J Cell Biol. 2013;202:563–77.

[18]   Tekin C, Aberson HL, Waasdorp C, Hooijer GKJ, de Boer OJ, Dijk F, et al. Macrophage-secreted MMP9 induces mesenchymal transition in pancreatic cancer cells via PAR1 activation. Cell Oncol. 2020;43:1161–74.

[19]   Gout J, Pommier RM, Vincent DF, Kaniewski B, Martel S, Valcourt U, et al. Isolation and Culture of Mouse Primary Pancreatic Acinar Cells. J Vis Exp. 2013;1–8.

[20]   Damhofer H, Ebbing EA, Steins A, Welling L, Tol JA, Krishnadath KK, et al. Establishment of patient-derived xenograft models and cell lines for malignancies of the upper gastrointestinal tract. J Transl Med. 2015;13:1–14.

[21]   Bolger AM, Lohse M, Usadel B. Trimmomatic: a flexible trimmer for Illumina sequence data. Bioinformatics. 2014;30:2114–20.

[22]   Harrow J, Denoeud F, Frankish A, Reymond A, Chen CK, Chrast J, et al. GENCODE: producing a reference annotation for ENCODE. Genome Biol. 2006;7 Suppl 1:S4.

[23]   Kim D, Langmead B, Salzberg SL. HISAT: a fast spliced aligner with low memory requirements. Nat Methods. 2015;12:357–60.

[24]   Anders S, Pyl PT, Huber W. HTSeq--a Python framework to work with high-throughput sequencing data. Bioinformatics. 2015;31:166–9.

[25]   Love MI, Huber W, Anders S. Moderated estimation of fold change and dispersion for RNA-seq data with DESeq2. Genome Biol. 2014;15:550.

[26]   R: A language and environment for statistical computing. R Foundation for Statistical Computing, Vienna, Austria

[27]   Huch M, Bonfanti P, Boj SF, Sato T, Loomans CJM, Van De Wetering M, et al. Unlimited in vitro expansion of adult bi-potent pancreas progenitors through the Lgr5/R-spondin axis. EMBO J. 2013;32:2708–21.

[28]   Tekin C, Shi K, Daalhuisen JB, ten Brink MS, Bijlsma MF, Spek CA. PAR1 signaling on tumor cells limits tumor growth by maintaining a mesenchymal phenotype in pancreatic cancer. Oncotarget. 2018;9:32010–23.

[29]   Badea L, Herlea V, Dima SO, Dumitrascu T, Popescu I. Combined gene expression analysis of whole-tissue and microdissected pancreatic ductal adenocarcinoma identifies genes specifically overexpressed in tumor epithelia. Hepato-

gastroenterology. 2008;55:2016–27.

[30]   Yang S, He P, Wang J, Schetter A, Tang W, Funamizu N, et al. A Novel MIF Signaling Pathway Drives the Malignant Character of Pancreatic Cancer by Targeting NR3C2. Cancer Res. 2016;76:3838–50.

[31]   Pei H, Li L, Fridley BL, Jenkins GD, Kalari KR, Lingle W, et al. FKBP51 Affects Cancer Cell Response to Chemotherapy by Negatively Regulating Akt. Cancer Cell. 2009;16:259–66.

[32]   Zhang G, Schetter A, He P, Funamizu N, Gaedcke J, Ghadimi BM, et al. DPEP1 Inhibits Tumor Cell Invasiveness, Enhances Chemosensitivity and Predicts Clinical Outcome in Pancreatic Ductal Adenocarcinoma. El-Rifai W, editor. PLoS One. 2012;7:e31507.

[33]   Bailey P, Chang DK, Nones K, Johns AL, Patch A-M, Gingras M-C, et al. Genomic analyses identify molecular subtypes of pancreatic cancer. Nature. 2016;531:47–52.

[34]   Nones K, Waddell N, Song S, Patch A-MM, Miller D, Johns A, et al. Genome-wide DNA methylation patterns in pancreatic ductal adenocarcinoma reveal epigenetic deregulation of SLIT-ROBO, ITGA2 and MET signaling. Int J Cancer. 2014;135:1110–8.

[35]   Pérez-Mancera PA, Rust AG, van der Weyden L, Kristiansen G, Li A, Sarver AL, et al. The deubiquitinase USP9X suppresses pancreatic ductal adeno-carcinoma. Nature. 2012;486:266–70.

[36]   Pinho A V., Van Bulck M, Chantrill L, Arshi M, Sklyarova T, Herrmann D, et al. ROBO2 is a stroma suppressor gene in the pancreas and acts via TGF-β signalling. Nat Commun. 2018;9:5083.

[37]   Chou A, Waddell N, Cowley MJ, Gill AJ, Chang DK, Patch A-M, et al. Clinical and molecular characterization of HER2 amplified-pancreatic cancer. Genome Med. 2013;5:78.

[38]   Raphael BJ, Hruban RH, Aguirre AJ, Moffitt RA, Yeh JJ, Stewart C, et al. Integrated Genomic Characterization of Pancreatic Ductal Adenocarcinoma. Cancer Cell. 2017;32:185-203.e13.

[39]   Muraro MJ, Dharmadhikari G, Grün D, Groen N, Dielen T, Jansen E, et al. A Single-Cell Transcriptome Atlas of the Human Pancreas. Cell Syst. 2016;3:385-394.e3.

[40]   Kobayashi H, Spilde TL, Li Z, Marosky JK, Bhatia AM, Hembree MJ, et al. Lectin as a marker for staining and purification of embryonic pancreatic epithelium. Biochem Biophys Res Commun. 2002;293:691–7.

[41]   Liberzon A, Birger C, Thorvaldsd??ttir H, Ghandi M, Mesirov JP, Tamayo P. The Molecular Signatures Database Hallmark Gene Set Collection. Cell Syst. 2015;1:417–25.

[42]   Grippo PJ, Sandgren EP. Acinar-to-ductal metaplasia accompanies c-myc-induced exocrine pancreatic cancer progression in transgenic rodents. Int J Cancer. 2012;131:1243–8.

148

[43]   Fletcher S, Prochownik E V. Small-molecule inhibitors of the Myc on-coprotein. Biochim Biophys Acta - Gene Regul Mech. 2015;1849:525–43.

[44]   Houbracken I, de Waele E, Lardon J, Ling Z, Heimberg H, Rooman I, et al. Lineage Tracing Evidence for Transdifferentiation of Acinar to Duct Cells and Plasticity of Human Pancreas. Gastroenterology. 2011;141:731-741.e4.

[45]   Rooman I, Real FX. Pancreatic ductal adenocarcinoma and acinar cells: A matter of differentiation and development? Gut. 2012;61:449–58.

[46]   Demcollari TI, Cujba AM, Sancho R. Phenotypic plasticity in the pancre-as: new triggers, new players. Curr Opin Cell Biol. 2017;49:38–46.

[47]   Shi G, DiRenzo D, Qu C, Barney D, Miley D, Konieczny SF. Main-tenance of acinar cell organization is critical to preventing Kras-induced aci-nar-ductal metaplasia. Oncogene. 2013;32:1950–8.

[48]   Johnson CL, Peat JM, Volante SN, Wang R, McLean CA, Pin CL. Acti-vation of protein kinase Cδ leads to increased pancreatic acinar cell dedifferenti-ation in the absence of MIST1. J Pathol. 2012;228:351–65.

[49]   Benitz S, Regel I, Reinhard T, Popp A, Schäffer I, Raulefs S, et al. Poly-comb repressor complex 1 promotes gene silencing through H2AK119 mo-no-ubiquitination in acinar-to-ductal metaplasia and pancreatic cancer cells. On-cotarget. 2016;7:11424–33.

[50]   Arora P, Cuevas BD, Russo A, Johnson GL, Trejo J. Persistent transac-tivation of EGFR and ErbB2/HER2 by protease-activated receptor-1 promotes breast carcinoma cell invasion. Oncogene. 2008;27:4434–45.

[51]   Huang Y-L, Shi G-Y, Lee H, Jiang M-J, Huang B-M, Wu H-L, et al. Thrombin induces nestin expression via the transactivation of EGFR signalings in rat vascular smooth muscle cells. Cell Signal. 2009;21:954–68.

[52]   Darmoul D, Gratio V, Devaud H, Peiretti F, Laburthe M. Activation of proteinase-activated receptor 1 promotes human colon cancer cell prolifera-tion through epidermal growth factor receptor transactivation. Mol Cancer Res. 2004;2:514–22.

[53]   Liu X, Yu J, Song S, Yue X, Li Q. Protease-activated receptor-1 (PAR-1): A promising molecular target for cancer. Oncotarget. 2017;8:107334–45.

[54]   Wojtukiewicz MZ, Hempel D, Sierko E, Tucker SC, Honn K V. Prote-ase-activated receptors (PARs)—biology and role in cancer invasion and metas-tasis. Cancer Metastasis Rev. 2015;34:775–96.

[55]   Borensztajn KS, Spek CA. Protease-activated receptors, apoptosis and tumor growth. Pathophysiol Haemost Thromb. 2008;36:137–47.

[56]   Spek CA, Tekin C, Bijlsma MFF. Protease-activated receptor-1 impedes prostate and intestinal tumor progression in mice: comment. J Thromb Haemost. 2019;17:235–8.

[57]   Auvergne R, Wu C, Connell A, Au S, Cornwell A, Osipovitch M, et al. PAR1 inhibition suppresses the self-renewal and growth of A2B5-defined glioma progenitor cells and their derived gliomas in vivo. Oncogene. 2016;35:3817–28.
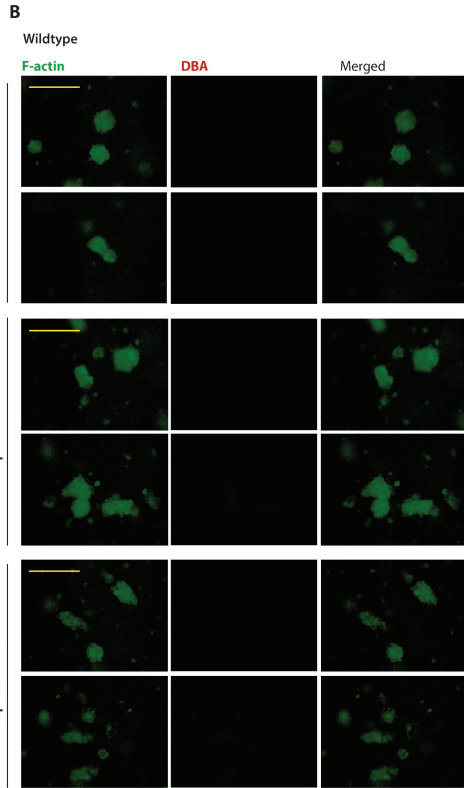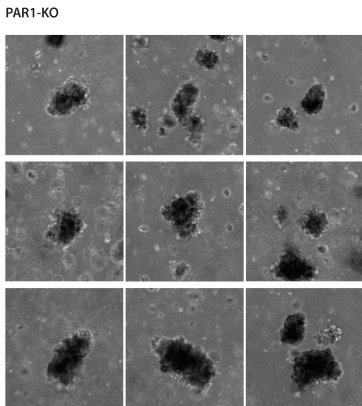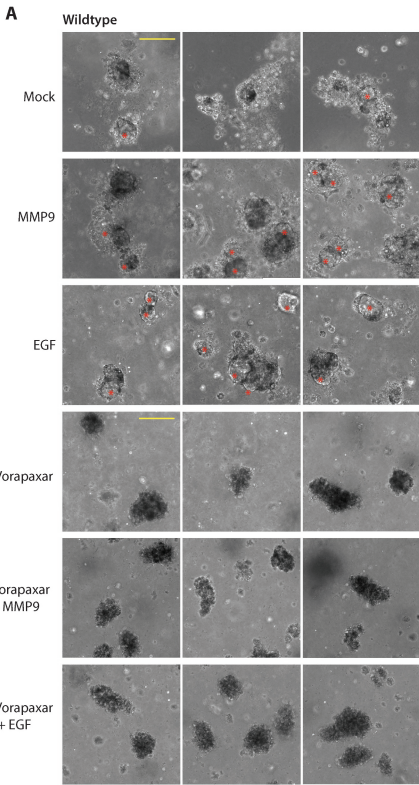
5

[58] Villares GJ, Zigler M, Wang H, Melnikova VO, Wu H, Friedman R, et al. Targeting melanoma growth and metastasis with systemic delivery of liposome-incorporated protease-activated receptor-1 small interfering RNA. Cancer Res. 2008;68:9078–86.

[59] Adams GN, Rosenfeldt L, Frederick M, Miller W, Waltz D, Kombrinck K, et al. Colon cancer growth and dissemination relies upon thrombin, Stromal PAR-1, and fibrinogen. Cancer Res. 2015;

[60] Adams GN, Sharma BK, Rosenfeldt L, Frederick M, Flick MJ, Witte DP, et al. Protease-activated receptor-1 impedes prostate and intestinal tumor progression in mice. J Thromb Haemost. 2018;16:2258–69.

[61] Versteeg HH, Schaffner F, Kerver M, Ellies LG, Andrade-Gordon P, Mueller BM, et al. Protease-Activated Receptor (PAR) 2, but not PAR1, Signaling Promotes the Development of Mammary Adenocarcinoma in Polyoma Middle T Mice. Cancer Res. 2008;68:7219–27.

SUPPORTING INFORMATION
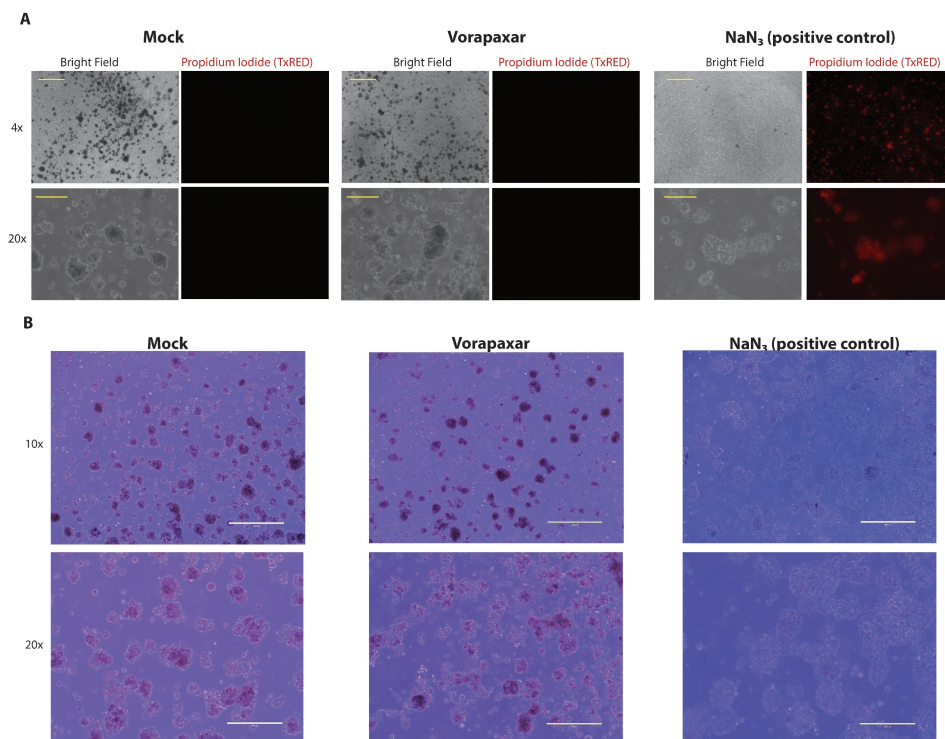
Supplementary Figure 1

Viability of 3D collagen embedded pancreatic acinar cells. A) Acinar spheroids were treated with mock (DMSO), 1 μM Vorapaxar, and 0.5 mM NaN3 on the day of cell seeding. Pictures were taken 4 days after cell seeding/treatment. Propidium Iodide (20μg/ml) was supplemented 15 minutes prior to imaging. Phase-contrast and TxRed (red fluorescence) images are shown at 4X and 20X magnifications. Scale bars indicate 500 μm on 4X, and 200 μm on 20X images. B) Resazurin (blue)- Resofurin (pink) conversion for detection of mitochondrial activity in acinar cultures. Acinar cells were treated as for panel A. 200 μl of CellTiter Blue reagent (resazurin) was added to 1000 μl of culture media and was incubated for 4 hours. Phase-contrast images are given at 10X and 20X magnifications. Scale bars indicate 400 μm on 10X, and 200 μm on 20X images. All images are taken with the EVOS FL cell imaging system.

A

Wildtype

Mock

MMP9

EGF

Vorapaxar

Vorapaxar + MMP9

Vorapaxar + EGF

PAR1-KO

Mock

MMP9

EGF

B

Wildtype

F-actin | DBA | Merged

Vorapaxar

Vorapaxar + MMP9

Vorapaxar + EGF

Supplementary Figure 2

PAR1 deficiency and PAR1 inhibition limit ductal differentiation of 3D collagen-embedded acinar cells. A) Phase-contrast images of 3D collagen embedded acinar cells from wildtype and PAR1-deficient acinar cells are shown. Wildtype (upper panel) or PAR1 deficient (lower panel) acinar cells were treated with DMSO as mock or with 1μM Vorapaxar (only on the wildtype group), and 1 ng/ml MMP9, or 50 ng/ml EGF for 5 days. Image acquisition was performed on day 5 at 20X magnification with the EVOS FL cell imaging system. Ductal structures are marked with an asterisk (red). B) Fluorescence images of 3D collagen embedded acinar cells from wildtype acinar cells with vorapaxar treatment. Acinar cells were treated with 1 μM vorapaxar and with 1 ng/ml MMP9, or 50 ng/ml EGF for 5 days. Image acquisition was performed on day 5 at 20X magnification with EVOS FL cell imaging system with YFP (F-actin) and Tx-Red (DBA) channels. YFP and Tx-Red channels were merged on ImageJ. Scale bars indicate 200 μm.

5
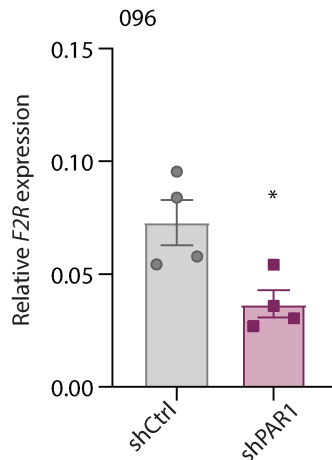
Supplementary Figure 3

shRNA knockdown confirmation of the primary 096 PDAC cell line. Shown mRNA expression for PAR1 (F2R) is relative to TBP. Shown is the mean±SEM (n=4); * $p < 0.05$, Student´s t-test.
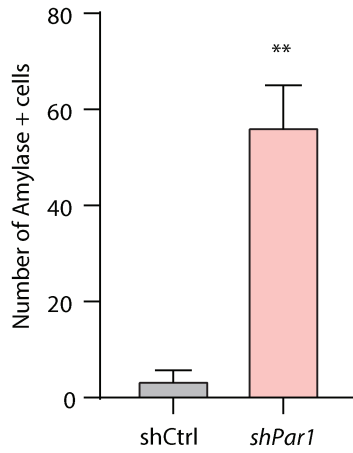
Supplementary Figure 4

Amylase expression increases in shPar1 tumors in the murine orthotopic KP model. Amylase-positive nuclei were counted on 4X images of 2 independent tumors in both the shCtrl and shPar1 group with the Image J IHC toolbox for DAB staining and nuclei detection (https://imagej.nih.gov/ij/plugins/ihc-toolbox/index.html). Shown is the mean±SEM (n=2); ** $p<0.01$, Student´s t-test.

Chapter 6

PAR1: Not such a good target as anticipated for cancer patients?

C Arnold Spek, Cansu Tekin, Maarten F Bijlsma

COMMENTARY

Protease activated receptor 1 (PAR-1), originally identified as the thrombin receptor on platelets and vascular endothelial cells, is expressed on numerous cells throughout the body. Tumor cells, and cells in the tumor microenvironment like cancer-associated fibroblasts, macrophages, T cells and endothelial cells, are no exception and PAR-1 expression is abundant in a variety of cancer tissues [1,2]. The potential relevance of PAR-1 expression for tumor growth is underscored by observations that PAR-1 expression levels correlate with cancer progression and overall survival [1,2]. Consistent with such clinical data hinting towards a tumor-promoting effect of PAR-1, experimental studies seem to provide solid evidence for activated PAR-1 as a driver of cancer progression. Indeed, PAR-1 activation induces proliferation, migration and invasion of cancer cells in different in vitro experiments (excellently reviewed in references [2,3]) whereas tumor cell specific PAR-1 overexpression potentiates tumor growth in preclinical animal models of breast and prostate cancer **(Table 1)** [4-6]. In line, shRNA-mediated inhibition of tumor cell PAR-1 [7,8], stromal PAR-1 depletion [9,10] or pharmacological PAR-1 inhibition [11] consistently suppress tumor growth in animal models. As a consequence, the current paradigm dictates that PAR-1 drives cancer progression based upon which PAR-1 has been suggested as a promising target for the treatment of cancer [1]. Intriguing recent data are however at odds with this paradigm and suggest that PAR-1 could also harbor tumor suppressive functions.

Table 1

Overview of studies targeting PAR-1 in experimental animal models of cancer.

Tumor type	PAR-1 modulation	Tumor site	Animals	Key finding	Reference
Breast cancer	PAR-1 deficient mice crossed into polyoma middle T mice.	Orthotopic	C57Bl/6 mice	Appearance of palpable tumors, tumor expansion, and metastasis was indistinguishable between wild-type and PAR-1 deficient mice.	Versteeg et al [19].
Breast cancer	PAR-1 overexpressing tumor cells in wild type animals.	Orthotopic	Nude mice	Large and highly vascularized tumors were generated by cells over-expressing wild type PAR-1, whereas small or no tumors developed in cells over-expressing truncated PAR-1 and/or control cells.	Cohen et al [4]; Kancharla et al [20].
Breast cancer	PAR-1 overexpressing tumor cells in wild type animals.	Orthotopic	Nude mice	PAR1 is both required and sufficient to promote growth and invasion of breast carcinoma cells.	Boire et al [5].
Colon cancer	Wild type tumor cells in PAR-1 deficient animals.	Subcutaneous	C57Bl/6 mice	Palpable tumors developed in the same time frame in both wild type and PAR-1 deficient mice but tumors growing in PAR-1 deficient mice grew significantly slower than those in wild type mice.	Adams et al [9].
Colon cancer	PAR-1 deficient mice crossed with APC$^{min/+}$ mice.	Orthotopic	C57Bl/6 mice	PAR-1-deficient APC$^{Min/+}$ mice developed more adenomas than PAR-1 expressing mice, and the adenomas that formed were significantly larger.	Adams et al [12].
Glioma	PAR-1 deficient tumor cells in wild type animals	Intracranial	NOG mice	shRNA-dependent PAR-1 silencing suppressed tumor expansion and prolonged survival.	Auvergne et al [7].
Lung cancer	Systemic PAR-1 inhibition in wild type animals.	Subcutaneous	Nude mice	Monotherapy with the PAR-1 pepducin P1pal-7 provided 75% inhibition of lung tumor growth.	Cisowski et al [11].
Melanoma	PAR-1 deficient tumor cells in wild type animals.	Subcutaneous	Nude mice	Decreased tumor growth in mice injected with PAR-1 silenced cells.	Villares et al [8].
Melanoma	Systemic PAR-1 inhibition in wild type animals.	Subcutaneous	Nude mice	Decreased tumor growth in mice treated with liposome-incorporated PAR-1 shRNA.	Villares et al [8].
Pancreatic cancer	Wild type tumor cells in PAR-1 deficient animals.	Orthotopic	C57Bl/6 mice	PAR-1 expression in the microenvironment drove tumor progression and induced chemoresistance.	Queiroz et al [10].
Pancreatic cancer	PAR-1 deficient tumor cells in wild type animals.	Orthotopic	C57Bl/6 mice	Tumor cell PAR-1 negatively affected tumor growth, yet promoted metastasis.	Tekin et al [13].
Prostate cancer	Inducible PAR-1 over-expressing tumor cells in wild type animals.	Subcutaneous	Copenhagen rats.	Doxycycline-dependent PAR-1 induction increased tumor mass and angiogenesis.	Yin et al [6].
Prostate cancer	PAR-1 deficient mice interbred with mice carrying the TRAMP transgene.	Orthotopic	C57Bl/6 mice	PAR-1 deficiency resulted in larger and more aggressive prostate tumors.	Adams et al [12].

In a recent issue of the Journal of Thrombosis and Haemostasis, Adams and colleagues elegantly addressed the importance of PAR-1 in spontaneously developing tumor models and showed that the genetic elimination of PAR-1 in fact aggravated tumor development [12]. Interbreeding PAR-1 deficient mice with TRAMP (transgenic adenocarcinoma of the mouse prostate) mice that spontaneously develop prostate tumors led to significantly larger tumors with features of aggressive growth. Moreover, PAR-1 deficient Adenomatous Polyposis Coli min (APCmin/+) mice developed more and larger adenomas as compared to PAR-1 wild type APCmin/+ mice. In a concurrently published paper from our own group, we showed that PAR-1 silencing in cancer cells induced well-differentiated tumors with enhanced growth characteristics in an orthotopic pancreatic cancer model [13]. These intriguing novel studies emphasize that the role of PAR-1 in cancer biology is not as straightforward as anticipated and highlight that PAR-1 may not be the anticipated promising target for the treatment of cancer.

PAR-1 is traditionally known to be activated by the blood coagulation factor thrombin and the potential importance of thrombin (or blood coagulation in general) in cancer was already described by Bouillard and Trousseau in the 19th century [14]. Due to an intense research effort, thrombin is now accepted to be a key player in various cellular processes relevant to tumor growth and metastasis [3,16]. Initial clinical studies confirmed this notion by showing that anticoagulant treatment prolonged overall survival of cancer patients, but subsequent studies were unable to make good on the promise of anticoagulants in cancer treatment. Although several hypotheses have been put forward, the minimal effect of anticoagulants on the overall survival of cancer patients remained puzzling [14]. The recent papers of Adams [12] and Tekin [13] may provide an interesting explanation. As excellently reviewed in reference [15], most (if not all) of the thrombin effects are suggested to be PAR-1 mediated. It is thus well conceivable that the observed tumor-impeding effects of PAR-1 are also thrombin dependent and that anticoagulant treatment would consequently provoke tumor growth in certain contexts.

The opposing results from preclinical PAR-1 studies strongly support the no-

tion that PAR-1 plays a context-dependent role in tumor biology. Indeed, stromal depletion of PAR-1 limits pancreatic cancer progression [10], whereas PAR-1 depletion from tumor cells potentiates tumor growth in a similar orthotopic pancreatic cancer model [13]. Likewise, colon cancer growth is inhibited when wild type (PAR-1 expressing) colon cancer cells are implanted in PAR-1 deficient mice [9], but is increased in a model in which both tumor and stromal cells are PAR-1 deficient. It thus seems that PAR-1 exerts an opposing role in the stroma and tumor cells, indicating that the effects seen in PAR-1 targeting studies may critically dependent on the chosen model (i.e. stromal versus tumor cell targeting). Of note, all studies that demonstrated that tumor cell PAR-1 drives tumor progression employed immune-compromised mice (either nude or NOG, see Table 1 for an overview). Considering the importance of immune cells in the stromal compartment [16,17], it is tempting to speculate that the presence or absence of immune cells determines the outcome of tumor cell PAR-1 targeting studies. Importantly, the two most recent studies showing that PAR-1 limits cancer progression [12,13] were performed in immune-competent mice in which immune cells are omnipresent. The actual importance of PAR-1 on immune cells in the setting of cancer biology remains to be established however but it would be interesting to directly compare the growth dynamics of PAR-1 deficient tumor cells in immune-competent versus immune-compromised mice.

In their search for the mechanism that underlies the growth inhibiting effect of PAR-1 in TRAMP and/or APCmin mice, Adams and colleagues observed a dramatic reduction in apoptotic cells in PAR-1 deficient tumors [12]. Next, they elegantly showed that activated protein C- but not thrombin- mediated PAR-1 activation induced apoptosis of prostate cancer cells in vitro. The agonist-dependent divergent response of PAR-1, referred to as biased agonism [18], strongly suggests that the endogenous activating protease(s) dictate(s) the context-dependent role of PAR-1 in tumor progression. Such a hypothesis underscores the importance of the preclinical animal model and the lack of immune cells in nude mouse models may obscure data interpretation. Indeed, immune cells secrete PAR-1 agonists like MMPs and Granzymes themselves, whereas they may also impact upon PAR-1 agonist expression by tumor cells. The lack of immune cells

6

thus changes the protease composition in the tumor microenvironment thereby affecting the dynamics of PAR-1 activation and potentially masking the tumor suppressive roles of PAR-1. It is however not before we identify the endogenous PAR-1 agonist driving apoptosis of tumor cells that we could prove or refute this hypothesis.

The PAR-1-cancer biology field is currently bustling with important questions remaining to be answered. It is pivotal to fully understand the context-dependent role of PAR-1 and to assess whether PAR-1 indeed plays opposing roles in tumor cells and the stromal compartment. Moreover, it will be of great interest to assess whether immune cells are key mediators in PAR-1 dependent tumor growth and whether tumor cell PAR-1 would be pro-tumorigenic in the absence of immune cells but anti-tumorigenic in their presence. Finally, it has to be established whether the tumor suppressive and tumor promoting functions of PAR-1 in vivo are mediated by different PAR-1 agonists and whether specifically targeting the tumor promoting agonist would hold clinical promise. Irrespective of the answers to these questions, the paradigm shift from PAR-1 as strictly tumor-promoting to a potential context-dependent tumor suppressor establishes that PAR-1 is currently not an attractive target to pursue in a cancer setting. Next to potential bleeding complications that already were a major concern for long term treatment, PAR-1 inhibition may even potentiate tumor development in certain patients. The latter also directly implies that it will be pivotal to carefully monitor patients on Vorapaxar treatment not only for bleeding complications but also for unfavorable effects on tumor development.

REFERENCES

[1]   Liu X, Yu J, Song S, Yue X, Li Q. Protease-activated receptor-1 (PAR-1): a   promising molecular target for cancer. Oncotarget 2017; 8: 107334-45.

[2]   Wojtukiewicz MZ, Hempel D, Sierko E, Tucker SC, Honn KV. Protease-activated receptors (PARs)--biology and role in cancer invasion and metastasis. Cancer Metastasis Rev 2015; 34: 775-96.

[3]   Borensztajn K, Spek CA. Protease-activated receptors, apoptosis and tumor growth. Pathophysiol Haemost Thromb 2008; 36: 137-47.

[4]   Cohen I, Maoz M, Turm H, Grisaru-Granovsky S, Maly B, Uziely B, Weiss E, Abramovitch R, Gross E, Barzilay O, Qiu Y, Bar-Shavit R. Etk/Bmx regulates proteinase-activated-receptor1 (PAR1) in breast cancer invasion: signaling partners, hierarchy and physiological significance. PLoS One 2010; 5: e11135.

[5]   Boire A, Covic L, Agarwal A, Jacques S, Sherifi S, Kuliopulos A. PAR1 is a matrix metalloprotease-1 receptor that promotes invasion and tumorigenesis of breast cancer cells. Cell 2005; 120: 303–13.

[6]   Yin YJ, Salah Z, Maoz M, Even Ram SC, Ochayon S, Neufeld G, Katzav S, Bar-Shavit R. Oncogenic transformation induces tumor angiogenesis: a role for PAR1 activation. FASEB J 2003; 17: 163-74.

[7]   Auvergne R, Wu C, Connell A, Au S, Cornwell A, Osipovitch M, Benraiss A, Dangelmajer S, Guerrero-Cazares H, Quinones-Hinojosa A, Goldman SA. PAR1 inhibition suppresses the self-renewal and growth of A2B5-defined glioma progenitor cells and their derived gliomas in vivo. Oncogene 2016; 35: 3817-28.

[8]   Villares GJ, Zigler M, Wang H, Melnikova VO, Wu H, Friedman R, Leslie MC, Vivas-Mejia PE, Lopez-Berestein G, Sood AK, Bar-Eli M. Targeting melanoma growth and metastasis with systemic delivery of liposome-incorporated protease-activated receptor-1 small interfering RNA. Cancer Res 2008; 68: 9078-86.

[9]   Adams GN, Rosenfeldt L, Frederick M, Miller W, Waltz D, Kombrinck K, McElhinney KE, Flick MJ, Monia BP, Revenko AS, Palumbo JS. Colon Cancer Growth and Dissemination Relies upon Thrombin, Stromal PAR-1, and Fibrinogen. Cancer Res 2015; 75: 4235-43.

[10]   Queiroz KCS, Shi K, Duitman J, Aberson HL, Wilmink JW, Van Noesel CJM, Richel DJ, Spek CA. Protease-activated receptor-1 drives pancreatic cancer progression and chemoresistance. Int J Cancer 2014; 135: 2294–304.

[11]   Cisowski J, O'Callaghan K, Kuliopulos A, Yang J, Nguyen N, Deng Q, Yang E, Fogel M, Tressel S, Foley C, Agarwal A, Hunt SW 3rd, McMurry T, Brinckerhoff L, Covic L. Targeting protease-activated receptor-1 with cell-penetrating pepducins in lung cancer. Am J Pathol 2011; 179: 513-23.

[12]   Adams GN, Sharma BK, Rosenfeldt L, Frederick M, Flick MJ, Witte DP,

6

Mosnier LO, Harmel-Laws E, Steinbrecher KA, Palumbo JS. Protease activated receptor-1 impedes prostate and intestinal tumor progression in mice. J Thromb Haemost 2018, epub ahead of print.

[13]   Tekin C, Shi K, Daalhuisen JB, Ten Brink MS, Bijlsma MF, Spek CA. PAR1 signaling on tumor cells limits tumor growth by maintaining a mesenchymal phenotype in pancreatic cancer. Oncotarget 2018; 9: 32010-23.

[14]   Spek CA, Versteeg HH, Borensztajn KS. Anticoagulant therapy of cancer patients: Will patient selection increase overall survival? Thromb Haemost 2015; 114: 530-6.

[15]   Han N, Jin K, He K, Cao J, Teng L. Protease-activated receptors in cancer: A systematic review. Oncol Lett 2011; 2: 599-608.

[16]   Mahajan UM, Langhoff E, Goni E, Costello E Greenhalf W, Halloran C, Ormanns S, Kruger S, Boeck S, Ribback S, Beyer G, Dombroswki F, Weiss FU, Neoptolemos JP, Werner J, D'Haese JG, Bazhin A, Peterhansl J, Pichlmeier S, Büchler MW, Kleeff J, Ganeh P, Sendler M, Palmer DH, Kohlmann T, Rad R, Regel I, Lerch MM, Mayerle J. Immune Cell and Stromal Signature Associated with Progression-free Survival of Patients with Resected Pancreatic Ductal Adenocarcinoma. Gastroenterology 2018, epub ahead of print.

[17]   Gajewski TF, Schreiber H, Fu YX. Innate and adaptive immune cells in the tumor microenvironment. Nat Immunol 2013; 14: 1014-22.

[18]   Zhao P, Metcalf M, Bunnett N.W. Biased signaling of protease-activated receptors. Front Endocrinol (Lausanne) 2014; 5: 67.

[19]   Versteeg HH, Schaffner F, Kerver M, Ellies LG, Andrade-Gordon P, Mueller BM, Ruf W. Protease-activated receptor (PAR) 2, but not PAR1, signaling promotes the development of mammary adenocarcinoma in polyoma middle T mice. Cancer Res 2008; 68: 7219-27.

[20]   Kancharla A, Maoz M, Jaber M, Agranovich D, Peretz T, Grisaru-Granovsky S, Uziely B, Bar-Shavit R. PH motifs in PAR1&2 endow breast cancer growth. Nat Commun 2015; 6: 8853.

Chapter 7

General Discussion and Future Perspectives

General Discussion and Future Perspectives

PAR1 activation, biased signaling, and the downstream pathway

PAR1 is a member of the G-protein coupled receptor (GPCR) family. The conventional mechanism for GPCR activation involves conformational changes in the receptor following agonist binding, subsequently translating into the activation of different downstream G-protein subunits [1]. The PAR family fundamentally differs from other GPCRs and carries their endogenous ligands on the N-terminal arm of the receptor. Receptor cleavage by extracellular proteases releases the tethered ligand, which then folds back and binds the receptor, initiating the conformational changes that commence downstream signaling [2]. After proteolytic activation, PAR1 is transported from the cell membrane to the endosome for degradation in the lysosomes [3].

The first identified PAR1 agonist was Thrombin (gene name: coagulation factor II, F2); hence PAR1 is also known as the thrombin receptor (F2R). Thrombin cleaves the PAR1 N-terminal arm between arginine and serine at position 46, and this cleavage is considered the canonical mode of activation for this receptor. However, other proteases such as matrix metalloproteases (MMPs) cleave PAR1 at different sites, and these cleavages are considered non-canonical cleavage events. The canonical and non-canonical cleavage of PAR1 can result in different, albeit subtle conformational changes and allosteric mechanisms that govern downstream signal transduction [4]. The different pathways can trigger highly divergent physiological outcomes [5,6]. In addition to canonical and non-canonical activation of PAR1, some proteases such as elastase and plasmin cleave PAR1 further downstream from the activation sites leading to inactivating of the receptor [7]. The ability of different proteases to interact with the same GPCR to trigger different signaling pathways that may lead to vastly different physiological consequences is called biased signaling (or biased agonism) [8]. Knowledge of the PAR1 agonist(s) present in a particular context and the site cleaved is essential to understand why certain, often seemingly contradictory, responses are observed following PAR1 activation [4].

PAR1 activity in epithelial-to-mesenchymal transition and tumor growth

In cancer, the ubiquitous expression of PAR1 and persistent stimulation of its known downstream pathway components such as AKT, NF-κB, ERK1/2, and HIF-1α impacts cell growth and apoptosis, thereby aiding tumor growth [9–12]. Furthermore, PAR1 has been shown to transactivate the epidermal growth factor receptor (EGFR) [13–15] and to interact with the Hippo-YAP pathway, both of which are signaling cascades known to promote tissue growth and tumorigenesis [16]. In agreement, experimental work on PAR1 shows that the majority of downstream signaling activities contribute to poor prognosis by enhancing tumor growth [17–21], epithelial-to-mesenchymal transition (EMT) and the resultant tumor cell motility [17,22–29], and tumor angiogenesis/endothelial barrier function [18,30,31]. Among all these potential pro-tumorigenic properties, the most important effect seems to be PAR1-dependent increased cell motility, metastasis, and invasive growth. PAR1 mediates tumor cell invasiveness through different mechanisms. For instance, PAR1 activity on tumor cells results in increased adhesion of platelets to tumor cells and of tumor cells to the extracellular matrix (ECM). As a consequence, it is likely that PAR1 increases ECM invasion, and platelet interactions protect tumor cells from shear stress in the bloodstream and allow evasion from immune surveillance [32–37].

Based upon the well-known importance of EMT in tumor cell migration and the potential involvement of PAR1 in EMT, it is tempting to suggest that PAR1 also contributes to differentiation to mesenchymal cell states that support metastasis and consequently poor prognosis in PDAC. In Chapter 2, we address the importance of PAR1 in the EMT of PDAC cells and show that PAR1 plays a vital role in the maintenance of a mesenchymal cell state. The key finding of Chapter 2 is that PAR1 limits tumor growth by inducing EMT, causing tumor cells to reduce proliferation but instead disseminate from the primary tumor to form distant metastasis. Previous work showed that PAR1 deficiency in the stroma also reduced metastasis but promoted primary tumor growth. Indeed, the inoculation of wild-type tumor cells into PAR1 deficient animals (hence PAR1 competent tumor cells in a PAR1 deficient environment) resulted in smaller tumors as compared to the inoculation in wild type animals [17]. Together these studies highlight that PAR1 plays a context-dependent pleiotropic role in tumor biology and that PAR1 targeting should be approached with caution. For instance, explicitly targeting stromal

7

PAR1 could be an intriguing new concept to reduce the metastatic burden of PDAC. Alternatively, the identification of PAR1 agonists that specifically mediate the growth inhibitory effect on tumor cells could hold therapeutic promise. Finally, the efficacy of PAR1 inhibition could be increased by only targeting signaling cascades/PAR1 agonists that mediate the pro-tumorigenic effects of PAR1.

Macrophage influx and PAR1 driven tumor-macrophage crosstalk
Monocyte recruitment to tissues is the innate immune system's initial response to tissue damage or inflammation. Upon entry into the tissue, monocytes get activated to become macrophages, and these newly activated naïve macrophages further differentiate into a broad spectrum of specialized macrophage phenotypes (from pro-inflammatory to anti-inflammatory) in response to micro-environmental cues [38]. In many solid tumors, including PDAC, macrophage infiltration is common, and increased macrophage numbers are often associated with poor prognosis and enhanced metastasis [39,40]. Interestingly, studies using different solid tumor models have shown that tumor-associated macrophages (TAMs) induce EMT [41–43], which (as indicated above) may drive tumor progression and metastasis. Of particular interest given the above, PAR1 activation induces the secretion of monocyte chemoattractant protein-1 (MCP-1), a cytokine required for monocyte recruitment [44]. Furthermore, using an orthotopic pancreatic cancer grafting model, a previous study showed that PAR1-deficient animals exhibited decreased macrophage infiltration into the tumor, accompanied by smaller tumors and increased gemcitabine resistance compared to wild-type animals [17]. These findings suggest that PAR1 may aid metastatic potential and therapy resistance in cancers by driving monocyte/macrophage infiltration through the production of MCP-1 [45].

A question that remained is how the recruited macrophages, once migrated into the tumor, interact with PAR1 to increase tumor progression. In Chapter 3, we report that naïve (M0) macrophages secrete MMP9, we identify MMP9 as a novel agonist for tumor cell PAR1, and we show that MMP9-dependent PAR1 activation drives EMT. Interestingly, the MMP9-dependent induction of EMT on tumor cells also renders tumor cells resistant to M0 macrophage-induced cytotoxicity. The findings in this chapter thus suggest that targeting MMP9 rather

than PAR1 could be effective against PAR1-driven EMT and resistance against M0-macrophage-induced cytotoxicity. This would allow specific targeting of the pro-tumorigenic activities of PAR1, leaving the anti-tumorigenic effects of PAR1 untouched.

In Chapter 4, the anti-tumorigenic activities of naive M0 macrophages were further analyzed in detail in a PAR1-independent manner. In this chapter, we show that the anti-tumorigenic capacities of M0 macrophages are dependent on TNF-α secretion. Indeed, naïve M0 macrophages secrete large amounts of TNF-α, and TNF-α inhibition prevents M0-induced cytotoxicity. Moreover, the differentiation of naïve M0 macrophages into specialized subtypes, either by tumor cells or by specific cytokines, diminishes TNF-α secretion and a loss of the cytotoxic effects of macrophages.

An essential aspect of M0 macrophage differentiation in the tissue microenvironment (TME) is that their secretion patterns may change after differentiation. It, therefore, remains to be seen whether M2/TAM differentiated macrophages still secrete MMP9. In addition, it may well be that differentiated macrophages predominantly secrete other (PAR1 cleaving) proteases, and the interaction of these proteases with PAR1 may yield a different cellular outcome due to PAR1 biased signaling [5]. Therefore, protease expression profiling of macrophages at different stages of differentiation and other members of the tumor microenvironment such as pancreatic stellate cells and cancer-associated fibroblast populations could yield specific pro-tumorigenic PAR1 agonists. In other words, an in-depth understanding of PAR1-driven cellular pathways (both up-and downstream of PAR1 cleavage) together with expression patterns and dynamics of agonists at different stages in the TME can yield novel therapeutic targets against metastatic disease or primary tumor progression.

PAR1 activity in acinar-to-ductal metaplasia
Acinar-to-ductal metaplasia (ADM) is an event that occurs in the pancreas, whereupon injury, pancreatic acinar cells differentiate into duct-like cells with progenitor cell properties. ADM contributes to tissue regeneration and is essential for the homeostasis of the pancreas. However, in case of oncogenic mutations or

7

sustained stress, ADM can lead to pancreatic intraepithelial neoplasia (PanIN), which is a common premalignant precursor lesion often observed in PDAC patients [46,47]. This thesis provides the first clues that PAR1could play a key role in ADM in the pancreas. As shown in Chapter 5, PAR1 activation induced ductal differentiation of wild-type acini, whereas PAR1 deficient acini were shown to be resistant to the induction of ADM. Although of evident importance, PAR1 driven ADM is not the only novel finding in this chapter. We also showed that silencing PAR1 in terminally differentiated PDAC cells provoked a marked increase in acinar-related gene expression patterns and a decline in ductal transcriptional programs – an unforeseen but exciting finding as it was previously believed that terminally differentiated ductal cancer cells could not re-gain acinar cell-related expression patterns. Our data refute this paradigm and instead show that through continuous PAR1 inhibition, ductal cell identities can be shifted towards acinar fates. However, it must be noted that PAR1 knockout mice show no defects in pancreatic development or ductal structures, suggesting that PAR1 is likely not be involved in embryonic development of the ductal lineage. Also shown in Chapter 5 is that PAR1 driven maintenance of the ductal lineage is linked to Myc activity. Myc is a highly deregulated proto-oncogene in >50% of cancers that plays an essential role in cell proliferation, metabolism, and differentiation [48]. Of note, we show that Myc inhibition mimics PAR1 deficiency in enhancing acinar programs in healthy organoids and PDAC cells. The underlying mechanism by which the PAR1/Myc axis drives ADM remains elusive, however. A (future) more detailed analysis of the molecular mechanism on PAR1-driven ADM incorporating Myc activity and elucidating PAR1/Myc target genes/pathways may identify essential players in ductal transdifferentiation. At this moment, it is tempting to speculate that Myc inhibition, as the secondary member behind PAR1-initiated ADM, may yield a novel therapeutic window to prevent disease progression. Importantly, however, no clinically approved specific Myc inhibitors are currently available. PAR1-mediated ADM is a potential early event in PDAC development, but patients are not typically diagnosed at an early stage. Therefore, the big question in future studies would be whether reversal of ductal cells to acinar-like cells has therapeutic potential in both premalignant and established PDACs. To this end, genetic animal models in which the premalignant and the late stages of PDAC are captured (with and without genetic or pharmacological perturbation of PAR1)

could be used. The reason for using model systems combining PAR1 deficiency with KRAS mutations is that the KRAS oncogene is one of the most predominantly mutated genes in human malignancies. In pancreatic cancer, more than 90% of the patient samples are positive for KRAS mutations [49,50]. The constitutively active KRAS G12D mutation is the most frequent KRAS mutation in the pancreas and is detected frequently in the most common precursor lesions such as pancreatic intraepithelial neoplasia (PanIN) [51,52]. Furthermore, studies with mouse models have shown that oncogenic KRAS is a prerequisite for PanIN formation [53,54]. Therefore, combining PAR1 deficiency with oncogenic KRAS in a pancreas-specific model to assess disease progression over time can shed a brighter light on the extent of the therapeutic potential and provide more evidence for targeting PAR1 (or its activating proteases) in combatting disease progression in PDAC.

Clinical Relevance and Future Perspectives
Systemic inhibition of PAR1 should be applied with caution, considering that systemic treatment is not expected to act on tumor cells alone. This is particularly important as blocking thrombin-PAR1 dependent platelet aggregation impairs coagulation and may lead to bleeding complications. In fact, the TRA*CER trial, a placebo-controlled phase III trial in which vorapaxar was added to the standard of care to treat acute coronary syndromes, reported an increased risk of bleeding in the vorapaxar group, and the trial was terminated prematurely due to the bleeding complications [55,56]. Instead of PAR1 inhibition, dominant/highly expressed agonists or downstream signaling pathways (e.g., Myc) in the target tissue could therefore be more suitable targets to achieve therapeutic goals. In addition, patient stratification based on PAR1 and/or agonist expression will inform the dominant agonists in the given subgroup, which could be used for targeted and personalized therapies.

It would be interesting to address whether PAR1 inhibition or agonist / downstream pathway inhibition could be utilized in patients who suffer from acute or chronic pancreatitis and for those who are at higher risk for developing PDAC. Furthermore, early-stage inhibition of PAR1 or its protumorigenic agonist could limit tumor progression and decrease the metastatic burden, thereby increasing

7

the window of opportunity for tumor resection. However, it must be noted that animal studies combining PAR1 deficiency with oncogene-driven pancreatic cancer progression are needed to obtain pre-clinical evidence before clinical trials could be initiated. As already mentioned before, PAR1 inhibition should be handled with care, given that systemic targeting may cause severe bleeding complications. Again, identifying (and targeting) the protumorigenic PAR1 agonist may hold more significant clinical promise.

REFERENCES

[1]   Neves SR. G Protein Pathways. Science (80-). 2002;296:1636–9.

[2]   Soh UJ, Dores MR, Chen B, Trejo J. Signal transduction by protease-activated receptors. Br J Pharmacol. 2010;160:191–203.

[3]   Grimsey N, Lin H, Trejo J. Endosomal signaling by protease-activated receptors. In: Methods in Enzymology. 2014.

[4]   Covic L, Kuliopulos A. Protease-activated receptor 1 as therapeutic target in breast, lung, and ovarian cancer: Pepducin approach. Int J Mol Sci. 2018;19:1–16.

[5]   Zhao P, Metcalf M, Bunnett NW. Biased signaling of protease-activated receptors. Front Endocrinol (Lausanne). 2014;5:1–16.

[6]   Mosnier LO, Sinha RK, Burnier L, Bouwens EA, Griffin JH. Biased agonism of protease-activated receptor 1 by activated protein C caused by non-canonical cleavage at Arg46. Blood. 2012;120:5237–46.

[7]   Flaumenhaft R, De Ceunynck K. Targeting PAR1: Now What? Trends Pharmacol Sci. 2017;38:701–16.

[8]   Kenakin T. Functional selectivity and biased receptor signaling. J Pharmacol Exp Ther. 2011;336:296–302.

[9]   Liu X, Yu J, Song S, Yue X, Li Q. Protease-activated receptor-1 (PAR-1): A promising molecular target for cancer. Oncotarget. 2017;8:107334–45.

[10]   Wang Q, Liu Q, Wang T, Yang H, Han Z, Zhang P. Endothelial cell protein C receptor promotes MGC803 gastric cancer cells proliferation and migration by activating ERK1/2. Med Oncol. 2015;32:162.

[11]   Maeda S, Nakajima K, Tohyama Y, Kohsaka S. Characteristic response of astrocytes to plasminogen/plasmin to upregulate transforming growth factor beta 3 (TGFβ3) production/secretion through proteinase-activated receptor-1 (PAR-1) and the downstream phosphatidylinositol 3-kinase (PI3K)-Akt/PKB signaling cascade. Brain Res. 2009;1305:1–13.

[12]   Chang LH, Chen CH, Huang DY, Pai HC, Pan SL, Teng CM. Thrombin induces expression of twist and cell motility via the hypoxia-inducible factor-1α translational pathway in colorectal cancer cells. J Cell Physiol. 2011;226:1060–8.

[13]   Arora P, Cuevas BD, Russo A, Johnson GL, Trejo J. Persistent transactivation of EGFR and ErbB2/HER2 by protease-activated receptor-1 promotes breast carcinoma cell invasion. Oncogene. 2008;27:4434–45.

[14]   Huang Y-L, Shi G-Y, Lee H, Jiang M-J, Huang B-M, Wu H-L, et al. Thrombin induces nestin expression via the transactivation of EGFR signalings in rat vascular smooth muscle cells. Cell Signal. 2009;21:954–68.

[15]   Darmoul D, Gratio V, Devaud H, Peiretti F, Laburthe M. Activation of proteinase-activated receptor 1 promotes human colon cancer cell proliferation through epidermal growth factor receptor transactivation. Mol Cancer Res.

7

2004;2:514–22.

[16]   Mo J-S, Yu F-X, Gong R, Brown JH, Guan K-L. Regulation of the Hippo-YAP pathway by protease-activated receptors (PARs). Genes Dev. 2012;26:2138–43.

[17]   Queiroz KCS, Shi K, Duitman J, Aberson HL, Wilmink JW, Van Noesel CJM, et al. Protease-activated receptor-1 drives pancreatic cancer progression and chemoresistance. Int J Cancer. 2014;135:2294–304.

[18]   Cisowski J, O'Callaghan K, Kuliopulos A, Yang J, Nguyen N, Deng Q, et al. Targeting protease-activated receptor-1 with cell-penetrating pepducins in lung cancer. Am J Pathol. 2011;179:513–23.

[19]   Boire A, Covic L, Agarwal A, Jacques S, Sherifi S, Kuliopulos A. PAR1 is a matrix metalloprotease-1 receptor that promotes invasion and tumorigenesis of breast cancer cells. Cell. 2005;120:303–13.

[20]   Pang L, Li J fang, Su L, Zang M, Fan Z, Yu B, et al. ALEX1, a novel tumor suppressor gene, inhibits gastric cancer metastasis via the PAR-1/Rho GT-Pase signaling pathway. J Gastroenterol. 2018;53:71–83.

[21]   Sayyah J, Bartakova A, Nogal N, Quilliam LA, Stupack DG, Brown JH. The Ras-related protein, Rap1A, mediates thrombin-stimulated, integrin-dependent glioblastoma cell proliferation and tumor growth. J Biol Chem. 2014;

[22]   Yang E, Cisowski J, Nguyen N, O'Callaghan K, Xu J, Agarwal A, et al. Dysregulated protease activated receptor 1 (PAR1) promotes metastatic phenotype in breast cancer through HMGA2. Oncogene. 2016;35:1529–40.

[23]   Zhong W, Chen S, Qin Y, Zhang H, Wang H, Meng J, et al. Doxycycline inhibits breast cancer EMT and metastasis through PAR-1/NF-κB/miR-17/E-cadherin pathway. Oncotarget. 2017;8:104855–66.

[24]   Wang Y, Liu J, Ying X, Lin PC, Zhou BP. Twist-mediated Epithelial-mesenchymal Transition Promotes Breast Tumor Cell Invasion via Inhibition of Hippo Pathway. Sci Rep. 2016;

[25]   Kancharla A, Maoz M, Jaber M, Agranovich D, Peretz T, Grisaru-Granovsky S, et al. PH motifs in PAR1&2 endow breast cancer growth. Nat Commun. 2015;

[26]   Yang E, Boire A, Agarwal A, Nguyen N, O'Callaghan K, Tu P, et al. Blockade of PAR1 signaling with cell-penetrating pepducins inhibits Akt survival pathways in breast cancer cells and suppresses tumor survival and metastasis. Cancer Res. 2009;

[27]   Arakaki AKS, Pan W-A, Lin H, Trejo J. The α-arrestin ARRDC3 suppresses breast carcinoma invasion by regulating G protein–coupled receptor lysosomal sorting and signaling. J Biol Chem. 2018;293:3350–62.

[28]   Villares GJ, Zigler M, Wang H, Melnikova VO, Wu H, Friedman R, et al. Targeting melanoma growth and metastasis with systemic delivery of liposome-incorporated protease-activated receptor-1 small interfering RNA. Cancer Res. 2008;68:9078–86.

[29]   Wang T, Jiao J, Zhang H, Zhou W, Li Z, Han S, et al. TGF-β induced PAR-1 expression promotes tumor progression and osteoclast differentiation in giant cell tumor of bone. Int J Cancer. 2017;141:1630–42.

[30]   Agarwal A, Tressel SL, Kaimal R, Balla M, Lam FH, Covic L, et al. Identification of a metalloprotease-chemokine signaling system in the ovarian cancer microenvironment: Implications for antiangiogenic therapy. Cancer Res. 2010;

[31]   Andrikopoulos P, Kieswich J, Harwood SM, Baba A, Matsuda T, Barbeau O, et al. Endothelial angiogenesis and barrier function in response to thrombin require Ca2+ influx through the Na+/Ca2+exchanger. J Biol Chem. 2015;

[32]   Zigler M, Kamiya T, Brantley EC, Villares GJ, Bar-Eli M. PAR-1 and thrombin: The ties that bind the microenvironment to melanoma metastasis. Cancer Res. 2011;71:6561–6.

[33]   Moon JY, Franchi F, Rollini F, Angiolillo DJ. Role for Thrombin Receptor Antagonism With Vorapaxar in Secondary Prevention of Atherothrombotic Events: From Bench to Bedside. J Cardiovasc Pharmacol Ther. 2018;23:23–37.

[34]   Mahajan VB, Pai KS, Lau A, Cunningham DD. Creatine kinase, an ATP-generating enzyme, is required for thrombin receptor signaling to the cytoskeleton. Proc Natl Acad Sci U S A. 2000;

[35]   Even-Ram SC, Maoz M, Pokroy E, Reich R, Katz BZ, Gutwein P, et al. Tumor Cell Invasion Is Promoted by Activation of Protease Activated Receptor-1 in Cooperation with the ??v??5 Integrin. J Biol Chem. 2001;276:10952–62.

[36]   Wang S, Li Z, Xu R. Human cancer and platelet interaction, a potential therapeutic target. Int J Mol Sci. 2018;19:1–15.

[37]   Nieswandt B, Hafner M, Echtenacher B, Männel DN. Lysis of tumor cells by natural killer cells in mice is impeded by platelets. Cancer Res. 1999;59:1295–300.

[38]   Mosser DM, Edwards JP. Exploring the full spectrum of macrophage activation. Nat Rev Immunol. 2008;8:958–69.

[39]   Pollard JW. Tumour-educated macrophages promote tumour progression and metastasis. Nat Rev Cancer. 2004;4:71–8.

[40]   Jung KY, Cho SW, Kim YA, Kim D, Oh B-C, Park DJ, et al. Cancers with Higher Density of Tumor-Associated Macrophages Were Associated with Poor Survival Rates. J Pathol Transl Med. 2015;49:318–24.

[41]   Su S, Liu Q, Chen J, Chen J, Chen F, He C, et al. A Positive feedback loop between mesenchymal-like cancer cells and macrophages is essential to breast cancer metastasis. Cancer Cell. 2014;25:605–20.

[42]   Fan QM, Jing YY, Yu GF, Kou XR, Ye F, Gao L, et al. Tumor-associated macrophages promote cancer stem cell-like properties via transforming growth factor-beta1-induced epithelial-mesenchymal transition in hepatocellular carcinoma. Cancer Lett. 2014;352:160–8.

[43]   Liu CY, Xu JY, Shi XY, Huang W, Ruan TY, Xie P, et al. M2-polarized tumor-associated macrophages promoted epithelial-mesenchymal transition in

pancreatic cancer cells, partially through TLR4/IL-10 signaling pathway. Lab Invest. 2013;93:844–54.

[44]   Chen D, Carpenter A, Abrahams J, Chambers RC, Lechler RI, McVey JH, et al. Protease-activated receptor 1 activation is necessary for monocyte chemoattractant protein 1-dependent leukocyte recruitment in vivo. J Exp Med. 2008;205:1739–46.

[45]   Kothari A, Flick MJ. Coagulation Signaling through PAR1 as a Therapeutic Target in Pancreatic Ductal Adenocarcinoma. Int J Mol Sci. 2021;22:5138.

[46]   Kopp JL, von Figura G, Mayes E, Liu F-F, Dubois CL, Morris JP, et al. Identification of Sox9-Dependent Acinar-to-Ductal Reprogramming as the Principal Mechanism for Initiation of Pancreatic Ductal Adenocarcinoma. Cancer Cell. 2012;22:737–50.

[47]   Wei D, Wang L, Yan Y, Jia Z, Gagea M, Li Z, et al. KLF4 Is Essential for Induction of Cellular Identity Change and Acinar-to-Ductal Reprogramming during Early Pancreatic Carcinogenesis. Cancer Cell. 2016;

[48]   Chen H, Liu H, Qing G. Targeting oncogenic Myc as a strategy for cancer treatment. Signal Transduct Target Ther. 2018;3:1–7.

[49]   Hruban RH, Wilentz RE, Maitra A. Identification and Analysis of Precursors to Invasive Pancreatic Cancer. In: Pancreatic Cancer. New Jersey: Humana Press; 2005. p. 001–14.

[50]   Jones S, Zhang X, Williams Parsons D, Cheng-Ho Lin J, Leary RJ, Angenendt P, et al. Core Signaling Pathways in Human Pancreatic Cancers Revealed by Global Genomic Analyses NIH Public Access. Science (80-). 2008;321:1801–6.

[51]   Klimstra DS, Longnecker DS, Hruban RH, DiGiuseppe JA, Offerhaus GJA. K-ras mutations in pancreatic ductal proliferative lesions [Internet]. Vol. 145, American Journal of Pathology. American Society for Investigative Pathology; 1994. p. 1547–50.

[52]   Morris JP, Wang SC, Hebrok M. KRAS, Hedgehog, Wnt and the twisted developmental biology of pancreatic ductal adenocarcinoma. Nat Rev Cancer. 2010;10:683–95.

[53]   Hingorani SR, Petricoin EF, Maitra A, Rajapakse V, King C, Jacobetz MA, et al. Preinvasive and invasive ductal pancreatic cancer and its early detection in the mouse. Cancer Cell. 2004;5:103.

[54]   Aguirre AJ, Bardeesy N, Sinha M, Lopez L, Tuveson DA, Horner J, et al. Activated Kras and Ink4a/Arf deficiency cooperate to produce metastatic pancreatic ductal adenocarcinoma. Genes Dev. 2003;17:3112–26.

[55]   Tra T, Executive CER, Committees S. The Thrombin Receptor Antagonist for Clinical Event Reduction in Acute Coronary Syndrome (TRA•CER) trial: study design and rationale. Am Heart J. 2009;158:327-334.e4.

[56]   Tricoci P, Huang Z, Held C, Moliterno DJ, Armstrong PW, Van de Werf F, et al. Thrombin-Receptor Antagonist Vorapaxar in Acute Coronary Syndromes.

N Engl J Med. 2012;366:20–33.

Annexes

Summary
Nederlandse Samenvatting
PhD Portfolio
List of Publications
Curriculum Vitae
Acknowledgments

182

Summary

Pancreatic Ductal Adenocarcinoma (PDAC) is a highly lethal disease with 5-year survival rates of around 10%, and pancreatic cancer-associated mortality is becoming increasingly common over the years. Unfortunately, despite many years of research and accumulating knowledge, only a modest improvement is achieved in patient outcomes. One of the reasons for the high mortality rate is the lack of effective treatment options. Therefore, research efforts, including those described in this thesis, are directed towards a better understanding of the underlying mechanisms that drive disease progression to ultimately broaden the therapeutic window.

In this thesis, **Chapter 1** provides an introduction to PDAC, macrophages, and protease-activated receptor-1 (PAR1). PAR1 is well-known to be associated with disease progression and poor overall survival in different cancer types, and it was previously shown that stromal PAR1 accelerates tumor growth and induces chemoresistance in PDAC. To follow up on these previous findings, we focused in **Chapter 2** on the role of tumor cell PAR1 in PDAC progression. Using orthotopic mouse models grafted with wild type and PAR1-deficient PDAC cells, PDAC gene expression datasets, and PDAC cell lines, we show that PAR1 is a crucial player in maintaining a partial mesenchymal tumor cell state. Indeed, PAR1 deficient tumors have a well-differentiated morphology in vivo, and gene expression analysis revealed an association of PAR1 with epithelial characteristics. Furthermore, PAR1 activation significantly enhanced the migratory capacity of PDAC cells, suggesting that its contributions to a mesenchymal-like state are functionally linked to metastasis. These findings show that the contribution of PAR1 on tumor cells differs from those previously shown for stromal PAR1. Therefore, targeting PAR1 in PDAC should be implemented with care.

To further our understanding of how PAR1 drives mesenchymal phenotypes, we investigated PAR1 interactions with tumor microenvironment (TME) components. Since PAR1 activity was previously shown to correlate with macrophage infiltration into the tumor in vivo, we next investigated whether PAR1 activity on tumor cells can be linked to macrophage secreted proteases (i.e., tentative PAR1 agonists). In **Chapter 3**, using patient data expression sets, we show that a macro-

phages themselves are not positive for PAR1. To elucidate the interaction of macrophages upon entry into the tumor tissue with tumor cell-expressed PAR1, we utilized naïve macrophages (M0) in medium transfer experiments. By analyzing known and potential PAR1 agonists secreted from M0-macrophages, we identified MMP9 as the dominant macrophage-secreted PAR1 agonist. Functional assays with PAR1 and/or MMP9 inhibitors together in M0-macrophage medium transfer experiments revealed that M0-macrophages drive epithelial-to-mesenchymal transition (EMT) by MMP9-dependent PAR1 activation. Another interesting finding in this chapter was that M0-macrophages had cytotoxic effects on tumor cells, which could be further increased via PAR1 or MMP9 inhibition. We proposed that EMT induction could act as a survival mechanism against M0 macrophage-induced cytotoxicity. Indeed, preventing EMT via ZEB1 silencing diminished the ability of tumor cells to survive macrophage-induced cytotoxicity, further strengthening the notion that MMP9-driven PAR1 activation on tumor cells induces EMT and enhances tumor cell viability under selective pressure.

The M0 macrophage-induced cytotoxicity found in **Chapter 3** is an unanticipated finding. Traditionally, macrophage influx is associated with accelerated tumor growth, and macrophages are accepted to exert pro-tumorigenic activities. To understand what drives M0 macrophage-induced cytotoxicity, we investigated M0 macrophage-induced cytotoxicity on PDAC cell lines in **Chapter 4**. We compared naive M0 macrophages to other specifically differentiated macrophages such as M1, M2, and tumor-associated macrophages (TAMs) in cell viability and cell death analysis. Interestingly, of all subtypes, only naïve M0 macrophages were found to induce cell death. Furthermore, we found that TNF-α secretion was exceptionally high in the M0 subtype and that TNF-α inhibition using Infliximab diminished the cytotoxic effect of naïve macrophages. Altogether, these findings suggest that reestablishing TNF-α secretion in differentiated macrophages (especially in the TAM subtype) could potentially re-activate their anti-tumorigenic properties.

Pancreatic acinar cells show cellular plasticity and, upon injury, can transdifferentiate into duct-like cells to contribute to the tissue remodeling during healing. This transdifferentiation of acinar cells into ductal cells is called acinar-to-ductal metaplasia (ADM). In normal tissue homeostasis, ADM is reversible; however,

the presence of oncogenic cues can render ADM irreversible and give rise to preneoplastic lesions that develop into PDAC. It has been previously shown that macrophages are key drivers of ADM through macrophage secreted factors such as MMP9. In **Chapter 5**, we demonstrated that the tumor cell-macrophage cross-talk through MMP9-dependent PAR1 activation contributes to ADM and pancreatic cell fates. Specifically, we found that PAR1 deficiency increases acinar-related gene expression in the healthy pancreas and limits ADM in acinar cells ex vivo. Moreover, silencing PAR1 in PDAC cell lines increases acinar marker expression. We found that the PAR1-mediated cell identity transitions rely on Myc activity, and continuous PAR1 and Myc inhibition on ductal organoids was found to reestablish acinar cell fates, even in tumor cells already committed to the ductal lineage. In conclusion, in **Chapter 5**, we identified the PAR1-Myc axis as a driver of ADM and ductal cell fates in premalignant pancreas and PDAC. Additionally, we showed that acinar cells are not the only cell type in the exocrine pancreas that shows cellular plasticity and that ductal cells can also transition into acinar-like cells even in the context of oncogenic KRAS activation.

In **Chapter 6**, we present a commentary on a study on PAR1 in prostate and intestinal tumor progression. In this chapter, we discuss how these findings relate to other findings on PAR1 in different tumor types and compare research outcomes. Contradicting results from different preclinical studies in PAR1 deficient backgrounds strongly suggest that PAR1 has divergent roles in tumor biology. The main focus is to highlight whether, due to different contributions to tumor growth depending on the context, PAR1 may be a promising target for cancer treatment. We conclude that the paradigm shift from PAR-1 as strictly tumor-promoting to a potential context-dependent tumor suppressor establishes that PAR-1 is currently not an attractive target to pursue in a cancer setting. Next to potential bleeding complications that already were a major concern for long-term treatment, PAR-1 inhibition may even potentiate tumor development in certain patients. Therefore, as touched upon in the general discussion section, we envision that explicitly targeting the protumorigenic PAR1 agonist may hold more significant therapeutic potential as full-blown PAR1 inhibition.

Nederlandse Samenvatting

Alvleesklierkanker is een zeer dodelijke ziekte met een gemiddelde overlevings-duur van ongeveer 9 maanden. Vijf jaar na diagnose is ruim 90% van de patiënten overleden, terwijl de sterfte na 10 jaar rond de 99% ligt. Een van de belangrijkste redenen voor dit hoge sterftecijfer is het gebrek aan effectieve behandelingsmo-gelijkheden. Voor het ontwikkelen van nieuwe behandelingen is het van groot belang meer inzicht te verkrijgen in mechanismen die ten grondslag liggen aan alvleesklierkanker.

In dit proefschrift wordt in **Hoofdstuk 1** een inleiding gegeven over alvlees-klierkanker, een specifieke soort immuuncellen die we macrofagen noemen, en protease geactiveerde receptor 1 (PAR-1). Het is bekend dat PAR1 is geasso-cieerd met snelle ziekteprogressie en een relatief korte overleving in verschillen-de kankertypes. Verder is eerder aangetoond dat PAR1 expressie in cellen ron-dom de eigenlijke tumorcellen (ook wel stromale expressie genoemd) de groei van alvleesklierkanker versnelt en daarnaast de tumor minder gevoelig maakt voor chemotherapie. Gebaseerd op deze eerdere bevindingen hebben wij ons in **Hoofdstuk 2** gericht op de rol van tumorcel PAR1 in de progressie van alvlees-klierkanker. Met behulp van muismodellen, genexpressie datasets, en cellijnen, vonden we dat PAR1 een cruciale rol speelt bij de morfologie van alvleesklier-kankercellen en de groei van de cellen. PAR1 bevattende alvleesklierkankercellen bleken langzamer te groeien dan alvleesklierkankercellen zonder PAR1. Naast dit tumor-remmende effect van PAR1 bleek de PAR1 afhankelijke morfologie veran-dering echter ook te leiden tot een verhoogde bewegelijkheid van de tumorcellen, die leidt tot meer uitzaaiingen. Gebaseerd op de snellere groei van tumorcellen die geen PAR1 tot expressie brengen lijkt het remmen van PAR1 in patiënten, on-danks dat dit uitzaaiingen zou kunnen voorkomen, op dit moment geen goed idee.

Eerdere studies lieten zien dat de activiteit van PAR1 correleert met de hoeveel-heid macrofagen in alvleesklierkankerweefsel. In **Hoofdstuk 3** laten we zien dat expressie van PAR1 inderdaad correleert met zogeheten markers voor macrofa-gen, maar dat macrofagen zelf geen PAR1 tot expressie brengen. In plaats daar-van blijken macrofagen een specifiek eiwit (te weten matrix metalloprotease 9; MMP-9) uit te scheiden dat PAR1 op de alvleesklierkankercellen activeert. Deze

activatie leidt tot het ontstaan van meer mobiele, makkelijker uitzaaiende alvleesklierkankercellen. Een andere interessante bevinding in dit hoofdstuk was dat macrofagen in staat bleken alvleesklierkankercellen te doden (zoals macrofagen horen te doen als immuun cellen), maar dat de activatie van PAR1 dit grotendeels voorkwam. De differentiatie van alvleesklierkankercellen na PAR1 activatie lijkt dus te werken als een overlevingsmechanisme tegen macrofaag-geïnduceerde celdood. Het blokkeren van dit resistentie mechanisme in alvleesklierkankercellen bleek inderdaad te leiden tot een toename in macrofaag afhankelijke celdood. Dit suggereert dat tumorcellen PAR1 misbruiken om macrofaag-geïnduceerde celdood te omzeilen en dat het remmen van PAR1 mogelijk de effectiviteit van macrofagen zou kunnen vergroten.

De macrofaag-geïnduceerde celdood zoals waargenomen in **Hoofdstuk 3** is een onverwachte bevinding. Traditioneel wordt de instroom van macrofagen in tumorweefsel namelijk geassocieerd met versnelde tumorgroei, en macrofagen worden daarom beschouwd als tumorgroei-bevorderende cellen. Om deze ogenschijnlijk tegenstrijdige waarnemingen te verklaren, onderzochten we macrofaag-geïnduceerde celdood van alvleesklierkankercellen in **Hoofdstuk 4**. Hierbij bleek dat alleen naïeve macrofagen, die pas kort in het tumorweefsel aanwezig geweest zijn, alvleesklierkankerceldood induceren. Macrofagen die als gevolg van de interactie met (en instructie door) alvleesklierkankercellen een andere identiteit aannamen, voorkwamen celdood. Verder vonden we dat de productie van een bekend tumorcel dodend eiwit (te weten TNF-α) hoog was in naïeve, ongedifferentieerde macrofagen maar niet in gedifferentieerde macrofagen. Het remmen van TNF-α bleek tenslotte het celdodende effect van naïeve / ongedifferentieerde macrofagen te verminderen. Bij elkaar suggereren deze bevindingen dat het herstellen van de TNF-α secretie in gedifferentieerde macrofagen mogelijk zou kunnen leiden tot een effectievere celdood van alvleesklierkankercellen.

De alvleesklier kan na beschadiging herstellen. Hiertoe differentiëren de acinaire cellen, de cellen die de verteringsenzymen maken, in een proces dat bekend staat als acinaire naar ductale metaplasie (ADM). Onder normale omstandigheden is ADM omkeerbaar en transdifferentiëren de ductale cellen weer terug naar hun acinaire oorsprong. De aanwezigheid van specifieke oncogene DNA mutaties kan ADM echter onomkeerbaar maken en aanleiding geven tot het ontstaan van

alvleesklierkanker. Eerder is aangetoond dat macrofagen bij dit proces een belangrijke rol spelen door de uitscheiding van MMP-9. Aangezien we eerder hebben aangetoond dat MMP9 kan leiden tot PAR1 activatie hebben we in **Hoofdstuk 5** bestudeerd of MMP9 via PAR1 bijdraagt aan ADM en het ontstaan van alvleesklierkanker. Hierbij vonden we inderdaad dat acinaire cellen PAR1 gebruiken om te differentiëren en dat het remmen van PAR1 ADM voorkwam. Deze data suggereren dat PAR1 een belangrijke rol speelt bij de initiatie van alvleesklierkanker.

Hoofdstuk 6 is een beschouwing van een gepubliceerde studie naar de rol van PAR1 in prostaat- en darmkankerprogressie. We bespreken hoe de bevindingen uit het gepubliceerde artikel zich verhouden tot andere bevindingen in de wetenschappelijke literatuur over PAR1 in verschillende tumortypes. Tegenstrijdige resultaten van verschillende studies suggereren dat PAR1 onder bepaalde omstandigheden tumorgroei kan remmen en uitzaaiing kan voorkomen maar dat het onder andere omstandigheden juist tumorgroei kan bevorderen. Als gevolg hiervan concluderen we dat het remmen van PAR-1 momenteel geen goede optie is voor kankerpatiënten. Naast potentiële bloedingscomplicaties als gevolg van langdurige PAR1 remming zou PAR-1 remming bij bepaalde patiënten zelfs de ontwikkeling of groei van tumoren kunnen versterken. Daarom denken wij, zoals we in de algemene discussie uitgebreid beschreven hebben, dat toekomstige onderzoeken zich expliciet moeten richten op de specifieke factoren die de tumor-bevorderende activiteiten van PAR1 mediëren. De identificatie van deze factoren zal de mogelijkheid bieden om de tumor-bevorderende rol van PAR1 te remmen zonder de tumor-remmende werking te verminderen.

PhD Portfolio

Cansu Tekin

PhD Period: November 2015-October 2021

Total ECTS: 29.1

General Courses	Year	ECTS
Laboratory Animal Science	2015	3
Workshop R2: Analysis of Tumor Genomics	2015	0.1
Basic Laboratory Safety	2016	0.4
OOA Microscopy Course	2016	1.5
Endnote	2016	0.1
Mass Spectrometry, Proteomics and Protein Research	2017	2.1
Computing in R	2018	0.4
OOA Histopathology of Human Tumors	2018	0.6
Practical Biostatistics	2020	1.4

Conferences and Presentations	Year	ECTS
Cancer Center Amsterdam Annual Retreat (Noordwijkerhout, NL)	2017-2020	3
Annual OOA PhD Retreat (Renesse, NL)	2017	1
AACR Annual Meeting (Chicago, IL, USA)	2018	1.5

Seminars	Year	ECTS
Department Seminars (CEMM)	2015-2021	6
AMC Oncology Seminars (OASIS)	2015-2019	8

List of Publications

Publications that are included in this thesis

Tekin C, Shi K, Daalhuisen JB, ten Brink MS, Bijlsma MF, Spek CA. PAR1 signaling on tumor cells limits tumor growth by maintaining a mesenchymal phenotype in pancreatic cancer. Oncotarget. 2018;9:32010–23.

Spek CA, **Tekin C,** Bijlsma MF. Protease-activated receptor-1 impedes prostate and intestinal tumor progression in mice: comment. J Thromb Haemost. 2019;17:235–8.

Tekin C, Aberson HL, Waasdorp C, Hooijer GKJ, de Boer OJ, Dijk F, Bijlsma MF, Spek CA. Macrophage-secreted MMP9 induces mesenchymal transition in pancreatic cancer cells via PAR1 activation. Cell Oncol. 2020;43:1161–74.

Tekin C, Aberson HL, Bijlsma MF, Spek CA. Early macrophage infiltrates impair pancreatic cancer cell growth by TNF-α secretion. BMC Cancer. 2020;20:1–9.

Tekin C, Scicluna BP, Lodestijn SC, Shi K, Bijlsma MF, Spek CA. Protease-activated receptor-1 drives and maintains ductal cell-fates in the premalignant pancreas and ductal adenocarcinoma. Mol Oncol. 2021;

Publications that are *not* included in this thesis

Slapak EJ, Duitman J, **Tekin C**, Bijlsma MF, Spek CA. Matrix Metalloproteases in Pancreatic Ductal Adenocarcinoma: Key Drivers of Disease Progression? Biology (Basel). 2020;9:80.

Steins A, van Mackelenbergh MG, van der Zalm AP, Klaassen R, Serrels B, Goris SG, Kocher HM, Waasdorp C, de Jong JH, **Tekin C** et al. High-grade mesenchymal pancreatic ductal adenocarcinoma drives stromal deactivation through CSF-1. EMBO Rep. 2020;21:e48780.

Curriculum Vitae

Cansu Tekin was born on March 21st, 1991, in Ankara, Turkey. At a school science fair, she got introduced to Dolly the sheep, which immediately clicked her excitement and molecular biologists became her version of "I want to be an astronaut". Nevertheless, in the following years, her childhood passion persisted, and while in high school, she was elected as the school delegate to compete in the National Biology Olympics. This journey made her passion burn brighter, leading her to study Molecular Biology and Genetics at Bilkent University in 2009. During her Bachelor's studies, she had worked in various labs and explored different fields such as breast cancer research, bioengineering, metabolism, and cardiovascular research, eventually finding her way to the Biomedical Sciences: Medical Biology Master's program at the University of Amsterdam in 2013. After completing her internships at the Amsterdam UMC, under the supervision of Joost Meijers, and in Maastricht UMC, under the supervision of Gerry Nicolaes, she had completed her Master's with an unsatiated wish to dive deeper into medical biology. Meanwhile, the beautiful country Netherlands had a strong pull on her to stay longer, which eventually led her to pursue a Ph.D. at CEMM at the Amsterdam UMC.

In her spare time, she paints, makes sculptures, and explores movies and literature.

Acknowledgments

After five and a half years of running through the G2 and CEMM-tower (not to mention various other locations in the AMC where this department was spread over), this thesis is marking the end of my time in the CEMM/LEXOR.

I want to start my gratitude for my time here by thanking my promotor and co-promotors, **Jan Paul**, **Arnold**, and **Maarten**, for giving me the opportunity to work as a Ph.D. student in this department.
First of all, **Jan Paul**, thank you for all the discussion and quick-witted responses during PION meetings and during symposia. I always admired your energy and your passion for science. I will always remember you as an invincible cyclist and a great scientist.

Arnold, I am ever grateful and consider myself very lucky to have you as a supervisor. Your gentle, passionate, calm, and friendly aura became my beacon during this ride. I always enjoyed talking to you, and you always reciprocated, even at the cost of me stealing your coffee time. You always welcomed me with a big smile and helped me right away. Whenever I had exciting results, rushing to your office and sharing the news with you and getting your positive feedback right away with a big smile was equally nice to obtain those results in the first place. It was a great pleasure to share my scientific quest with you, talking and discussing also non-scientific stuff over coffee.

Maarten, despite many years sitting across the meeting table, I still don't have a precise method to tell whether you were joking or serious. However, I admire your goal-oriented approach and straightforward thinking, which saved us an immense amount of time while preparing and publishing our manuscripts. Plus, your meticulousness, attention to detail and refined taste in how everything should look was another lesson that I took from you. Many thanks for keeping the projects and the graphics on a straight trajectory.

Joost Meijers, in the first months of my time in the Netherlands, I started my internship in your lab and still remember those days with a warm smile on my face. You were a great mentor to me; I learned a great deal from you. Thank you for accepting to be on my thesis committee; I am delighted to see you again, and it is a great honor.

Hanneke, I admired your strong stand and encouraging presence during the PION meetings. **Louis**, you are truly inspiring as a scientist, and your way of thinking is teaching others a great deal. I am honored to have you both on my thesis committee.

Alex de Vos, your energetic presence in the G2 lab was genuinely remarkable. Many thanks for helping me out whenever I am looking for a fringe reagent in the lab, and also, many thanks for being on my thesis committee.

I want to express many thanks and gratitude to **Carlie de Vries** and **Henri Versteeg** for accepting to be on my thesis committee, making time to evaluate and read my thesis.

Hella, you are definitely the rockstar of the Stolling group, solving problems with ease and keeping our lovely corner lab in order as if it's an easy-peasy thing to do. I enjoyed your gezelligheid and admired your orderliness. It was a great pleasure to work with you and talk with you. I will never forget your positive attitude, your laughter against funny stuff happening in and around our lab.

Jan Willem, your dedication and discipline are definitely admirable. In my first days in the lab, you helped me a lot and taught me a lot, of which I am ever grateful. I always enjoyed your company in the lab and your comments during our group meetings. I am thrilled to hear that your scientific career is advancing, and I am sure many more success stories are ahead of you.

Maaike and **Lin**, thank you for the gezelligheid in the lab; I wish I had more time with you in the lab. All the best for your future endeavors.

Kun, as your successor on the PAR1 project, you and your work became cornerstones for this thesis. I benefited greatly from your animal studies, and for this, we both can be happy that those animals were sacrificed for a more significant cause. I really enjoyed your company during our trip to EACR in Manchester. I appreciate all the friendly guidance you gave me both scientifically and for my career.

Brendon, I must thank you for many things. First, for helping me out big time for the RNA sequencing, setting this straight and running. This was a part where I learned a lot and had great fun. Second, thank you for your very insightful comments and enthusiastic scientific discussions.

Onno, **Gerrit**, and **Frederike**, without your input and help, one of the chapters in this book would not be where it is today. Thank you for joining our project, helping, and teaching me.

Joost and **Marieke**, words wouldn't be enough to express my gratitude for you to help me out during the animal experiments. Without your help, I wouldn't be able to finish any of those animal studies.

Leonie, your friendly attitude and curiosity is really remarkable. I hope you never lose that light in your eyes, and you can keep your interest alive. I am sure you will do a great job and get a lot of success out of your Ph.D. **Etienne**; I am truly impressed with your strong stand in life and admire your persona (and shirt-sock combinations). Having you around in the lab was almost like having a sunny day in the Netherlands. I hope your energy never dies.

Preeti, Paris, Ronja, Vaishali, Nesrin, Clara, and **Sanne ten Hoorn**, I think words cannot do the work when I try to express how much I enjoyed our lunch and coffee breaks. Our close-knitted bond and support for each other were some of the greatest gifts to have out of my time in CEMM. **Preeti**, I haven't met anybody who has your shining and warm aura. You are an incredible person, and I have no doubts that you will achieve many great things. **Clara**, you are a wonder-woman; your dedication inspires me. Thank you so much for your feedback and your guidance in our office whenever I wanted to get your opinion. S**anne ten Hoorn**, your energy is definitely lifting others. I admired your go-getter personality and your friendliness.

Sophie, thank you for helping me out with the organoids and for giving me your strong support. **Anne**, you are extremely funny, friendly and hard-working. I wish you all the best in life. **Veronique**, many thanks for your discussion and support. **Eva**, I missed you a lot after you have left. Your big smile and helpful attitude were one of the highlights in my early years. **Cynthia**, you are the centerpiece of the Bijlsma lab, and without you, nothing would be the same. Thank you for helping me out, and I wish you all the best.

Mark, Amber, and **Sanne Bootsma,** it was a great pleasure to culture together in the ML2 and thank you for all the laughs and gezelligheid. **Maartje, Joyce, Janneke, Kate, Patricia, Robin,** and **Leandro** thanks for the company, talks and gezelligheid during memorable borrels. I had a great time during these happy hours.

Berke, hem Utrecht'te hem G2'de dostluğun ve desteğinle hep yanımda oldun. Bilime duyduğun aşk ve ilginç konulara olan çekimin gerçekten özenilesi. Arkadaşlığın ve desteğin için çok teşekkür ederim.

Gül, Nur, Umut, Deniz, Çağlar, Efe, Ayça, ve **Berke**, Utrecht'te bana ikinci bir aile ve bu süreçte en büyük desteğim oldunuz. Beraber geçirdiğimiz bütün anlar için çok teşekkürler. Daha nice güzel günlerde görüşmek dileğiyle.

Tatjana, Luka, and **Roberto, Katja**, thank you for all the wonderful trips, dinners, board game nights, and drinks. It was a pleasure hanging out with you and talking until late at night. I am ever grateful for all of our time.

Ripunjay, Miriam, Max, Johannes, Jan-Matthis, and **Emrah**, thank you for giving your support, friendship, and being part of my other friend-family in Germany.

Gizem, Elifcan, Seza, Uğur, Ece, Cansu, Çağan, ve **Barış**, Köln'deki günlerime sizin dostluğunuz ve desteğiniz damgasını vurdu desem yeridir. Akademik dertleşmelerimiz, desteğiniz bu tezin yazıldığı günlerde yaşam sevinci oldu, varlığınıza minnettarım.

Emre ve **Marie**, sizin güzel dostluğunuz ve eksik etmediğiniz desteğiniz için size minnettarım. Merci pour tout, tous les bons moments et votre amitié. Let's cheer for the adventures ahead of us.

Didem, **Çağlar** ve **Hakan**. Ankara'ya ziyaretlerimin en güzel anları ve hiç eksik etmediğiniz dostluğunuz için size çok teşekkür ederim.

Ilkin, Ezgi, Erdi, ve **Ferhat,** Bilkent'te başlayan yolculuklarımız sınırları aşıp bugünlere geldi ve bütün bu yıllar boyunca dostluğunuz, varlığınız bana güç verdi. Hepinize ayrı ayrı minnettarım. Birlikte daha nice güzel şeylere, günlere kavuşmak dileğiyle.

Dilege, bütün bu süreci benimle beraber el ele yürüdüğün için sana çok teşekkür ederim. Varlığınla ve sonsuz desteğinle bana güç oldun, bana ne kadar güçlü olduğumu yılmadan hep hatırlattın. Sana ne kadar minnettar olsam, ne kadar teşekkür etsem az. Bu yolculuğu senin desteğin olmadan tamamlamak çok zor olurdu. İyi ki varsın.

Canım **annem** ve **babam**, sizler olmadan ne bugünlere gelebilir ne de bu eğitimi tamamlayabilirdim. Bana olan sonsuz desteğiniz ve inancınız için çok teşekkür ederim.